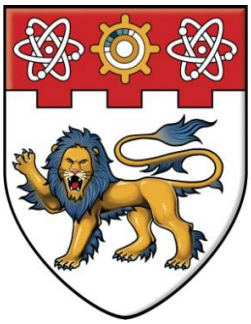

NANYANG TECHNOLOGICAL UNIVERSITY

The Development of Improved Strategies to Monitor and Control Biofouling of Membranes in the Water Industry

LOW JIUN HUI

Interdisciplinary Graduate School

Nanyang Environment and Water Research Institute

Singapore Membrane Technology Centre

2016

The Development of Improved Strategies to Monitor and Control Biofouling of Membranes in the Water Industry

LOW JIUN HUI

Interdisciplinary Graduate School
Nanyang Environment and Water Research Institute
Singapore Membrane Technology Centre

A thesis submitted to the Nanyang Technological University in partial fulfillment of the requirement for the degree of
Doctor of Philosophy

2016

ACKNOWLEDGEMENTS

First of all, I would like to thank my academic supervisor Associate Professor Scott A. Rice for his mentorship, supervision and support throughout my candidature. This thesis would not be complete without his continual encouragement and advice.

I would like to show my appreciation to Professor Harvey Winters, Professor Yehuda Cohen, Professor Anthony Gordon Fane and Associate Professor Diane McDougald for their valuable advices that were directly or indirectly beneficial to my learning during my PhD candidature.

I would also like to thank Associate Professor Rong Wang and Assistant Professor Tzyy Haur Chong for their support in my research work carried out at the Singapore Membrane Technology Centre (SMTC). This research work also would not be possible without the help from colleagues and friends in Nanyang Environment and Water Research Institute (NEWRI) and collaborators from Singapore Centre for Environmental Life Sciences Engineering (SCELSE). Special shout-out to Dr. Robert Barnes, Dr. Miles Edward Rzechowicz, Dr. Hyun-Suk Oh, Dr. Stanilaus Raditya Surwano, Dr. Victor Sim, Dr. Martin Tay, Ms. Jia Shin Ho, Mr. Kunli Goh and Ms. Bibianna Yeo.

I would like to acknowledge the Interdisciplinary Graduate School (IGS) and SCELSE for providing me with financial support for me to attend international conferences and the SCELSE summer school, which allowed me to broaden both my networks and my knowledge in the field of membranes and microbiology.

Last but not least, I want to thank my family for supporting me unreservedly in my decision to pursue this PhD journey

TABLE OF CONTENTS

ABSTRACT

The use of membranes in water treatment processes has greatly increased our global supply of portable water and helped alleviate water scarcity. However, the problem of membrane fouling, especially biofouling, continues to plague the water industry and hinders our quest in making clean water readily available to more people at lower costs. In this study, various strategies were developed and investigated in an attempt to further understand the causes of reverse osmosis biofouling, prevent or delay the onset of biofouling, and to monitor the rate of biofouling online. The effects of three main biofilm exopolysaccharides produced by *Pseudomonas aeruginosa*, Psl, Pel, and alginate, on RO membrane performance were investigated. Among the three, it was found that the presence of the Psl polysaccharide in *P. aeruginosa* biofilms contributed the most to biofilm resistance, with up to 69% faster fouling rates and 70% increase polysaccharide production, and the absence of Pel and alginate polysaccharide did not have a significant impact on *P. aeruginosa* biofouling, contributing to only a 3% difference in fouling rates.

Nitric oxide (NO) has recently been shown to function as a signal for the dispersal of biofilms formed by a wide range of microorganisms. At the concentrations at which NO acts as a signal, it is non-toxic to bacteria and thus represents a molecule with significant potential to disperse mixed species biofilms responsible for RO biofouling based on an environmentally responsible and non-toxic approach. The efficacy NO as treatment to control fouling of RO membranes was investigated, and it was found that NO significantly reduced biofouling rates for both single and mixed species biofouling by 52% and 92% respectively, without significantly altering the community diversity of the mixed species biofilm.

A complementary approach to the control of biofouling is to develop strategies to determine when fouling is occurring, but to do so at an early stage, before it is a problem

so that remedial action can be implemented to control fouling. To address this, a canary cell was developed to model biofouling in an industrial spiral wound module under similar hydrodynamic conditions. Non-invasive techniques including ultrasonic time domain reflectometry and electrochemical impedance spectroscopy were also investigated as tools to provide real-time biofouling information that precedes the actual rise in transmembrane pressure such as in situ biofilm thickness measurements and changes in electrical conductivity at the membrane boundary layer, allowing for the early detection of biofouling.

The findings in this study have demonstrated that alternative, non-toxic strategies can be effective in controlling biofilm and have also shown that different polysaccharides have specific roles in mediating biofouling. In addition, the development and optimization of a canary modeling technique allows for future development of sensors to monitor biofouling in RO operations.

LIST OF TABLES

LIST OF FIGURES

LIST OF SYMBOLS AND ABBREVIATIONS

RO	Reverse Osmosis
SWRO	Seawater reverse osmosis
$\Delta\pi$	Osmotic pressure difference
ρ	Density
g	Acceleration due to gravity
h	Height
J_v	Water output flux
TMP	Transmembrane pressure
M	Viscosity
R_T	Total membrane resistance, consisting of intrinsic resistance and resistance due to fouling
CP	Concentration polarization
R_{int}	Intrinsic membrane rejection
C_p	Concentration of a solute in permeate stream
C_m	Concentration of a solute in feed stream
MWCO	Molecular weight cut-off
C_w^{salt}	Boundary layer salt concentration
C_B^{salt}	Bulk flow layer salt concentration
EPS	Extracellular polymeric substances
DNA	Deoxyribonucleic acid
CFU	Colony forming unit
CF	Cystic fibrosis
QS	Quorum sensing
AHL	N-acylhomoserine lactone

O&M	Operations and maintenance
UV	Ultraviolet radiation
UTDR	Ultrasonic Time Domain Reflectometry
EIS	Electrochemical Impedance Spectroscopy
c	Speed of UTDR acoustic wave
Z	Impedance
A	Amplitude
t	Time
d	Distance
ω	Angular frequency
C	Capacitance
G	Conductance
PBS	Phosphate Buffer Solution
NB	Nutrient Broth
TOC	Total Organic Carbon
LMH	Litres per square metre per hour
CLSM	Confocal Laser Scanning Microscopy
MQ	MilliQ deionised water
BSA	Bovine serum albumin
CFV	Crossflow velocity
SD	Standard deviation
MBR	Membrane bioreactor
R2A	Reasoner's 2A culture media
PCR	Polymerase chain reaction
OTUs	Operational Taxonomic Units
CIP	Cleaning in place

SWM	Spiral wound module
ε	channel voidage
l_m	mesh size
d_f	spacer filament diameter
Re	Reynolds number

LIST OF PUBLICATIONS AND CONFERENCE PROCEEDINGS

R. J. Barnes, R. R. Bandi, F. Chua, J. H. Low, T. Aung, N. Barraud, et al., "The roles of *Pseudomonas aeruginosa* extracellular polysaccharides in biofouling of reverse osmosis membranes and nitric oxide induced dispersal," Journal of Membrane Science, vol. 466, pp. 161-172, 9/15/ 2014.

R. Barnes, J. H. Low, R. Bandi, M. Tay, F. Chua, T. Aung, et al., "Nitric Oxide Treatment for the Control of Reverse Osmosis Membrane Biofouling," Applied and Environmental Microbiology, vol. 81, pp. 2515-2524, 2015.

M. F. Siddiqui, M. Rzechowicz, H.-S. Oh, N. Saeidi, J. H. Low, H. Winters, et al., "The efficacy of tannic acid in controlling biofouling by *Pseudomonas aeruginosa* is dependent on nutrient conditions and bacterial density," International Biodeterioration & Biodegradation, vol. 104, pp. 74-82, 10// 2015.

J. H. Low, "The roles of *Pseudomonas aeruginosa* extracellular polysaccharides in reverse osmosis membrane biofouling and nitric oxide biofouling control," in The 7th International Desalination Workshop, Lotte City Hotel Jeju, Korea, 2014.

J. H. Low, "Anti-biofouling electrospun nanosilver functionalized nylon 6 nanofibrous membranes for reverse osmosis prefiltration," in 2nd International Conference on Desalination using Membrane Technology, Singapore Expo Convention and Exhibition Centre, Singapore, 2015.

J. H. Low, "In-situ Nitric Oxide treatment to control biofouling in membrane-based water treatment process," in Euromembrane 2015, Eurogress Aachen, Germany, 2015.

CHAPTER 1 LITERATURE REVIEW

1.1 The need for access to clean water

Water is essential to, and forms the basis of, all life on Earth, where for example, the total amount of water in an average human amounts to about two thirds of their weight. One of the reasons why life as we know it is only found on planet Earth so far is because our planet is in a habitable zone whereby the conditions are right for liquid water to exist. Water covers about 70% of the Earth's surface, but the bulk of it is saline and only 2.5% exists as freshwater (Figure 1.1). Among the sources of freshwater, only 1.3% is available to humans as surface water. Therefore, it is very important to conserve these limited sources of water and to also look for alternate sources of water.

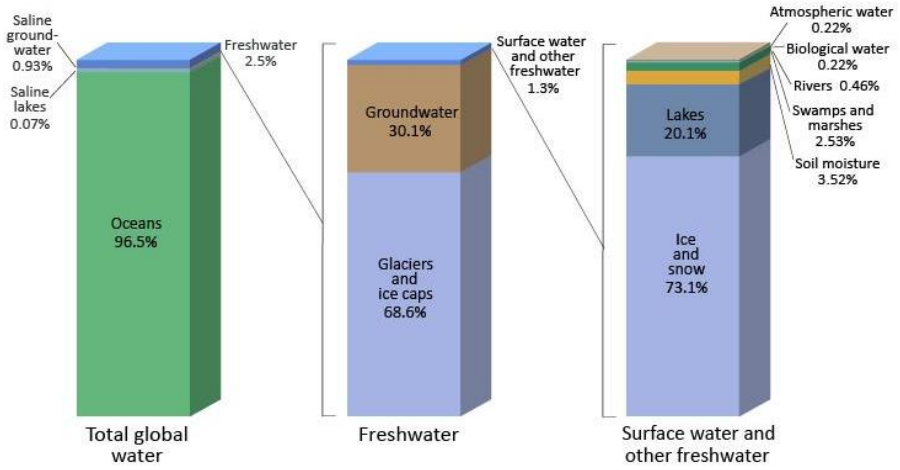

Figure 1.1 Distribution of Earth's Water.[1]

Scarcity of water is one of the more serious, if not the most, global challenges of our time. Currently, over a third of the planet's population lives in countries which are water-stressed and by 2024 and this figure is predicted to increase to approximately two-thirds.[2] According to the United Nations, over one billion people are inhabitants in areas that are physically short of water and more are going to experience water shortage.

Another 1.6 billion people also face economic water shortage, where they lack the physical infrastructure to obtain freshwater from its sources (Figure 1.2). Countries such as China, India, and many parts of Africa, already face moderate to severe fresh water shortages.

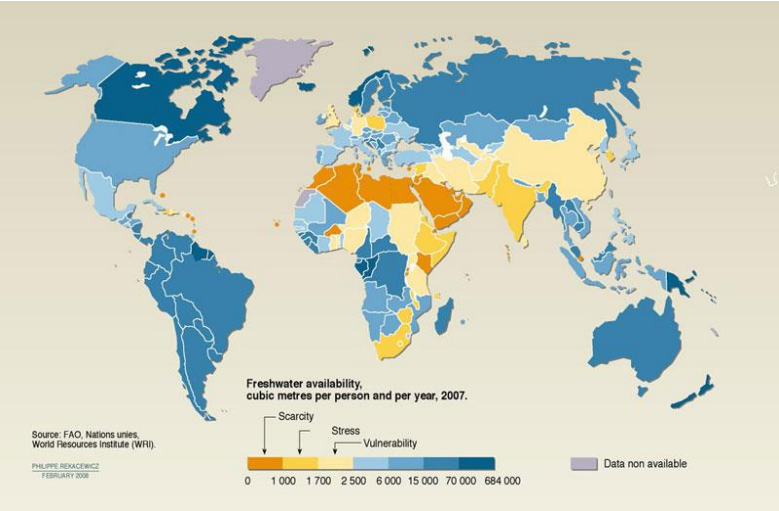

Figure 1.2 Freshwater availability across the world.[3]

Several measures have been implemented to alleviate the stresses we face on water supplies, such as the practice of water conservation, infrastructure repair, as well as improving current catchment and distribution systems. However, while these measures taken are very important, they can only improve the use of current existing water resources, but cannot increase the supply. The only known method to increase our water supply to a state beyond what is readily available are desalination and water recycling.[4] One of the most attractive technologies in desalination and water recycling is the use of Reverse Osmosis (RO) to obtain clean water from non-portable sources. RO uses hydraulic pressure to separate pure water from its contaminants, such as salts, via a semi-permeable membrane. The pores of the membrane are so small that theoretically only water molecules can pass through. This process does not require heat, which represents an energy cost, as compared to other popular methods of water purification like multi-stage

flash distillation and multi-effect evaporation. The amount of energy needed to power desalination in Seawater RO (SWRO) plants has declined significantly in the past 4 decades, from US$1.26 per cubic meter in the 1980s to less than US$0.50 per cubic meter in 2007.[5, 6] Currently, the largest SWRO desalination plant, Sorek in Israel, is capable of producing 627,000 cubic meters of water daily and profitably sells this water at US$0.58 per cubic meter. This decrease in consumption of energy is attributed to the continual improvements in technologies, including the development of higher-permeability membranes, the installation of devices that allows energy recovery, and the use of more energy-efficient pumps.[5] Thermodynamically, the minimum amount of energy required to extract 1 m^3 of freshwater at 50% recovery is about 1.1 kWh[7], which equates to about US$0.10/$m^3$ at current oil prices.

1.2 Reverse osmosis (RO)

Reverse osmosis (RO) is gaining worldwide acceptance in both water treatment and desalination applications. It is typically a pressure-driven process whereby a semi-permeable membrane rejects dissolved constituents present in the feed water. This rejection is due to exclusion of size, exclusion of charge and physical–chemical interactions between the solvents, solutes and membranes.[8, 9] Fundamentally, osmosis (forward osmosis) is defined as the resultant passage of liquid water across a partially permeable membrane driven by a net difference in osmotic pressure ($\Delta\pi$) across the partially permeable membrane [10], given by:

$$\Delta\pi = \rho g h$$

where ρ is the density of the liquid, g is the acceleration due to gravity and h corresponds to the height difference between the feed and draw solution at the end of the osmosis process (Figure 1.3A). In RO, an external hydraulic pressure of a larger magnitude than

that of the osmotic pressure difference is applied on the concentrated feed to force water to move through the semi-permeable membrane in the opposite direction, from a region having higher concentration of solute (feed) to a region having lower concentration of solute (permeate) (Figure 1.3B).

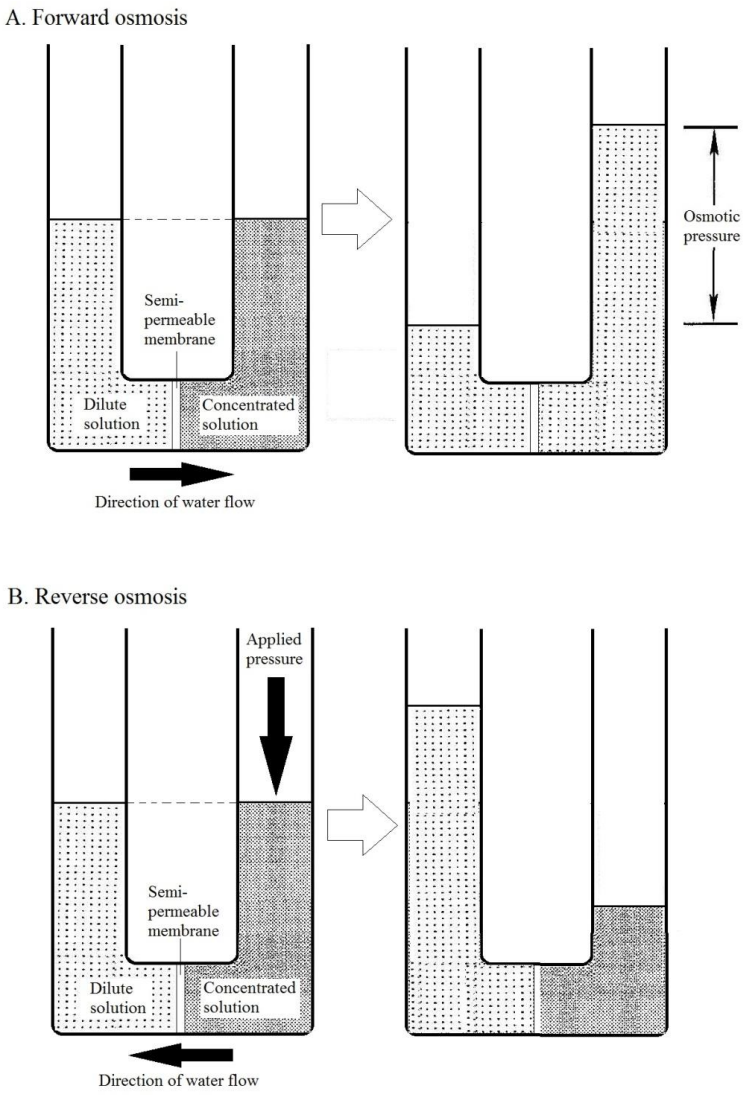

Figure 1.3 A simple diagram illustrating the principles of Forward and Reverse Osmosis, modified from [11]. In forward osmosis (A), water flows from the dilute to the concentrated solution through the semi-permeable membrane without any external hydraulic pressure applied. In reverse osmosis (B), an external hydraulic pressure is applied on the side with the concentrated solution, forcing water to move from the concentrated to the dilute solution.

Filtration can be carried out by either using dead-end filtration or crossflow filtration. The two types of filtration differ in the direction of feed water flow relative to permeate water flow (Figure 1.4).

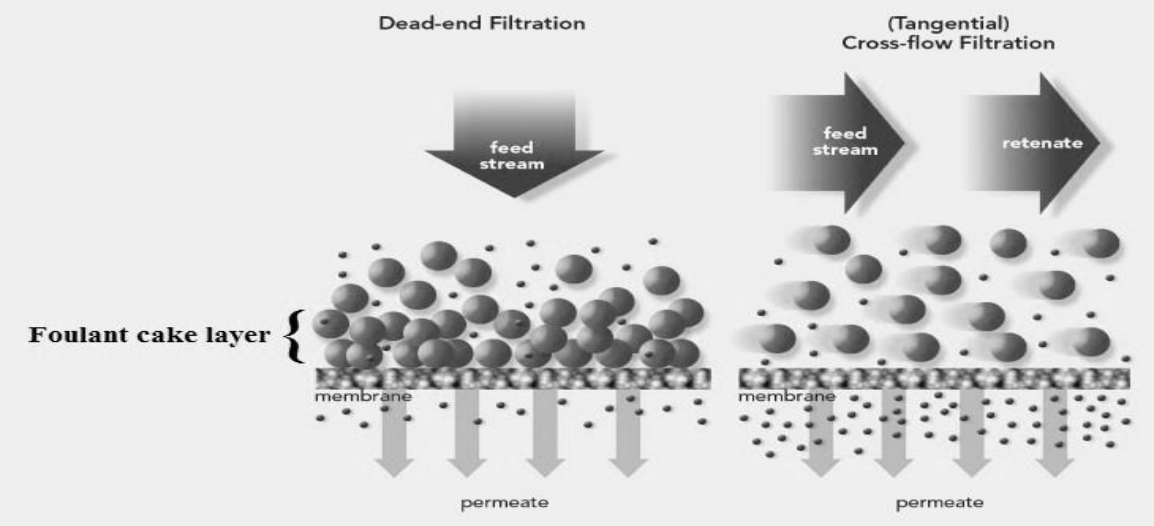

Figure 1.4 Comparison of Dead-end filtration vs. crossflow filtration (adapted from [12]). Dead-end filtration results in the formation of a foulant cake layer that impedes membrane performance.

In dead-end filtration, all of the feed solution is forced directly through the membrane. The solutes retained on the side of the membrane interfaced with the feed accumulates and forms a foulant cake layer [13] until the cake layer builds up to a point where the membrane no longer functions. At this time, the filtration process will have to be stopped and the membrane has to be cleaned before the process can continue; it is also known as batch filtration, as the filtration process occurs in batches.

In crossflow filtration, the filtrate flow is perpendicular to the main stream [13] and any cake layer formed will be removed by the shear force exerted by the water flow. This allows for a continuous process without having to stop the operation to remove the cake layer. It is the preferred process adopted in the water industry as there is less downtime, which translates to higher product yield, lower operating costs and increased profits.

1.3 RO membrane materials and module configurations

Semi-permeable membranes used in RO processes can be made from a range of materials, the most common being polyamide (PA) and cellulose acetate (CA). The first defect-free, high-flux, anisotropic RO membranes was developed by Loeb and Sourirajan [14] in 1963 using a composite solution of 22.2% CA, 66.8% acetone, 10% water and 1% $MgClO_4$.

Subsequently, membranes of different materials were made and they differ in their physical and chemical properties, fabrication process, membrane performance, and membrane application. CA membranes are hydrophilic and demonstrate a high level of resistance against fouling.[15] However, such membranes have a narrow pH operating range of between 4 and 6.5, making them incompatible with common cleaning protocols that use strong acid or alkali. CA is often used to make membranes for microfiltration and ultrafiltration processes because they are inexpensive and readily replaceable.

Polyamide thin film composite membranes, on the other hand, overcome some of the pH limitations faced by CA membranes, but have lower chlorine tolerance.[16] For example, DOW™ FILMTEC™ polyamide membranes have a typical free chlorine tolerance of no more than 0.1 ppm, thus chlorine-based cleaning agents e.g. bleach, cannot be used to clean polyamide membranes that are scaled or fouled. Thin film composite membranes comprises of two parts, a selective rejection layer and a microporous support layer (Figure 1.5). The selective top layer serves as the active layer to filter out contaminants and only allows water to pass through. The microporous support layer, consisting of a layer of microporous polysulfone and reinforcing fabric, acts to preserve the integrity of the membrane when operating under high pressure. The two layers are laminated onto each other via various techniques such as casting, dip-coating, gas-phase deposition, and interfacial polymerization.[17]

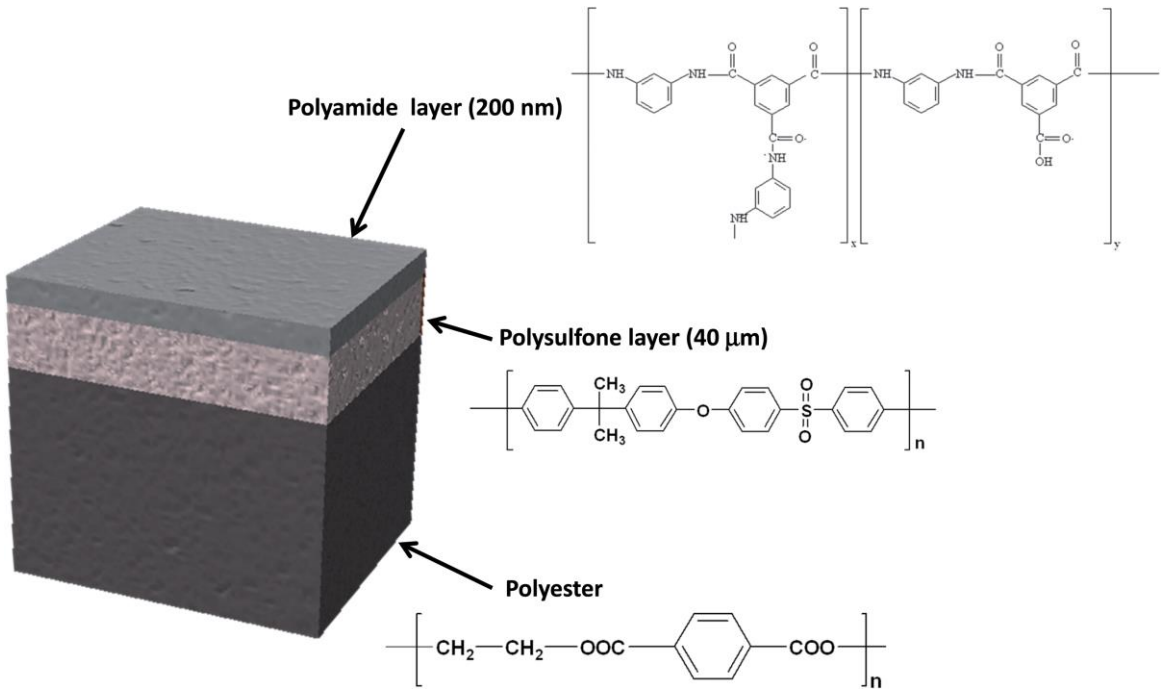

Figure 1.5 Diagram of a thin film composite RO membrane, showing a thin PA active layer above a microporous polysulfone layer and reinforcing polyester underneath.[18]

The thin film composite PA membranes dominate the RO membrane market, and are commercially available in several module configurations: Plate-and-frame; Hollow-Fiber; Tubular; and Spiral-wound. Among these membrane types, the spiral wound module (Figure 1.6) is the most common configuration adopted in the water industry. This is because it has several advantages over other configurations. It allows a high productivity per unit volume due to its large surface-to-volume ratio and packing density. The feed channel spacers between each individual flat sheet membrane within the module also allows any concentration polarization to be kept low and makes the module less prone to fouling.

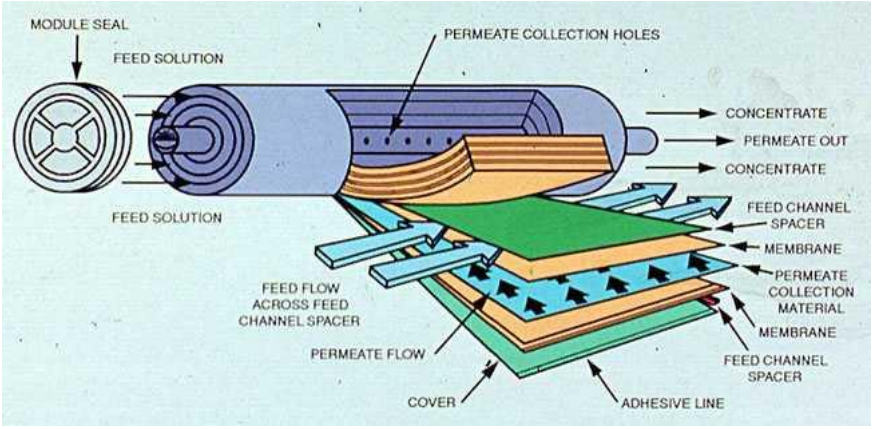

Figure 1.6 Schematic diagram of a spiral wound RO module, showing the arrangement of the membrane and feed channel spacers from within.[19]

1.4 RO performance

Performance for a membrane process can be determined by various parameters, including flux, recovery, rejection and molecular weight cut-off. All of these affect the quality and quantity of water output. In principle, these parameters could all be optimized to give the best possible output, in both quality and quantity. However, that would translate to high operating costs, which would not be practical, and would also accelerate problems such as fouling. Depending on the demand, different water treatment plants may optimize their membrane processes differently to best suit their water production needs, influent water quality as well as types of membranes used.

1.4.1 Flux

For a given applied pressure, the output flux or water production can be calculated using the following equation:

$$J_v = \frac{TMP - \Delta\pi}{\mu R_T}$$

Where J_v represents the output flux, TMP is the trans-membrane pressure, $\Delta\pi$ is the osmotic pressure difference, μ is the viscosity of water, and R_T is the resistance of the membrane due to its physicochemical properties (intrinsic membrane resistance) and additional resistance due to membrane fouling. Flux is also affected by concentration polarization, which is the increase in local solute concentration at the surface of the membrane resulting in increased effective osmotic pressure difference.

1.4.2 Constant flux vs constant pressure RO processes

Water production via RO can be operated under varying conditions, with the two most common being constant pressure or constant flux processes (Figure 1.7). In constant pressure processes, the TMP is fixed and the water flux will decline over time, due to apparent changes in membrane resistance due to CP and fouling. The decline in performance in this case is self-limiting, as a decline in flux results in a decline in foulant deposition. In constant flux processes, the flux is kept constant by adjusting the TMP applied. As the rate of foulant deposition is flux dependent, the decline in performance in a constant flux operation is self-accelerating, as more and more energy is required to maintain the same water output as fouling progresses.

1.4.3 Recovery

Recovery is the ratio of how much permeate is obtained from the system relative to the amount of feed water filtered. A RO membrane module has a recovery of about 7-12%. In a RO plant, usually 6 of these elemental membrane modules are arranged together linearly to from a RO vessel, and each vessel typically has a recovery of about 50%.[20] RO vessels are designed to maintain a balance between flux and operating costs.

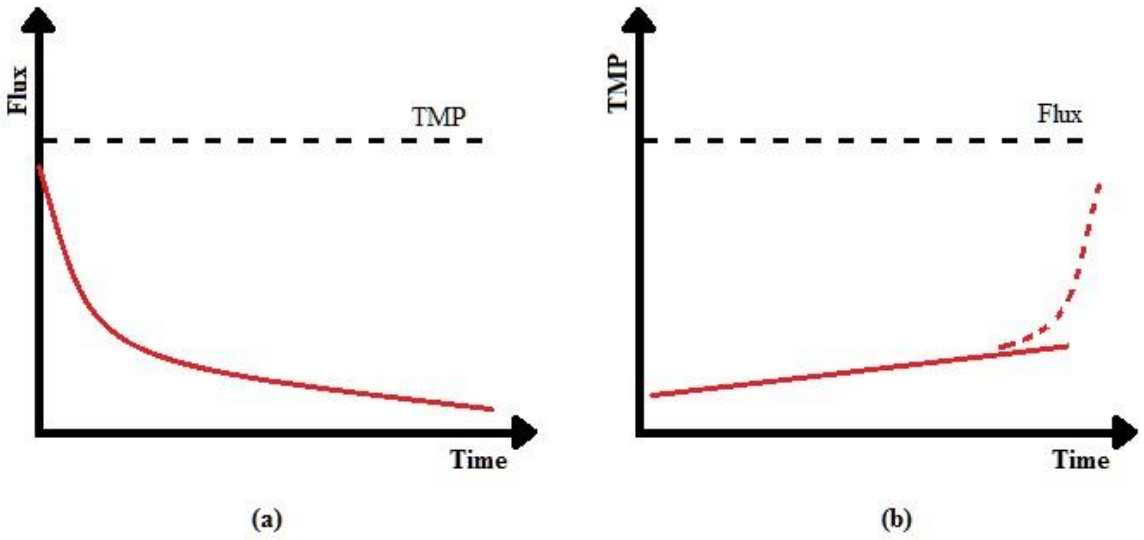

Figure 1.7 Schematic diagram of (a) flux profile in a constant TMP operation, and (b) TMP profile in a constant flux operation.

1.4.4 Rejection

Rejection is the ability to retain solutes in the feed side and is expressed as a percentage. For a given solute, the rejection is given by:

$$R_{int} = 1 - \frac{C_p}{C_m}$$

Typical RO membranes have salt rejection values of >95%.[21]

1.4.5 Molecular Weight Cut-Off (MWCO)

MWCO is a term to describe the pore size of a filtration membrane. The smaller the value of MWCO, the tighter the membrane pore size. A value of 100 means the membrane is capable of 90% rejection of a particle that has a molecular size of 100 Daltons. Most ultrafiltration membranes have molecular weight cut-off values up to 100,000 and even higher for nanofiltration and reverse osmosis membranes.

1.5 Challenges to the implementation of RO membranes for water purification

One issue faced in the implementation of RO in water purification is the cost involved, in terms of both capital and operational expenditure. Capital costs are more or less fixed as a result of the location, construction of the RO plant, the water pipelines and other infrastructure components. Operational costs include the form of energy required to drive the process, periodic cleaning of the system, and replacement of membrane modules when their performance decline beyond economical repair. Depending on the capacity of the plants and their standard operating protocols, membrane modules are replaced every 4-5 years after 11,303 - 39420 h of operating time at costs ranging between about 21,000 to 108,000 Euro.[22]

1.5.1 Concentration polarization (CP)

Concentration polarization is a physical phenomenon in which the concentration of solute or particle near the membrane surface is higher than that in the bulk solution. This phenomenon, inherent to all crossflow filtration processes, occurs as long as the membrane shows different permeability for the various components of the solution or suspension. The concentrated layer at the membrane surface that results increases the resistance of the filter and consequently reduces the permeate flux through the membrane. Concentration polarization is of considerable interest since a high permeate rate is most desirable in filtration processes.[23]

In reverse osmosis, where the solutes retained can have significant osmotic pressures, concentration polarization can result in osmotic pressures considerably higher than those represented by the bulk stream concentration (Figure 1.8). Higher feed pressures are required to overcome this increased osmotic pressure and produce reasonable flux.[24]

Concentration polarization is reversible and can be reduced through the decrease of flux or an increase in crossflow velocity, which reduces the boundary layer thickness or can be reversed by allowing for back-diffusive flow (achieved by closing the permeate outlet). If left unaddressed, CP can potentially lead to irreversible fouling (discussed below).

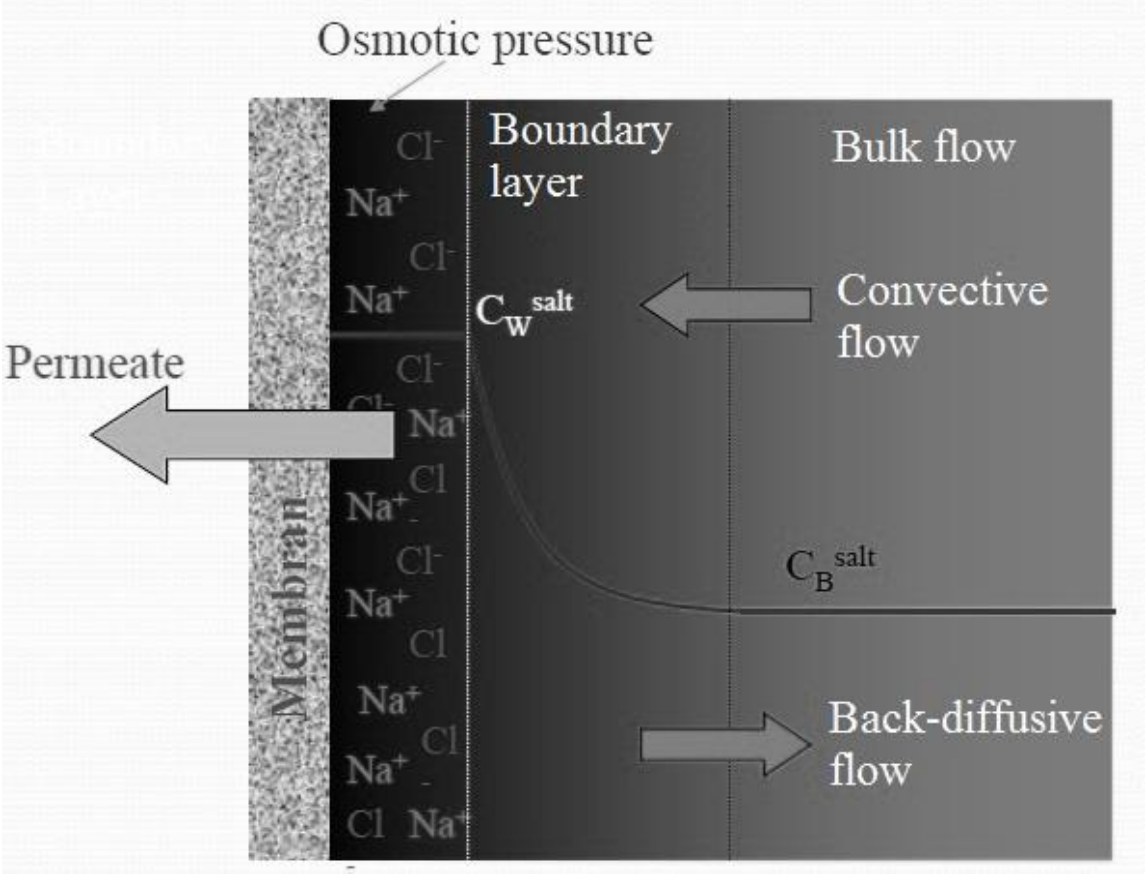

Figure 1.8 Illustration of concentration polarization of NaCl on membrane surface. Due to the direction of the convective flow, the salt ions accumulate at the surface of the membrane, resulting in a concentration C_W^{salt} at the boundary layer that is higher compared to the concentration in the bulk flow C_B^{salt}. [25]

1.5.2 Membrane fouling

Membrane fouling is the unwanted deposition of materials either on the surface of the membrane or into the membrane pores that results in a flux decline when a constant pressure is applied (constant pressure operation) or a TMP increase when a constant flux is maintained (constant flux operation). While concentration polarization is reversible, fouling is an accumulation of materials on the membrane surface, which may not be reversible. Sources of fouling include solid particles, inorganic ions, organic matter, colloids and microorganisms. Factors that escalate fouling includes the lack of pretreatment, insufficient fluid management in terms of the hydrodynamic environment, high flux and unsuitable membrane properties.[26] In this study, the focus is more on biofouling as it is currently of greater interest to industry and little is known about its mechanism of formation and how best it can be mediated, if not eradicated.

1.5.3 Biofouling

Biofouling is commonly defined as the undesirable deposition and growth of biofilms on surfaces. A biofilm is an aggregate of microbial cells that has associated irreversibly with a surface and embedded in a matrix of extracellular polymeric substances (EPS). Biofilms formation may occur on almost any surface, some of which include the tissues of living animals, ingrained medical devices, liquid water pipes, and aquatic systems and the details of biofilm formation and biofilm development has been reviewed extensively.[27-30]

Biofouling is a biofilm phenomenon [31] and in most biofilms, the microorganisms associated only account for less than one tenth of the dry mass, with the remaining biomass being comprised of the extracellular matrix that the organism produces and is embedded within. It consists of a assortment of different extracellular polymeric

substances (EPS) made of complex polysaccharides, proteins, DNA and other organics secreted by the bacterial cells, which provides the support for the biofilm and is also responsible for the cohesion and surface adhesion of the biofilm.[32] Water makes up the greatest fraction of the biofilm matrix by weight.[33] For example, biofilms have been shown to consist mainly >90% water, >50% organic content in dry mass, and $>10^6$ Colony Forming Units (CFU) cm^{-2} .[34] Biofouling is a costly problem as biofilms are common and ubiquitous.

Bacteria are able to switch between two different modes of survival: free moving, single cells (planktonic) and biofilms. Biofilms are often defined as a sessile microbial community characterized by adhesion to a solid surface and production of a matrix (the EPS), which surrounds the bacterial cells and includes extracellular polysaccharides, proteins and DNA. A variety of environmental and physiological cues regulates the transition from planktonic cells to biofilm growth, like bacterial cell density, nutrient availability and stress exposure.[35] The biofilm composition may vary greatly, depending on the kinds of microorganism involved, the composition of the raw water, the temperature and the hydrodynamic conditions.

In addition to the natural genetic program of biofilm formation, biofilm development may also be enhanced by a myriad of stress responses to enhance bacterial survival.[35] Some of these responses include oxidative stress responses, antibiotic stress responses, nutrient limitation and many more. Oxidative stress responses occur in many bacteria where certain genes are turned on to detoxify or evade the effects of reactive oxygen species such as peroxides and superoxides, which are byproducts of aerobic respiration in host immune cells.[36] For example, antibiotics that specifically target ribosomes [37] or nutrient limitation [38-40] also trigger specific genetic responses, which in some bacteria, leads to the formation of biofilms and in turn causes biofouling. Although antifouling

approaches, such as chlorination, oxidation and ultraviolet disinfection can partly control fouling, their effects are normally temporary and are not permanent as bacteria with the appropriate stress response will continue to thrive and proliferate and ultimately colonize all surfaces over time.[31]

1.6 Biofilm growth and development

The process of biofilm formation is thought to be a complex process, but generally, the biofilm forms through a series of stages, which while not present in all biofilm development cycles, are consistently observed across many bacterial species. Biofilm formation usually involves an attachment stage, where planktonic cells attaches onto a solid surface, before a growth stage where the bacterium multiplies and form microcolonies, and finally a detachment stage where the biofilm disperses to release cells back into the free-living stage (Figure 1.9).

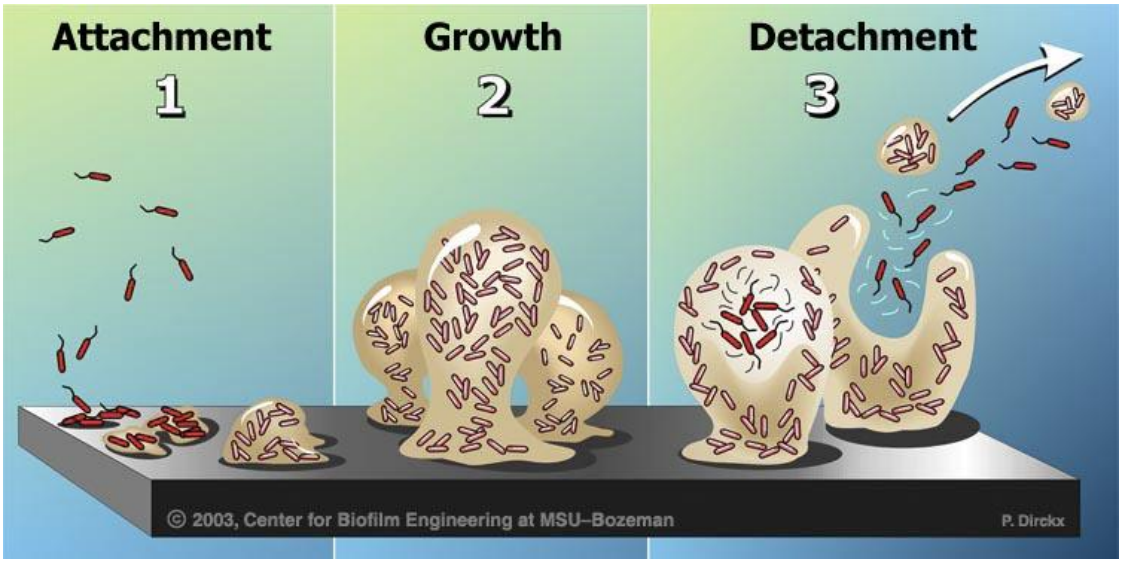

Figure 1.9 A typical biofilm life cycle involving three stages: Attachment, Growth, and Dispersal[41]

1.6.1 Biofilm life cycle

1.6.1.1 Attachment phase

Bacteria in the planktonic phase can attach to substrata that are either in pristine condition or surfaces that is covered with a conditioning film.[42] A conditioning film is defined as a layer of proteinaceous content that covers a surface and provides receptor sites for the adhesion of bacteria.[43] Microbial adhesion to surfaces which are pristine is mainly controlled by the macroscopic interactions such as surface charge and surface hydrophilicity, and this is a non-specific interaction.[44] In contrast, the deposition of microbes onto surfaces covered with conditioning film involves specific microscopic ligand – receptor interactions.[45]

1.6.1.2 Growth phase

Upon adhesion to the surface, bacteria will grow and multiply, forming colonies and producing EPS comprised of polysaccharides, proteins and other polymers that are sticky in nature. EPS further enhances the adhesive interaction and can assist the bacteria cells to anchor onto the surface.[46] EPS production and bacterial growth results in the formation of a thick biofilm layer, which increases its resistance to antimicrobials and environmental stresses.

1.6.1.3 Dispersal phase

Biofilm removal or sloughing can occur as a consequence of mechanical breakage of biofilms due to flow or shear stresses and is typically considered a passive process.[30] In contrast, the active escape of bacteria from the biofilm, called dispersal, is a genetically regulated process, which occurs in response to environmental cues, such as changes in nutrient availability,[47, 48] fluctuation in local oxygen concentrations [49] or increases in signals such as nitric oxide.[50] Dispersal is the last stage of biofilm development and

is essential for the survival of the biofilm bacteria where they may need to leave the biofilm in order to migrate to new sites to re-initiate the biofilm life cycle. Without this ability, the cells in the biofilm would effectively be trapped and would eventually die off due to the accumulation of waste products, or due to overcrowding and competition for resources.

1.6.2 Biofilm EPS formation and regulation

The biofilm EPS is composed of proteins, polysaccharides and nucleic acids, each performing a distinct role throughout biofilm formation.[51] The glucose-rich Pel and mannose-rich Psl polysaccharide were found to be required for formation of liquid-air interface pellicles and biofilms of *Pseudomonas aeruginosa*.[52] Extracellular DNA was discovered to be responsible in the initial attachment of bacterial cells as well as cell-to-cell interconnection and macrocolony formation.[53] A protein, CdrA, was found to crosslink the polysaccharide Psl and/or tether Psl to cell walls to stabilize the biofilm and extracellular matrix.[54] Biofilm bacteria have several advantages over single cells, including optimization of growth and survival, improved acquisition of nutrients and increased protection against stresses from the environment.[55] When a biofilm is formed, stress factors such as antibiotics and disinfectants diffuse through the biofilm matrix at a much retarded rate, allowing ample time for the bacteria to make adaptive responses such as the production of enzymes that can inactivate the antibiotic molecule.[56] Reduced growth rates of bacteria in the biofilm state also reduces the efficacy of growth-dependent antibiotics such as penicillin.[57] The presence of a subpopulation of persister cells, which are dormant antibiotic tolerant phenotypic variants, may also account for overall broad resistance in a biofilm.[58]

P. aeruginosa, a model gram negative biofilm-forming bacteria, is ubiquitous in water and soil and has been isolated from RO membranes biofilms originating from pre-treated

secondary effluents. This organism produces no less than three exopolysaccharides; alginate, Psl and Pel. Each polysaccharide has its own unique chemical structure and biosynthetic mechanisms, providing distinct physiological properties to the cells and biofilm matrix. The three polysaccharide types can be subdivided into two classes, capsular and aggregative. Alginate is a capsular polysaccharide, covering the exterior of one or more cells, whilst Pel and Psl are aggregative polysaccharides, providing structure and interacting with other matrix components.

Alginate is a high molecular weight acidic polysaccharide composed of non-repeating subunits α-L-guluronic acid and β-D-mannuronic acid.[59] Mucoid variants of *P. aeruginosa*, which over-produce alginate, have been isolated from lung tissues of patients suffering from chronic cystic fibrosis (CF).[60] Due to its association with chronic pulmonary infections, the biosynthetic pathway of alginate is the best characterized of the three polysaccharides. However, recent studies have shown that alginate is not responsible for the initial stage of biofilm formation by non-mucoid strains of *P. aeruginosa*, which represent the majority of clinical and environmental isolates. Instead, these bacteria primarily utilize the aggregative polysaccharides, Psl and Pel, for biofilm development.

Psl contains D-glucose, D-mannose, and L-rhamnose [61] and plays an important role in the initial attachment of sessile cells to both abiotic and biotic substrates.[62-65] Psl also has a role in biofilm development beyond just surface attachment, facilitating structural stability and architecture in mature biofilms.[66] It was suggested that Pel polysaccharide is rich in glucose based on initial carbohydrate analysis even though the definite structure remains largely unknown.[67, 68] Pel plays an essential role in the initiation and maintenance of cell-cell interactions, providing the community with structural support.[69]

1.6.3 Quorum sensing regulation

Biofilm formation is highly regulated in bacteria and the regulatory systems controlling biofilm development are of great interest as they are target sites for novel anti-biofilm strategies. One such regulatory system is quorum sensing (QS), which controls gene expression in response to cell-population density fluctuations. **B**acteria that exhibit quorum sensing produce and release signaling molecules known as autoinducers that increase in concentration as cell density increases. When a minimal threshold stimulatory concentration of an autoinducer is detected, gene expression becomes altered. QS is a mechanism in which gene expression in bacteria is controlled according to their local population density[70] or local diffusion limitations.[71, 72]

One of the best understood QS systems is the N-acylhomoserine lactone (AHL) signaling system, found primarily in gram-negative bacteria such as *P. aeruginosa* [73] and *Vibrio fischeri*.[74] Different Gram-negative bacteria produce and utilize different AHL molecules, and the basic structure of the AHL signal molecule family consists of a homoserine lactone functional group covalently linked to a N-acyl chain ranging in size from 4-14 carbons and which may be unsaturated or saturated and may or may not contain a hydroxy- or oxo-group at the 3-carbon position (Figure 1.10).

The basic QS gene circuit is comprised of an autoinducer synthase and receptor protein that can bind to the autoinducer molecules and alter gene expression directly or indirectly. The production of autoinducer molecules generally increases with an increase in bacterial cell densities. Most signals are produced intracellularly and are subsequently secreted in the extracellular environment, where they accumulate to a threshold concentration and subsequently binding to membrane bound receptors. In QS systems that use AHLs, the autoinducer synthase is a LuxI protein, and the receptor is a LuxR protein (Figure 1.11). QS in *P. aeruginosa* is regulated by two QS systems, *las* and *rhl*.[75] The *las* system is

comprised of the transcription activator LasR and the autoinducer (AI) synthase enzyme LasI, which controls synthesis of the signal molecule N-(3-oxododecanoyl) homoserine lactone (3-Oxo-C12- HSL). Similarly, the *rhl* system is comprised of the transcription activator RhlR and the RhlI AI synthase that synthesizes N-butyryl homoserine lactone (C4-HSL). It was also found that the LasR transcriptional activator also regulates the *rhl* system.

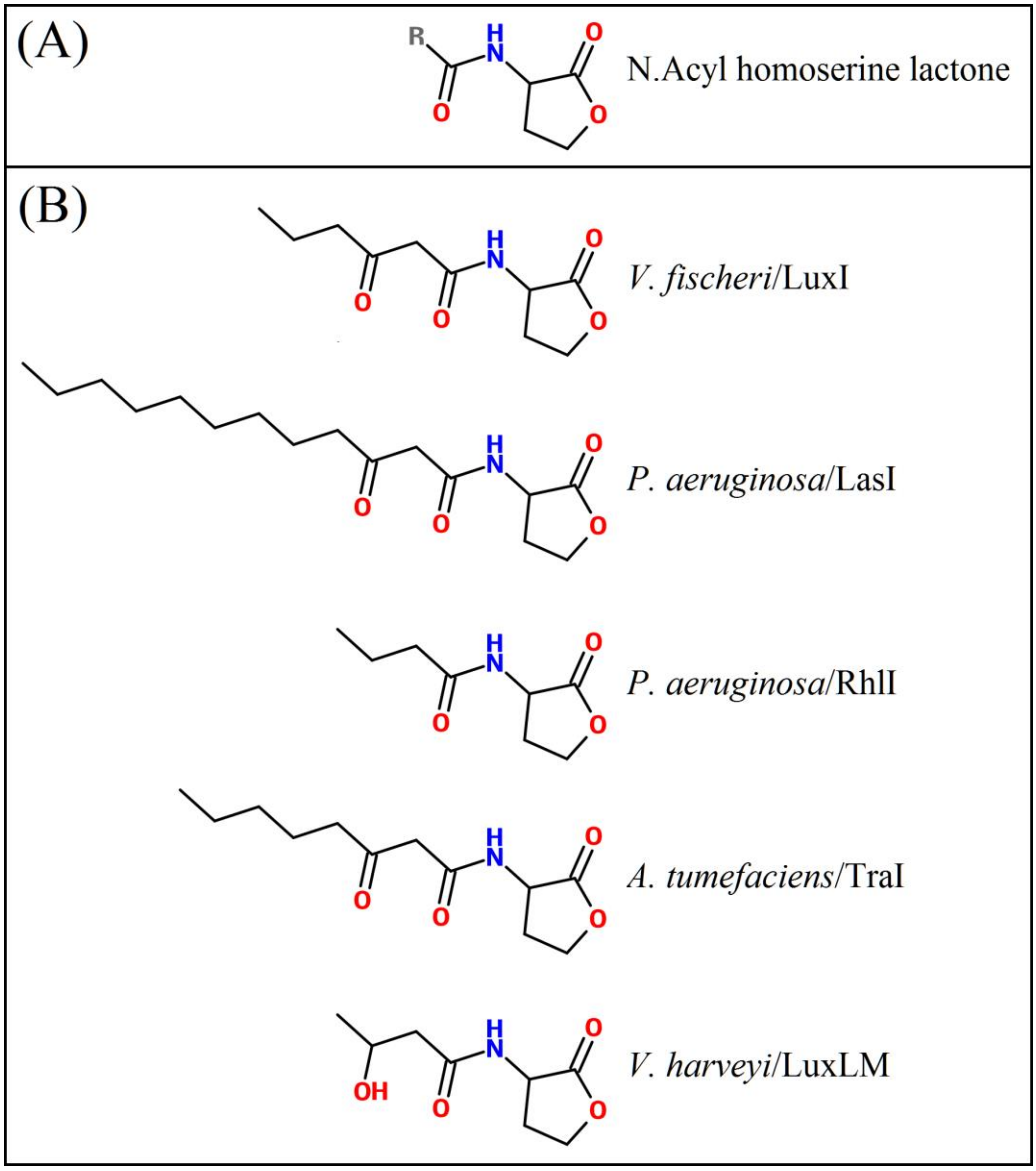

Figure 1.10 (A) General chemical structure of an AHL molecule, consisting of a homoserine lactone moiety adjoined with a N-acyl side chain. (B) Representative acyl-homoserine lactones used by Gram-negative bacteria and the associated genes that are responsible for the synthesis of the signals.[76-80]

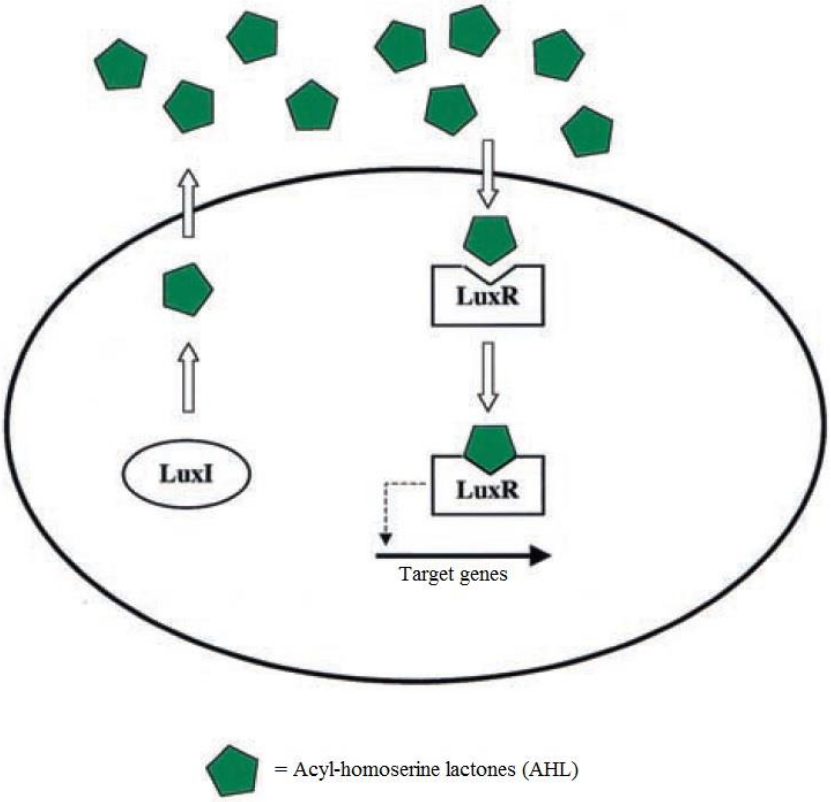

Figure 1.11 The LuxI/LuxR QS system of Gram-negative bacteria, regulated by two regulatory proteins. LuxI proteins are autoinducer synthases and they catalyze the formation of autoinducer molecules, in the case a specific acyl-homoserine lactone molecule, which diffuses out of the cell. Once the autoinducer molecules accumulate as a result of high cell density and signal production, the LuxR proteins will bind to these autoinducers to form a complex that will in turn bind to specific genes and activate transcription.[70, 74, 81]

QS plays an important role in the formation of bacterial biofilms. Studies have shown that in *P. aeruginosa* biofilm formation, strains that are deficient in the production of 3-oxo-C12-HSL, the *las* signal molecule, formed very thin, unstructured biofilms compared to the wild-type strain.[82] Biofilms from a *rhlI* mutant did not differ much from the wild-type and closely resembled the parent biofilm. These results suggest that the *las*, but not the *rhl*, QS system is critical in the *P. aeruginosa* biofilm formation.

1.6.4 Multi-species biofilms and synergistic interactions

While most studies focus on single species biofilms, naturally occurring biofilms are not normally formed by a single bacteria species. Nearly all biofilms in nature are comprised of a wide variety of microorganisms and communication among community members can facilitate biofilm development. For example, it was found that in the lungs of patients suffering from cystic fibrosis, at least two pathogens *P. aeruginosa* and *Burkholderia cepacia* can form mixed biofilms and both employ AHL-based QS systems to direct the expression of genes coding for virulence factors as well as biofilm formation.[83-85] When *B. cepacia* was grown with a *P. aeruginosa* that produces AHL, mixed biofilms were formed and *B. cepacia* was capable of recognizing the AHL signals produced by *P. aeruginosa*. When *B. cepacia* was grown with a mutant *P. aeruginosa* strain that could not produce AHL, separate microcolonies were formed.[86] This indicates that AHL-based signaling can influence the architecture of mixed community biofilms.

The close proximity and complex interactions within biofilms underlie both synergistic and antagonistic behaviors in that species within a biofilm can compete for resources or coordinate to better utilize nutrients or withstand harsh conditions.[87] Mixed biofilms were found to confer enhanced tolerance to antimicrobial treatments as compared to single species biofilms [88], by altering the components of the EPS matrix.[32] There is a need for a better understanding of the interactions and dynamics within these mixed communities, which is necessary to successfully prevent or deal with biofouling issues involving mixed biofilms.

Both the attachment of bacterial cells as well as the production of EPS contribute to performance declines in membrane-based processes. Bacterial cells bound to the membrane can impede the back diffusion of salt resulting in salt concentration polarization and an increased osmotic pressure on the surface of the membrane, and

therefore an increase in salt passage as well as permeate flux decrease leading to lower salt rejection and lower permeate quality. EPS contributes to the hydraulic resistance to permeate flow as well as an increase in biofilm-enhanced osmotic pressure [89, 90], resulting in lower salt rejection and lower permeate flux. Because of their prevalence and negative impact on RO operation, it is important to develop strategies to control biofouling.

1.7 Traditional Biofilm Control Methods

1.7.1 Chlorination

Chlorine acts as a biocide by directly disrupting bacterial cell membrane integrity or by damaging nucleic acids and enzymes via oxidation.[91] Although this method is effective in killing bacteria and thus preventing biofilm formation, the toxicity of chlorine and its by-products has prevented its widespread use in the RO industry.[92] Furthermore, chlorine causes damage to membranes and shortens the lifespan of the membranes, resulting in the need to replace membrane modules, which equates to higher operating costs.[93]

1.7.2 Ozonation

Ozone has been commonly used as a disinfecting agent for portable water treatment because of its strong oxidation potential and production of fewer halogenated by-products during disinfection than chlorine. However, as a consequence of its strong oxidizing abilities, it is known to rapidly degrade membrane surfaces [94] as well as breakdown larger molecular weight organic matter into easily assimilated forms that actually favor the growth of microorganisms.[95] By altering the water chemistry and thus the selection pressure, bacteria species that survive the ozone treatment can metabolize this, resulting

in the faster build-up of biofilms on membrane surfaces [96] and thus limiting the efficacy of ozonation in membrane-based processes.

The expenses incurred associated with the implementation of ozone disinfection systems varies depending on the manufacturer, the location, plant capacity, and the nature of the wastewater to be treated. Ozonation costs are generally high compared to other disinfection methods. For example, in two representative plants in the city of Indianapolis, each operating at 125 million gallons per day (mgd), each of the ozone disinfection systems accounts for about 8% of the total construction cost of each plant, while the Operation and Maintenance (O&M) of each ozone system cost approximately 1.9% and 3.7% respectively of the total O&M costs in each plant.[97]

O&M expenses and initial capital costs largely determine the overall cost of an ozone disinfection system. The annual costs of operating ozone based disinfection include, and is not limited to, energy usage, miscellaneous equipment repairs, supplies, and manpower requirements. Another cost consideration is that each ozonation system is site specific, and is dependent on the effluent limitations of the plant.[98]

1.7.3 Ultraviolet (UV) disinfection

UV disinfection involves exposure of water samples to UV radiation emitted from a mercury vapor arc lamp. UV performs well against bacteria and viruses by causing thymine dimerization, preventing DNA replication and effectively inactivates microorganisms.[95] However, bacteria in particles or flocs may 'shade' other bacteria inside the particle and prevent UV radiation from reaching bacteria inside the particle [99]. Like ozone, UV disinfection is able to destroy microbes in the water without leaving behind residues. However, when applied to the control of biofilms this characteristic can be a disadvantage as unlike chemical oxidants, UV disinfection leaves no residual and

there is no downstream protection against microbial growth once the treated water leaves the UV unit. Any viable bacteria that survive the UV process will then be free to grow and foul equipment downstream including the RO membranes. This technology is not only capital intensive and requires high amount of energy, it has also been shown to have reduced efficiency against biofilm bacteria compared to planktonic bacteria. These limitations with traditional biofouling control methods have lead to the need to develop novel anti-biofouling strategies. By understanding the biofilm life cycle, strategies have been developed to mimic the natural process of biofilm dispersal.

1.8 Alternative strategies - Quorum sensing antagonism

By interfering with the QS pathway, biofilm production can be reduced or prevented. Inhibition of QS could be done by inhibiting the production of signal molecules, degradation of the signaling molecules once they are produced, or the introduction of structurally-similar analogs to block the cognate signal from binding to the receptor protein. Compounds such as halogenated furanones [100] were found to be able to disrupt biofilm development without being biocidal, by binding to the LuxR proteins and destabilizing them, causing them to be unable to activate transcription of QS-related genes.

Nitric Oxide (NO), a water soluble free radical, was found to be a signaling molecule involved in many cellular processes in eukaryotes such as cell differentiation, apoptosis and proliferation.[101] It was also found to be involved in biofilm development and dispersal. At low, non-toxic concentrations, NO was found to act as signaling molecules to induce biofilm dispersal in *P. aeruginosa*.[102] Soluble compounds that release NO in aqueous solution, called NO donors, can be used to deliver NO to bacterial biofilms and to induce biofilm dispersal.

NO induces biofilm dispersal by stimulating phosphodiesterase activity, which results in the degradation of cyclic di-guanylate monophosphate (c-di-GMP), culminating in changes to gene expression that favour the planktonic mode of growth [103]. NO, which has a short half-life in aqueous environments can be delivered to biofilms by using chemical compounds that generate NO in solution. One such NO donor compound, sodium nitroprusside (SNP) was shown to disperse biofilms of the model organism *P. aeruginosa*, as well as other bacterial species, and mixed species biofilms at low, non-toxic concentrations [50, 102]. A recent study investigated the biofilm dispersal potential of three NO donor compounds (MAHMA NONOate, SNP and PROLI NONOate) using *P. aeruginosa* PAO1 as a model organism.[104]

1.9 RO Biofouling Monitors

Traditionally, a membrane is considered to be fouled when there is an irreversible exponential increase in TMP in a constant flux operation. Cleaning or backwashing procedures when applied at this point yield minimal membrane performance recovery. However, if membrane cleaning occurs before this point, it is possible to increase the recovery and therefore, there is great interest in the use of non-invasive fouling detection methods to detect fouling or biofouling even before the onset of TMP rise.

Fouling monitors can be categorized by optical methods or non-optical methods. Optical methods can provide real-time information and can be very sensitive. However, optical methods require the use of special membrane modules with an optical window for direct observation, and this design may not be feasible for RO processes due to its high pressure requirements. Optical resolution is also limited to a few hundred nanometers due to the wavelengths of visible light, and are unsuitable to visualize opaque samples or samples that are too concentrated. Non-optical, non-invasive methods such as Ultrasonic Time-Domain Reflectometry (UTDR) and Electrochemical Impedance Spectroscopy (EIS)

makes uses of non-optical properties such as acoustics and dielectric behaviors and can potentially overcome the limitations of optical methods.

1.9.1 Ultrasonic Time-Domain Reflectometry

In UTDR, an ultrasonic wave is generated and propagates through various media via compressions and rarefactions and this property can provide spatial information on the physical characteristics of the media through which it travels. Its velocity *c* is dependent of the property of the material through which the ultrasonic wave is being transmitted, with *c* increasing with increasing density, ρ, of the material. When the wave encounters an interface between two media, transmission, reflection, and phase change can occur. The magnitude of the reflected and transmitted waves is a function of the difference between the acoustic impedances of the media, Z_2 - Z_1, where $Z_i = \rho_i c_i$ and the subscripts 1 and 2 refers to the medium from which and into which the wave is propagating respectively. The amplitude *A* of the reflected wave relative to its incident wave perpendicular to an interface is given by [105]:

$$A = \frac{Z_2 - Z_1}{Z_2 + Z_1}$$

The time required t for a wave to propagate from a reflecting interface is a function of the distance between the transducer and the reflecting interface, Δd, and the velocity c and is given by:

$$t = \frac{2\Delta d}{c}$$

Figure 1.12 shows the principles of UTDR and how the different interfaces within the membrane cell reflect the acoustic signals differently, resulting in a characteristic amplitude profile against signal arrival time.

Since reflection A is unchanged and is used as a stationary point of reference, the time of arrival of peaks B and C can be used to establish the thickness of a fouling layer or the extent of membrane compaction. By superimposing the waveforms, the difference between the test and reference waveforms can be compared with a suitable software and signal analysis; UTDR resolution for the measurement of foulant thickness is dependent on the frequency of the transducer used and is typically between 100 - 750 nm.[106]

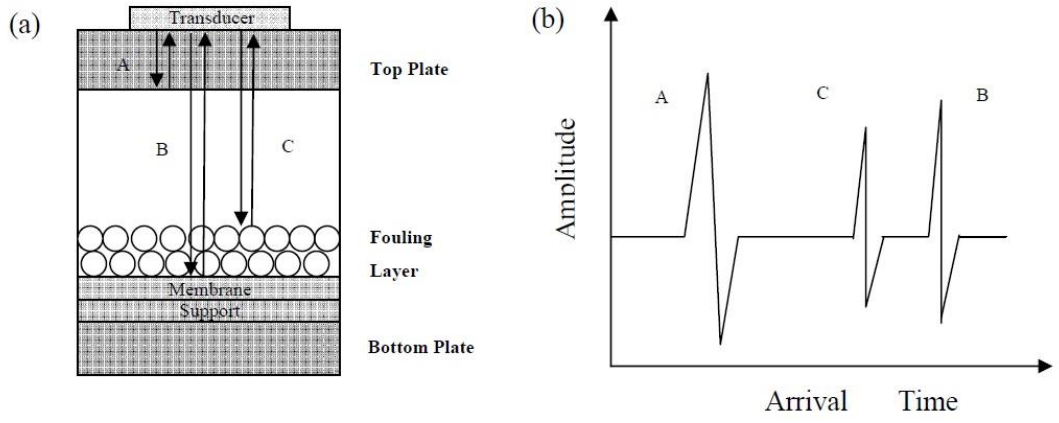

Figure 1.12 (a) Schematic diagram of the principle of UTDR measurement in a flat-sheet membrane module and (b) corresponding amplitude-time profile for such a configuration.

In order to employ UTDR to detect and monitor biofouling in real-time non-invasively, it is mandatory to increase the difference in acoustic impedance at the biofilm/water and membrane/biofilm interfaces as the presence of the biofilm layer on its own does not translate into a significant difference in acoustic impedance. This ‘acoustic enhancer’ should not interfere with the biofilm development nor should they compromise the RO process. Previous studies [107] have shown that colloidal silica can be used as acoustic enhancers for UTDR and its introduction is neither toxic nor affects biofilm development and has a negligible impact on RO performance.

1.9.2 Electrochemical Impedance Spectroscopy

The working principle of EIS revolves around the step-wise application of sinusoidal alternating current at a range of known frequencies into a system. Using digital techniques, the corresponding current and voltage magnitudes across the sample at each frequency, including the phase difference between each current–voltage pair, were measured. From this, the conductance and capacitance of the system can be deduced at each frequency. EIS is widely used to investigate processes and performance in dye-sensitized solar cells [108], to study corrosion in coatings and surfaces [109], and also in the field of biosensing.[110] For an RO system, changes in the capacitance and conductance dispersion with frequency provides a way of monitoring, in situ and in real time, the accumulation of particles that could potentially foul the membrane.

The electrical impedance, Z, is a complex quantity and is related to its real and imaginary parts, Z_{real} and Z_{img}, by the equation

$$Z = Z_{real} - iZ_{img}$$

Where Z_{real} and Z_{img} are related to the angular frequency ω, capacitance C and conductance G by the equations

$$Z_{real}(\omega) = G/(G^2+C^2\omega^2)$$

$$Z_{img}(\omega) = C\omega/(G^2+C^2\omega^2)$$

Therefore,

$$Z(\omega) = G/(G^2+C^2\omega^2) - iC\omega/(G^2+C^2\omega^2)$$

Graphically, the impedance data are presented on a complex plane Z*(w) known as a Nyquist plot. For a first-order system, the Nyquist plot can be described by

$$(Z_{real} - \frac{1}{2G})^2 + Z_{img}^2 = (\frac{1}{2G})^2$$

By measuring the EIS spectrum at the membrane surface, the derived Nyquist plot can provides a fingerprint of the foulant deposition layer as the membrane fouls in real time.

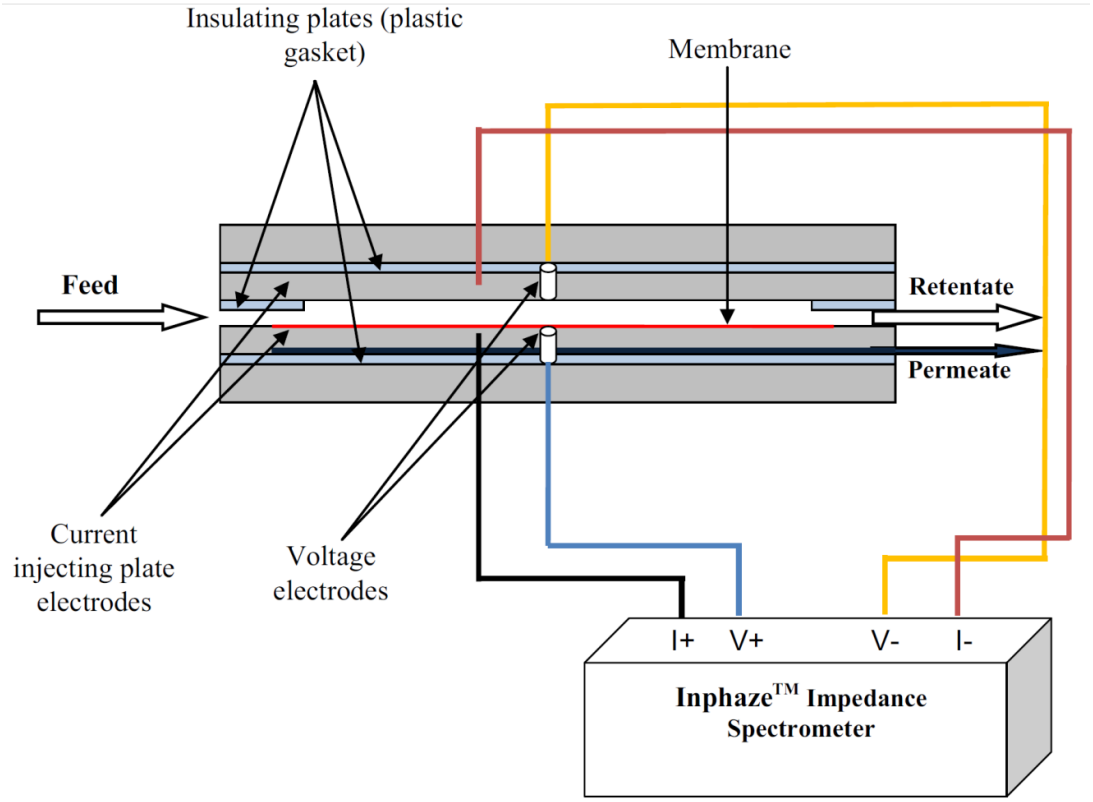

Figure 1.13 Cross sectional schematic view of a RO crossflow flat sheet module fitted with the current and voltage electrodes and connected to a impedance spectrometer.[111]

1.10 Problem Statement, Aims and Objectives

While reverse osmosis is well suited to generate potable water, it is not a perfect solution and faces several limitations. One of the least understood among these problems is biofouling. Membrane biofouling is a big challenge faced by the water industry and can cause advanced filtration technologies such as RO processes to be excessively costly. The

expenses associated with the problem of biofouling in water treatment plants is a combination of the following factors: plant performance deterioration, damage in the plant construction materials, decline in the quantity and quality of the product, the need for extensive cleaning, biocides addition, the need of additional processes such as using antifouling chemicals to treat the contaminated water, manpower costs involved in membrane cleaning or replacement and costs associated with the plant down-time.[42] The problem with current RO process management is the lack of appropriate approaches to a) detect membrane biofouling early, which can inform operators of when to take specific action and b) novel, non-toxic approaches to control fouling once it becomes a problem. Therefore, the goal of the undertaken in this thesis was to develop an understanding of the key processes in biofilm development as it relates to biofouling of membranes and loss of performance, to then test and validate the application of nitric oxide as a strategy to mitigate biofilm development and fouling, and to develop new tools for use as on line monitoring systems to aid in the decision process for when to implement fouling control measures. To achieve this, the thesis is divided into three, interlinked chapters.

Chapter 2 investigates the effects of bacterial biofilms on membrane biofouling, specifically the roles that different extracellular polysaccharides play were investigated.

Chapter 3 demonstrates the effect of nitric oxide donor compounds on bacterial biofilm growth and dispersal, their effects on membrane biofouling, and influence in biofilm community diversity were investigated.

Chapter 4 describes a canary cell approach to model biofouling in spiral wound RO modules was developed. Non-invasive in situ methods such as ultrasonic time domain reflectometry (UTDR) and electrochemical impedance spectroscopy (EIS) were also developed to complement traditional offline analysis in monitoring membrane biofouling.

In addition to developing and validating biofouling monitoring strategies, this thesis chapter also combines the application of the monitoring approach of xxx with NO treatment to show dispersal of the biofilm in real time.

Chapter 5 concludes this thesis with suggestions and recommendations for future work.

CHAPTER 2 THE ROLES OF BIOFILM MATRIX POLYSACCHARIDES IN RO BIOFOULING

2.1 Introduction

Membrane fouling due at least in part to the formation of bacterial biofilms on membrane surfaces remains a key challenge for membrane-based water purification systems.[112-114] Biofilm formation on membrane surfaces results in severe flux decline, increased transmembrane pressure (TMP), higher energy consumption and a faster rate of deterioration of system performance and production.[113-115] Extracellular polymeric substances (EPS) produced by microbial biofilms have been suggested to be the predominant cause of biofouling of water treatment membranes.[28, 89, 90, 116, 117] Therefore, understanding the importance of specific exopolysaccharides within the EPS matrix that contribute to biofouling may help in the development of new strategies for its prevention and control.

Pseudomonas aeruginosa has been shown to make at least three polysaccharides as part of the biofilm matrix, Psl, Pel and alginate. Depending on the strain studied, the roles of Psl and Pel, two important exopolysaccharides, in biofilm formation can vary drastically.[51, 118, 119] For example, *P. aeruginosa* PA14 and *P. aeruginosa* PAO1 differ in the primary polysaccharide used in the development of the biofilm. PAO1 relies primarily on Psl, while PA14 requires Pel production for mature biofilm development. Collectively these studies suggest that Pel and Psl are each capable of functioning as a structural adhesion involved in maintaining the integrity of the biofilm. When both *psl* and *pel* are intact, it appears that Psl is the predominant polysaccharide for *P. aeruginosa* PAO1, while Pel has only limited impact on single species biofilm phenotypes.[119] However, in another study, it was found that in the absence of Psl, Pel expressing biofilm were more viscous, which aids in expansion and spreading of the biofilm matrix. Pel-

based biofilms also facilitated integration with other species such as *Staphylococcus aureus* to form mixed biofilms whereas Psl-based biofilms favour monospecies biofilms.[120] It has been shown that Psl plays a critical and essential role in surface attachment in a range of clinical and environmental *P. aeruginosa* isolates, while Pel was not as important as an attachment determinant.[119] However, there was significant variability between strains in the contribution of Pel and Psl to mature biofilm structure.

Ghafoor *et al.* (2011) showed that Pel production in PAO1 is higher in the absence of Psl.[118] This raised the possibility that there can be cross regulation of polysaccharide operons or that there can be competition for precursors that account for limited production of individual polysaccharides.[67] The latter had been previously proposed to affect the production of other polysaccharides such as alginate. Colvin *et al.* (2012) demonstrated that elevated Pel expression in a mutant *psl* strain after extended cultivation could actually compensate for the loss of Psl, suggesting that an advantage of retaining the capability of producing multiple biofilm matrix polysaccharides is to reduce the impact of deleterious mutations on an important functions such as biofilm formation. Another hypothesis is that having the potential to secrete three different polymers with varying physicochemical properties may provide *P. aeruginosa* with the flexibility to survive in different niches.[121] Thus, depending on the environment, different polysaccharides might be employed as the primary matrix support.

Due to the negative impact of biofilms on the performance of RO membranes and processes, there is a need to develop strategies and countermeasures which are novel and more importantly non-toxic to control and/or prevent biofouling. Recent studies have demonstrated the possibility of using signaling molecules such as nitric oxide (NO) to induce the transition from biofilm growth mode to planktonic growth mode in some bacteria, thereby dispersing the biofilm. However, the presence or absence of biofilm

exopolysaccharides and its role in NO induced dispersal has not been extensively investigated. As biofilm dispersal is dependent on the ability of the bacteria cells to escape the biofilm matrix, differences in biofilm EPS composition would affect the mechanism or rate of dispersal. Understanding the roles that specific exopolysaccharides play in biofilm development, especially on the surfaces of water treatment membranes, is of importance in developing new methods and strategies to control biofouling in membrane processes. The aim of this chapter was to investigate the roles of Psl, Pel and alginate during biofilm development of PAO1 in a RO membrane system and how they influence the TMP and biofouling of RO processes.

2.2 Materials and Methods

2.2.1 Preparation of bacteria strains and mutants

P. aeruginosa PAO1 wild type and 4 mutants, each differing in its capacity to produce specific exopolysaccharides, were studied. The mutants PAO1Δ*alg8*Δ*psl*A, PAO1Δ*pelF*Δ*pslA*, PAO1Δ*alg8*Δ*pelF*, and the PAO1 isogenic alginate-overproducing MucA-negative mutant, PDO300, were kindly provided by Professor Bernd Rehm, Massey University, New Zealand. Full details of the construction of these mutants have been previously published.[118] A short summary of the polysaccharide-producing ability of each mutant can be found in Table 2.1. The fouling potential of the wild-type PAO1 on RO membranes was compared to the four polysaccharide mutants (PAO1Δ*alg*Δ*psl*, PAO1Δ*pel*Δ*psl*, PAO1Δ*alg*Δ*pel* and PDO300) to determine their relative tendency to foul. The bacteria were grown overnight in a 750 ml solution of 5 g l^{-1} Nutrient Broth (NB; Difco) and 0.034 M NaCl at 30^{o}C with shaking at 200 rpm. The bacterial cells were subsequently harvested by centrifugation at 18,514 *g* for 10 min. The pellet was washed and resuspended in sterile PBS to an OD_{600} of 0.1. The bacterial suspension was introduced into the RO system prior to the RO membrane cells to foul the membranes.

Table 2.1 Bacterial strains used in this study and their corresponding polysaccharide production capability.

P. aeruginosa **bacteria strain**	**Polysaccharide production**	**Reference or origin**
PA01	Alg(+)* Psl(+) Pel (+)	ATCC® BAA-47™
PA01Δ*alg*Δ*psl*	Alg(-) Psl(-) Pel (+)	Rehm [118]
PA01Δ*pel*Δ*psl*	Alg(+) Psl(-) Pel (-)	Rehm [118]
PA01Δ*alg*Δ*pel*	Alg(-) Psl(+) Pel (-)	Rehm [118]
PDO300	Alg(++) Psl(+) Pel (+)	Rehm [118]

*(+) represents normal production, (-) represents stunted production, (++) represents over-production.

2.2.2 Reverse Osmosis experimental setup

The RO system consisted of two identical RO cells running independently, with separate feed tanks (Figure 2.1). Each RO cell was made of stainless steel with plate geometry and flow channel of 150 x 30 x 0.8 mm with a net membrane surface area of 0.0045 m^2.

Using a centrifugal pump (Hydra-Cell, F21EASGSFEHG), the feed solution was pumped from a 10 l feed tank to the RO cell. The feed solution temperature was controlled at 23 ± 0.1^oC with a chiller (PolyScience). Pressure from the feed stream and cross-flow rates were adjusted by the use of pressure relief valves (Swagelok) and metering valves (Swagelok), respectively. Both the feed and permeate stream pressures were monitored by the use of pressure gauges (Ashcroft). The volumetric flow rate was monitored with a turbine flow meter (WF Waterflo) and the conductivity was measured using a conductivity meter (Thermo Scientific, model Alpha COND 500). Mass flow controllers (Brooks Instrument, model 5882/D1A1C3B001) were used to regulate the amount of permeate withdrawn in the permeate stream. The bacterial solution was introduced into the RO system before the RO membrane cell via a metering pump (ELDEX, model 5979-

OptosPump 2HM). Microfilters (5 μm and 0.2 μm) were installed on return and bypass flow of each RO cell, to prevent contamination of the feed tank by bacteria and essentially making the feed tank an active bioreactor.

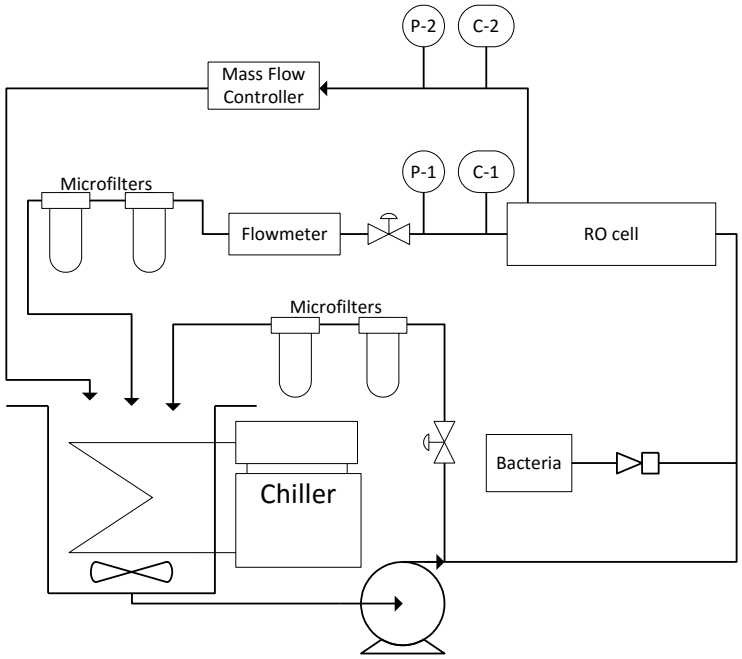

Figure 2.1 Schematic diagram of RO system used in this study. Feed water was pumped to the RO cell and both the retentate and permeate streams were channeled back to the feed tank to be recycled. Bacteria solution was injected into the system right before the RO cell and was filtered off by microfilters before the feed was recycled. TMP and salt concentrations were monitored by pressure gauges (P-1 and P-2) and conductivity meters (C-1 and C-2). Flux and flow rates were controlled by the mass flow controllers and the flow control valves.

2.2.3 RO biofouling experiments

RO membranes (TW-30, DOW Filmtec) were cut to size (3 cm × 15 cm) and soaked in MilliQ water overnight. The membranes were then soaked in 70% ethanol (Merck) for 1.5 h for sterilization followed by rinsing with MilliQ deionised water. The membranes were compacted at a flux of 60 l m^{-2} h^{-1} (LMH) overnight with MilliQ water to stabilize the flux, which was monitored using mass flow controller (model 5882, Brooks Instrument).

Following compaction, the flux was set to 30 LMH and a NaCl stock solution (200 g l^{-1}) was added to the feed tank to a final concentration of 2 g l^{-1}. The solution was left to mix for 1.5 h before a stock NB solution (8 g l^{-1}) was added to the feed tank to a final average background concentration of 24 mg l^{-1} NB, which translates to a TOC concentration of approximately 7.8 ml l^{-1}. The RO feed was left to mix for a further 1.5 h prior to the start of the experiment. The feed solution was replenished twice daily and the TOC was tested with a TOC analyser (Shimadzu, Model TOC-VWS) to ensure that the concentration of nutrients remained equal in each parallel unit. The RO system was operated in a closed loop where the retentate and permeate streams were reintroduced into the feed tank. Experiments were initiated by the start of continuous introduction of the bacterial suspension into the system at a dilution ratio of 1:800, giving an input load of 10^5 CFU ml^{-1}. The bacterial solution was replaced every 48 h to ensure bacteria viability. Experiments were done using constant flux (30 LMH) and the TMP continuously monitored. Fouling was defined here as the increase of TMP with time during the filtration process at constant flux. Therefore, a higher TMP within the same time frame or the same TMP within shorter time frame represents more severe fouling.

2.2.4 Membrane autopsy

The fouled membranes were removed from the RO modules for examination at the conclusion of the experiment and 1.5 cm was removed from each end of the membrane while the remainder was aseptically cut into 8 segments. Six segments (1 × 3 cm) of membrane covering the inlet, middle and outlet of the RO cell were analysed by fluorescence staining and CLSM observation to quantify the live and dead cells and the polysaccharide volume (representative of EPS). For the remaining two segments (3 × 3 cm), viable bacterial counts were determined as were the concentrations of polysaccharide and protein extracted from the membrane surface.

2.2.4.1 Fluorescent staining and CLSM

Segments of membrane were washed and stained using the LIVE/DEAD BacLight bacterial viability kit (Invitrogen) as per the manufacturer's instructions. The membranes were then washed again in 0.85% NaCl to remove excess stain. Live cells stained by SYTO-9 and dead cells stained by propidium iodide (PI) were visualized by confocal laser scanning microscopy (CLSM) (Nikon eclipse 90i, part of the A1R hybrid confocal spectral imaging system) at a magnification of ×200, with an argon laser (488 nm excitation for SYTO-9) and a diode laser (561 nm excitation for PI). For each section, z stack (3D) confocal images were obtained from 5 locations covering the membrane surface, and the average biovolume (μm^3) and surface coverage (%) was calculated using IMARIS (Bitplane, version 7.3.1). Biofilms were gently washed in 0.85% NaCl solution and for each slide, z stack (3D) confocal images were acquired from 9 different locations covering the membrane, and the average biovolume (μm^3) was calculated using IMARIS (Bitplane, version 7.3.1).

2.2.4.2 Viable bacterial counts

Using a cell scraper, the biofilm was removed from each 3 × 3 cm segment of membrane and resuspended in individual tubes containing 3 ml sterile PBS and vortexed for 30 s. Viable heterotrophic counts were determined using a modified Miles and Misra method (Miles & Misra 1938). In brief, three 10 µl drops of 10^{-1} to 10^{-6} dilutions were pipetted onto nutrient agar and incubated at ambient room temperature overnight before counting. Viable cells were expressed as colony forming units (CFUs) cm^{-2} of membrane.

2.2.4.3 EPS extraction and quantification

The remaining bacterial suspension was centrifuged at 18,514 *g* for 10 min and the supernatant transferred to a clean centrifuge tube for analysis of the soluble EPS fraction.

The bound EPS was extracted by adding 2 ml 8.5 g l^{-1} NaCl and 12 µl of 37% formaldehyde (Sigma) to the bacterial pellet, the suspension was vortexed and incubated at 4°C for 1 h. After incubation, 2 ml of 40 g l^{-1} NaOH and 0.5 ml MQ water were added, the solution was vortexed and incubated at 4°C for 3.5 h. Subsequently, the bacterial suspension was centrifuged at 18,514 *g* at 4°C for 20 min, and the supernatant was transferred to a clean centrifuge tube. Using the phenol-H_2SO_4 method[122], the polysaccharide content of the EPS was measured. Briefly, 0.5 ml of 50 g l^{-1} phenol (Sigma-Aldrich) and 2.5 ml of concentrated H_2SO_4 (Merck) were added to 1 ml of sample and incubated at room temperature for 10 min. The absorbance of the solution was measured at 492 nm (Shimadzu, model UV1800) and compared against a standard curve generated using glucose (Sigma-Aldrich). Using the Coomassie (Bradford) Protein Assay kit (Thermo Scientific), the protein content of the EPS was analysed. A 1 ml volume of the sample was added and mixed with 1 ml of reagent, incubated at room temperature for 10 min and the absorbance was measured at 595 nm (Shimadzu, model UV1800), as per the manufacturer's instructions. Bovine serum albumin (Thermo Scientific) was used as a standard for quantification of proteins.

2.3 Results

Three experiments were carried out using only PAO1 in order to observe the variability of fouling between the two RO modules. The results showed that the TMP rise in both modules was very similar, with only a 0.8% difference in the time required for a maximum TMP increase of 120%. If the experiment was stopped after one module had reached the maximum TMP percentage increase, a maximum TMP percentage difference between the two modules of only 9% was observed. Any difference between module fouling rates observed to be greater than 9% was therefore considered to be significant.

2.3.1 PAO1 vs PAO1Δ*pel*Δ*psl*

The RO membrane injected with PAO1 cells fouled in 124.6 h, resulting in a total TMP increase of 120% (Figure 2.2A). The TMP profile can be divided into two stages, as previously described.[123] The first stage was characterized by a slow increase in TMP, approximately 20% in the initial 90 h, followed by a second stage where an abrupt rise in TMP or 'TMP jump' was observed over the next 35 h.

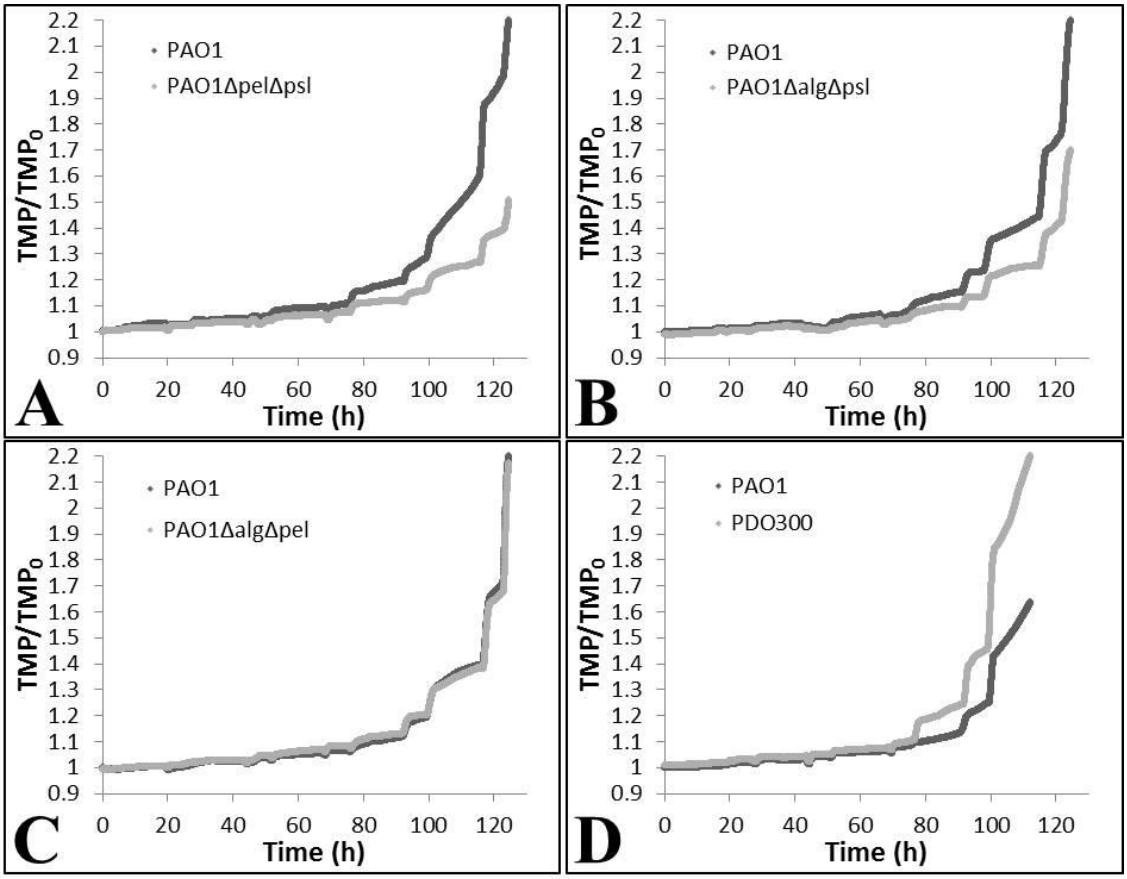

Figure 2.2 TMP profiles of the RO system inoculated with A) *P. aeruginosa* PAO1 vs PAO1Δ*pel*Δ*psl* B) PAO1 vs PAO1Δ*alg*Δ*psl* C) PAO1 vs PAO1Δ*alg*Δ*pel* D) PAO1 vs PDO300. The RO system was run using feed solution containing 24 mg l^{-1} of NB and 2 g l^{-1} NaCl, at a flux of 30 LMH and a CFV of 0.17 m s^{-1}. TMP values were recorded every 1 min over the experimental period.

Over the same 124.6 h time period, the TMP of the RO injected with the PAO1Δ*psl*Δ*pel* double mutant had only increased by 51%, resulting in a difference of 69% between the double mutant and the wild-type. Interestingly, the biofilm biovolumes and the viable bacteria counts of the two membranes were similar, with only a 13% and 9% difference, respectively (Figure 2.3A and 2.3E). Staining with Con-A-FITC revealed that the average polysaccharide biovolume was 24% less for the double mutant in comparison to the PAO1 (Figure 2.3B). This difference was also illustrated by the EPS extraction method, revealing a 70% reduction in PAO1Δ*pel*Δ*psl* polysaccharide (Figure 2.3C). A 24% reduction in protein was also observed for the double mutant (Figure 2.3D).

Differences in biofilm structure were observed for each strain (Figure 2.4). PAO1 formed a homogeneous biofilm (98% average surface coverage) 17 μm thick over the entire membrane surface (Figure 2.4A), whereas the biofilm structure of the double mutant appeared to be much more influenced by cross flow (Figure 2.4B), likely due to the lack of Psl, which is critical for cell attachment to surfaces. Rather than even attachment across the membrane surface, the biofilm appeared to have built up where some cells were able to attach onto the membrane due to flux. This resulted in deep furrows of bacterial cells (some 31 μm thick), separated by areas of unfouled membrane (51% average surface coverage).

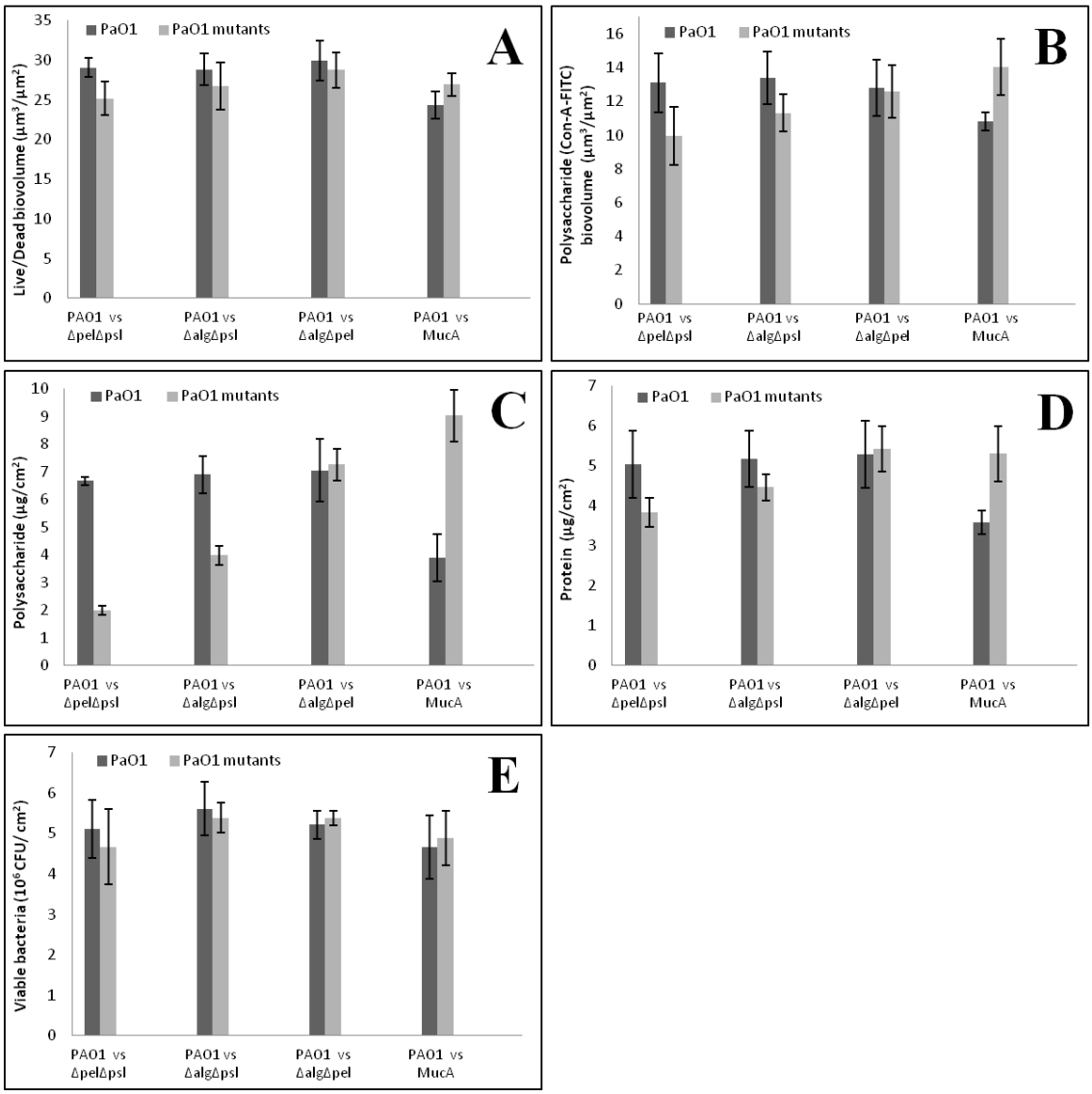

Figure 2.3 RO membrane autopsy results for *P. aeruginosa* PAO1 wild type vs PAO1 double mutants. (A) Biofilm biovolume for PAO1 and PAO1 mutants as determined by staining with SYTO 9 and PI (B) Biofilm biovolume for PAO1 and PAO1 mutants as determined by staining with ConA-FITC (C) Polysaccharide concentration of PAO1 and PAO1 mutants as determined by EPS extraction. (D) Protein concentration of PAO1 and PAO1 mutants. (E) Viable bacterial counts of PAO1 and PAO1 mutants as determined by CFU. Error bars are +/- one Std. Dev, n = 3.

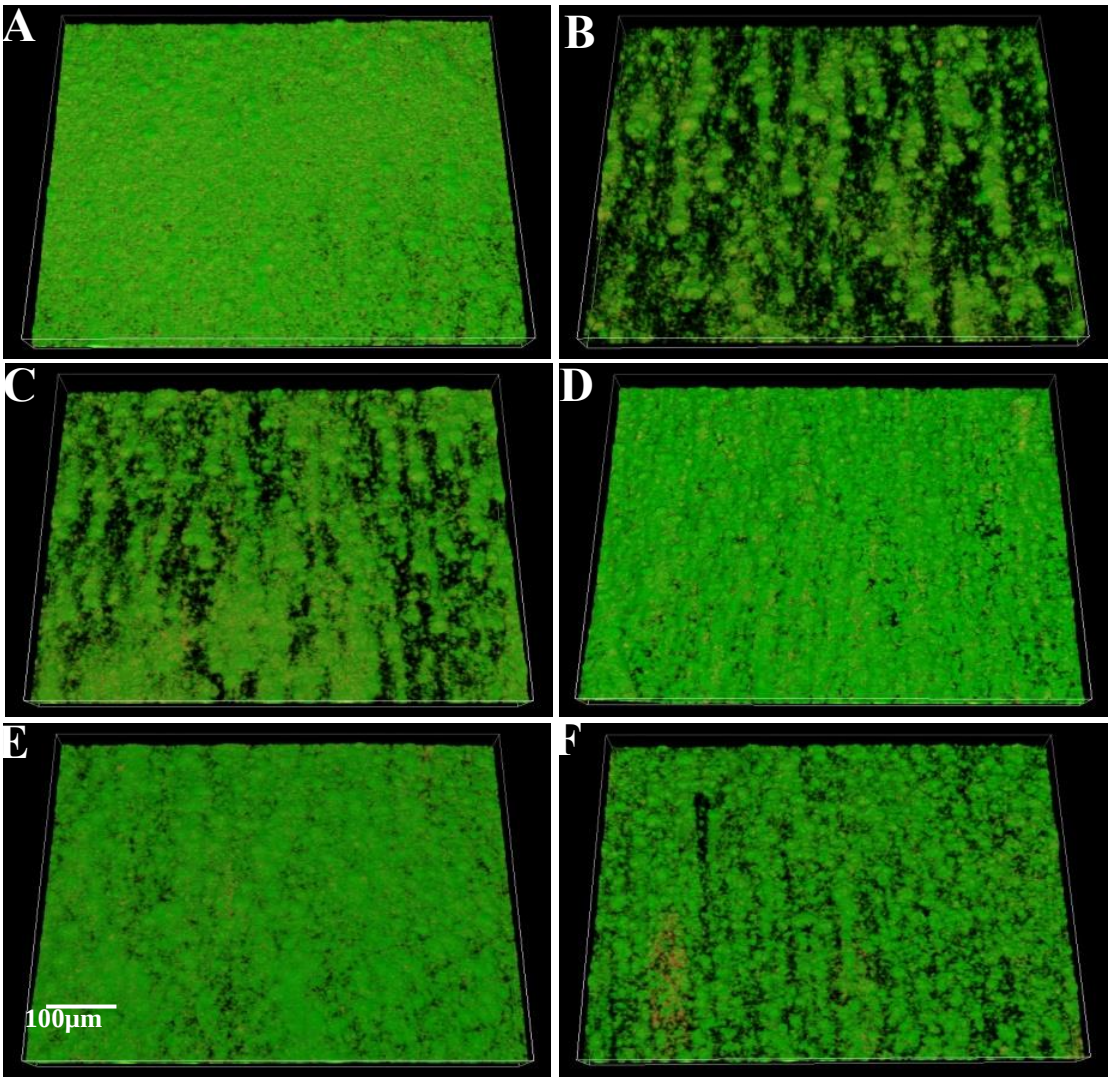

Figure 2.4 Biofilms of *P. aeruginosa* A) PAO1 wild type (125 h), B) PAO1Δ*pel*Δ*psl* (125 h), C) PAO1Δ*alg*Δ*psl* (125 h), D) PAO1Δ*alg*Δ*pel* (125 h), E) PDO300 (112 h) and F) PAO1 (112 h) strains on RO membranes. Representative confocal images showing biofilm structure via live and dead bacterial cells stained with SYTO9 and PI. Total magnification ×200. Scale bar = 100 µm.

2.3.2 *P. aeruginosa* PAO1 wild type vs PAO1Δ*alg*Δ*psl*

The RO membrane injected with wild-type PAO1 fouled in 125.1 h, with a 120% increase in TMP. Over the same period, the TMP of the RO injected with the PAO1Δ*alg*Δ*psl* double mutant had only increased by 70%, a difference of 50% (Figure 2.2B). The average total cell biofilm biovolume and the viable bacteria counts of the two membranes

were similar, with only a 7% difference between the biofilm biovolumes and a 4% difference between the viable CFU counts (Figure 2.3A and 2.3E). Average surface coverage of the PAO1Δ*alg*Δ*psl* fouled membrane was 68%. Staining with Con-A-FITC revealed that the average polysaccharide biovolume was 16% less for the double mutant in comparison to the wild-type (Figure 2.3B). This difference was also reflected by the chemical extraction and quantification of the EPS, which indicated that there was a 42% reduction polysaccharides for the PAO1Δ*alg*Δ*psl* mutant (Figure 2.3C). A 14% reduction in protein was also observed for the double mutant (Figure 2.3D). Similar to the PAO1Δ*pel*Δ*psl* double mutant, the biofilm structure appeared to be affected by cross flow, resulting in areas of unfouled membrane (Figure 2.4C).

2.3.3 *P. aeruginosa* PAO1 wild type vs PAO1Δ*alg*Δ*pel*

The PAO1 wild-type fouled the RO system within 124.8 h, resulting in a total TMP increase of 120%. Over the same time period, the TMP of the RO module injected with the PAO1Δ*alg*Δ*pel* double mutant had increased by 117%, a difference of only 3% (Figure 2.2C). The biofilm biovolume, based on Con-A-FITC stained polysaccharides, viable bacteria counts and EPS extracted polysaccharide and protein concentrations of the two membranes were very similar (Figure 2.3), with only a difference of 4%, 2%, 3%, 3% and 2%, respectively. The biofilm structures of both bacterial strains were observed to be similar, with an 18 µm thick, homogenous biofilm (98% and 96% average surface coverage) forming over the membrane surface (Figure 2.4D).

2.3.4 *P. aeruginosa* PAO1 wild type vs PDO300

The RO module inoculated with the PDO300 mutant fouled within 112.3 h, resulting in a 120% increase in TMP. Over the same time period, the TMP of the RO injected with the PAO1 wild type had only increased by 64% (Figure 2.2D). Although the experiment was stopped after the module with the PDO300 mutant had reached its maximum TMP, it is

likely that the PAO1 injected module would have fouled in approximately 125 h, as had been seen in the previous experiments. This would have resulted in a 10% difference in the time taken for each membrane module to achieve the maximum TMP. An increase in biofouling rate has been previously observed for a mucoid *P. aeruginosa* strain (FRD1) that overproduces alginate.[124] While it fouled the RO faster, the PDO300 mutant had only a slightly greater biofilm biovolume compared to the wild-type and only a slightly higher number of viable bacteria, with a 10% and 5% difference, respectively (Figures 2.3A and 2.3E). The biofilm thickness for both biofilms was also similar, 18 μm and 20 μm for PAO1 and PDO300, respectively. Staining with Con-A-FITC revealed that the average polysaccharide biovolume was 23% greater for the PDO300 mutant in comparison to the PAO1 wild type (Figure 2.3B). The chemical quantification of polysaccharides indicated there was a 57% increase in polysaccharide in the biofilm formed by the PDO300 strain (Figure 2.3C). A 32% increase in protein was also observed for the PDO300 mutant (Figure 2.3D). The biofilm formed by the PDO300 also had a more complete coverage over the membrane surface, 93% surface coverage versus 85% for the wild type (Figures 2.4E and 2.4F).

Interestingly, if the membrane autopsy results of the PDO300 mutant at the maximum TMP were compared to the average wild type PAO1 results at the maximum TMP from the previous experiments, some clear differences can be observed. The wild type strain fouled membranes had an 8% greater cell biofilm biovolume and 8% more viable bacteria in comparison to the PDO300 (Figure 2.3). However, Con-A-FITC staining revealed that the PDO300 biofilm had 7% more polysaccharide. EPS extraction revealed that the PDO300 biofilm had 24% more polysaccharide and 2% more protein per cm^2 of membrane and these results are similar to previously published observations.[124]

2.4 Discussion

The roles of various exopolysaccharides in membrane biofouling were investigated and it was demonstrated that at least one of the exopolysaccharides, Psl, was important in PAO1 biofilm development under a range of different conditions. Laboratory-scale RO experiments were designed to simulate full scale RO operations, where the feed included a steady supply of natural foulants such as bacteria and organic nutrients, was operated under crossflow and constant flux, experienced elevated salinity as a consequence of permeate production. As a consequence of the operational parameters, bacteria would essentially be filtered onto the membrane surface and proliferate, forming biofilms. Despite this effect, the PAO1 mutants incapable of producing Psl did not form a homogeneous biofilm on the membrane surface. Instead, these mutants appeared to be strongly influenced by crossflow, resulting in a unique pattern of biofilm, which led to large areas of unfouled membrane and significantly delayed the rate of biofouling, as measured by the rise in TMP. Previous work has shown that both EPS and bacterial cells contribute to a decline in RO performance.[89] Bacterial cells on the membrane surface impede the back diffusion of ions resulting in an inflated osmotic pressure on the membrane surface, and results in a decrease in permeate flux (or an increase in TMP at fixed flux) and salt rejection.[90] EPS add to the decline in membrane performance by adding to the hydraulic resistance to permeate flow.[125] In this study, the number of cells on the membrane surface was similar for all of the mutants tested. However, while the CFU and biofilm biovolumes based on cell staining did not differ significantly, a lower quantity of EPS components detected by both image quantification and chemical extraction for the Psl mutants suggested that the cells present lacked the ability to form a strong biofilm matrix. Reduced biofouling associated with a loss of Psl production emphasizes the importance of attachment polysaccharides in the ability for bacteria to foul industrial RO membranes and would explain the way some bacteria are more

successful primary colonisers in comparison to others.[126] These initial colonisers may then provide a support for the attachment of other organisms leading to highly diverse biofilm communities.[127, 128] The PAO1Δ*alg*Δ*pel* mutant fouled at the same rate as the PAO1, showing that the removal of alginate and Pel had no significant effect on the biofouling rate of the PAO1 biofilm. These polysaccharides therefore do not play a significant role in cell adhesion and biofilm formation in an RO system in the presence of Psl. In general agreement with a role of polysaccharides in the RO system, the PDO300 strain had a greater fouling effect than PAO1. Alginate overproduction has been observed to increase biofilm persistence by creating an extracellular matrix that promotes adherence.[129] One benefit of this in the RO system may be to increase the structural cohesion of the biofilm, which would presumably maintain the biofilm under conditions of high sheer. The data presented here supports this hypothesis, where the greater EPS production appeared to play a significant role in biofilm development and the decreased performance of the RO system.

Psl has been found to be critical for biofilm formation on RO membranes, while a loss of Pel had no apparent impact in its presence. Alginate played a role in the initial stage of biofilm formation, but not in longer term development. Interestingly, while Psl deficient mutants could form biofilms on RO membranes, they formed striated biofilms strongly influenced by cross flow, with open areas on the membrane and a low quantity of EPS components. The pattern of biofilm formation and amount of EPS produced, rather than the number of bacterial cells present, were most associated with RO performance, where the Psl devoid mutant showed the least impact on RO function and the alginate overproducing strain showed the greatest impact on RO performance. Therefore, the results from this study suggest that Psl played a crucial role in the establishment of a cohesive and dense biofilm in PAO1 which increases resistance to water passage in RO

membranes, and that the production of alginate may increase biofilm stability and maintenance under conditions that would normally induce dispersal.

While the above may be true for single species *P. aeruginosa*, the roles of these exopolysaccharides on mixed species biofilm and its effect on RO performance are not extensively studied and would be of great interest. It has been found that Pel was required for the integration of mixed species biofilm, and that Psl promoted distinct segregation of communities within the biofilm.[120] A deficiency or overproduction in each of the polysaccharides also influenced the relative abundance of *P. aeruginosa* in mixed biofilms as well as stress resistance of mixed species biofilms.[130]

This chapter highlighted that even within one class of biopolymer, e.g polysaccharides, the specific components do not contribute equally to the fouling process. Other components of the EPS may also affect biofilm development and membrane biofouling but were not investigated in this chapter. For example, it is clear that extracellular DNA and proteins, such as the large amyloid protein, CdrA are important for biofilm formation and these are also common to the matrix of other biofilm forming bacteria.[131-133] There is a lack of agreement in the field as to the relative importance of these different classes of biopolymers as it has been shown they contribute different rheological properties to the biofilm. However, it is clear from the data presented here that deletion of genes involved in their production have a significant impact on the biofilm structure and fouling of membranes. How these properties translate to membrane performance in RO systems is unknown and would be the next step forward in further understanding the roles of EPS on RO biofouling.

CHAPTER 3 THE APPLICATION OF NITRIC OXIDE FOR BIOFOULING CONTROL IN RO MEMBRANE SYSTEMS

3.1 Introduction

Membrane technology, for the conversion of seawater and wastewater through desalination and reclamation processes into potable water, is vital for sustainable water management. However, membrane fouling by bacterial biofilms continues to be a key challenge for water purification systems based on membranes.[112, 114, 134] The development of biofilm is a step-by-step process that is first initiated by the attachment and adhesion of planktonic cells to a membrane surface, followed by the forming of microcolonies and biofilm maturation, in which bacterial cells are ingrained in a self-produced matrix of extracellular polymeric substances (EPS).[112, 135, 136] Composed of proteins, polysaccharides and nucleic acids, the EPS gives the biofilm stability and enables it to withstand considerable shear forces.[134] Biofilm bacteria have several advantages over single cells, including optimization of growth and survival, improved acquisition of nutrients and increased protection against environmental stresses.[136, 137]

Biofilm formation on membrane surfaces results in a severe decline in flux, an increase in transmembrane pressure, high-energy consumption and a deterioration of system performance and product water production.[113-115] Typical techniques to mitigate fouling of membrane include membrane cleaning and pre-treatment of the untreated water. However, the effects of these treatments are generally only temporary. Microorganisms may withstand pre-treatment processes such as flocculation, coagulation, sand filtration, ultra filtration and cartridge filtration and they will eventually colonize a variety of surfaces within the plant.[114] Membrane cleaning, which involves physical or chemical methods, is used to regenerate the function of fouled membranes, and the methods used and the frequency of cleaning depend on the type of foulant as well as the

resistance of the membrane to chemical cleaning agent.[138] However, these cleaning methods shorten membrane life, further increasing operational costs.[89, 139] In addition, the chemicals used are often toxic biocides, which represent an environmental and health risk. Despite the widespread use of such chemicals, they are ineffective in destroying and/or completely removing the complicated multicellular structures of the membrane biofilms and its regeneration quickly results in a recurrence of system failure due to biofouling. They may also potentially select for resistant strains, which further exacerbates the problem. Therefore, new strategies of biofouling prevention are required to reduce such impacts.

Recent research has demonstrated that the gas molecule and important biological messenger nitric oxide (NO) is a signal for the dispersal of biofilm, by inducing the change from the biofilm growth mode to the planktonic state.[50, 103] NO brings about biofilm dispersal by stimulating the activity of phosphodiesterase, resulting in the degradation of secondary messenger molecule cyclic di-guanylate monophosphate (c-di-GMP), leading to changes to gene expression that support the planktonic mode of growth.[103] NO, which has a short half-life in aqueous environments can be delivered to biofilms by using chemical compounds that generate NO in solution. One such NO donor compound, sodium nitroprusside (SNP) was shown to disperse biofilms of the model organism *Pseudomonas aeruginosa*, as well as other bacterial species, and mixed species biofilms at low, non-toxic concentrations.[50, 102] A recent study investigated the biofilm dispersal potential of three NO donor compounds (MAHMA NONOate, SNP and PROLI NONOate) using *P. aeruginosa* PAO1 as a model organism.[104] The results showed that MAHMA NONOate could reduce bacterial biofilms by up to 40% over a 2 h exposure period, but that this reduction was partially due to growth inhibition. The addition of SNP reduced biofilm biovolume by 40% over a 24 h period but led to enhanced growth over shorter periods, likely due to the presence of iron in this

compound. PROLI NONOate quickly dispersed PAO1 biofilms, reducing the biovolume by 30% after 1 h exposure [104], with no inhibitory or growth effects observed.

Interestingly, it has also been shown that NO stimulates biofilm formation in *Nitrosomonas europaea* [140], *Azospirillum brasilense* [141] and *Shewanella oneidensis [142]*. Other reports have also suggested that NO has no effect on biofilms or may promote biofilm formation.[143, 144] Thus, different bacteria may show individual responses to NO and hence it is uncertain what the overall effect of NO might be on a natural, mixed species biofilm community. Therefore, the aim of this study was to determine the potential of PROLI NONOate to disperse biofilms generated by isolated bacteria from fouled industrial reverse osmosis (RO) and membrane bioreactor (MBR) membranes. In addition, this study aimed to examine the potential of PROLI NONOate dosing as a innovative strategy to curb biofouling of membranes in a laboratory-scale RO system.

3.2 Materials and Methods

3.2.1 Bacterial isolates

Biofilm scrapings were taken from six 9 cm^2 segments of membrane from a 5 year old spiral wound RO module obtained from the Kranji NeWater plant, Singapore. Membrane scrapings were mixed together and bulk genomic DNA was extracted from two 0.1 g samples using sodium dodecyl sulphate hexadecyltrimethyl ammonium bromide.[145] A portion of the biofilm scraping was cultured overnight in R2A broth at 30^oC with shaking at 200 rpm to prepare glycerol stocks of a mixed RO bacterial community for experimental work detailed in this study. DNA was extracted from the cultured cells, using the method above, to determine the shift in bacterial composition after culturing.

3.2.2 Reverse Osmosis (RO) system

The RO system used in this chapter was similar to the one described in Chapter two. The RO system was assembled as two independent cells in parallel, allowing one cell to be used as an untreated control in each of the NO treatment experiments. Each stainless steel RO cell had a flat plate geometry and flow channel sizes of 150 × 30 × 0.8 mm (L × W × H) with an effective area of 0.0045 m^2. Each 10 l feed tank was equipped with a stirrer (IKA, model Eurostar) and was cooled using a chiller (Polyscience) to maintain the feed solution at 23 ± 1 °C (Fig. 1). A high-pressure centrifugal pump (Hydra-Cell) was used to deliver the feed solution and maintain the cross-flow velocity (CFV) at 0.28 m s^{-1}, while system pressure was set to 362.6 psi using a flow control valve (Swagelok, model SS-4R3A). The feed flow rate was monitored with a turbine flow metre (WF Waterflo). The feed and permeate pressure were monitored by pressure transducers (Ashcroft). RO membranes (TW-30, DOW Filmtec) were cut to size (3 cm × 15 cm) and soaked in MilliQ water overnight. The membranes were then soaked in 70% ethanol (Merck) for 1.5 h for sterilization followed by rinsing with MilliQ water. The membranes were subjected to compaction at a flux of 60 l m^{-2} h^{-1} (LMH) overnight with MilliQ water until a stable flux was achieved, which was monitored using mass-flow controller (model 5882, Brooks Instrument). Following compaction, the flux was set to 30 LMH and a NaCl stock solution (200 g l^{-1}) was added to the feed tank to a final concentration of 2 g l^{-1}. The system was allowed to mix for 1.5 h before the nutrient source was added. For PAO1 experiments, a nutrient broth (NB) (Difco, BD) stock solution (8 g l^{-1}) was used to provide a final background nutrient concentration of 24 mg l^{-1}, which translates to a TOC concentration of approximately 7.8 mg l^{-1}.. For RO mixed community experiments, an R2A broth (1.25 g l^{-1} yeast extract, 1.25 g l^{-1} proteose peptone, 1.25 g l^{-1} casamino acids, 1.25 g l^{-1} glucose, 1.25 g l^{-1} starch, 0.75 g l^{-1} K_2HPO_4, 0.06 g l^{-1} anhydrous $MgSO_4$, 0.75 g l^{-1} sodium pyruvate) stock solution (7.81 g l^{-1}) was used to provide an final background

nutrient concentration of 25 mg l^{-1}, which translates to a TOC concentration of approximately 8 mg l^{-1}.. The RO feed was mixed for a further 1.5 h prior to the start of the experiment. The feed solution was replenished twice daily and the TOC was tested with a TOC analyser (Shimadzu, Model TOC-VWS) to ensure that the concentration of nutrients remained equal in each parallel unit.

3.2.3 NO treatment for prevention of membrane biofouling

The membrane fouling rate of an untreated RO cell was compared to that of one dosed with 40 µM PROLI NONOate every 24 h. The concentration of 40 µM was selected based on a previous optimization study.[104] The experiment was carried out using a single bacterial species (*P. aeruginosa* PAO1) and repeated using a mixed bacterial community cultured from a biofilm scraping from an industrial RO membrane. The bacteria were grown overnight in either 750 ml nutrient broth (PAO1) or R2A broth (mixed community) at 30^{o}C with shaking at 200 rpm. The bacterial cells were subsequently gathered by centrifugation at 18,514 *g* for 10 min. The pellet was washed and resuspended in 2 g l^{-1} NaCl to an OD600 of 0.1. The bacterial suspension was injected into the feed solution prior to the RO cells using an metering pump (ELDEX, model 5979-Optos Pump 2HM). The RO system was operated in closed loop where the retentate and permeate streams were returned to the feed tank. Micro-filters (KAREI, 5 and 0.2 µm) were installed downstream of the pressure cell to prevent excess bacteria from contaminating the feed tank. Experiments were initiated by the start of continuous injection of the bacterial suspension into the flow line at a dilution ratio of 1:800, giving an input load of 10^5 CFU ml^{-1}. The bacterial solution was replaced every 48 h. Experiments were conducted at a constant flux (30 LMH) and the TMP (difference in pressure between the feed and permeate stream) was monitored continuously. For PROLI NONOate injection, the bacterial suspension was replaced with sterile 2 g l^{-1} NaCl and the

bacterial injection tubing flushed for 10 min at 2 ml min^{-1} to remove excess bacterial cells, as shown in Figure 3.1. PROLI NONOate (2.19 g l^{-1}) in 0.4 g l^{-1} NaOH was then injected into the system for 30 min at a dilution ratio of 1:250 (1.6 ml min^{-1}), giving a final concentration of 8.76 mg l^{-1}. For the untreated cell, 0.4 g l^{-1} NaOH, without PROLI NONOate was used as a control. After dosing, the bacterial suspension was injected into the flow line as before. PROLI NONOate was injected into the treated cell every 24 h. Fouling was defined here as the increase in TMP over time during the filtration process at constant flux. Therefore, a higher TMP within the same time frame or the same TMP within shorter time frame represents more severe fouling.

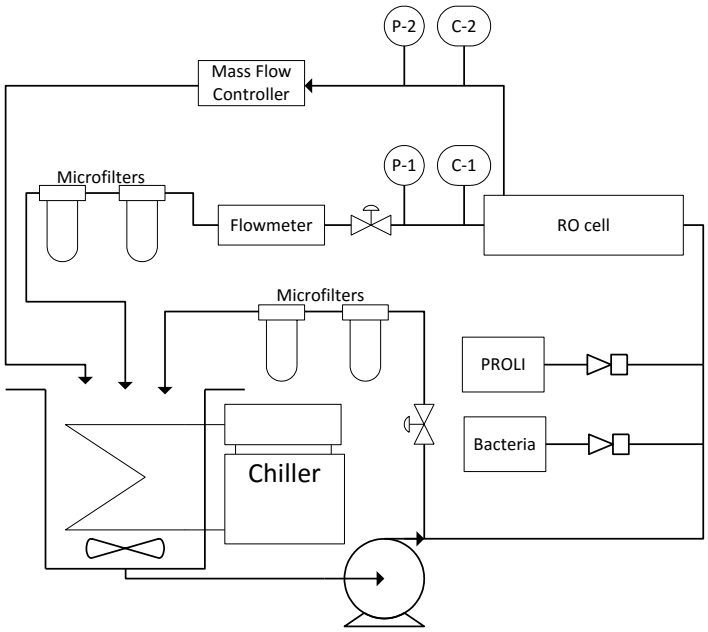

Figure 3.1 Schematic diagram of RO system used in this study. Feed water was pumped to the RO cell and both the rententate and permeate were returned to the feed tank to be recycled. Both bacteria and PROLI NONOate were injected into the system right before the RO cell, with the bacteria filtered off by microfilters before the feed was recycled. TMP and salt concentrations were monitored by pressure gauges (P-1 and P-2) and conductivity meters (C-1 and C-2). Flux and flow rates were controlled by the mass flow controllers and the flow control valves.

3.2.4 Membrane autopsy

The fouled membranes were removed from the RO modules for examination at the conclusion of the experiment and 1.5 cm was removed from each end of the membrane while the remainder was aseptically cut into 8 segments, as illustrated in Figure 3.2. Six segments (1 × 3 cm) of membrane covering the inlet, middle and outlet of the RO cell were analysed by fluorescence staining and CLSM observation to quantify the live and dead cells and the polysaccharide volume (representative of EPS). For the remaining two segments (3 × 3 cm), viable bacterial counts were determined as were the concentrations of polysaccharide and protein extracted from the membrane surface.

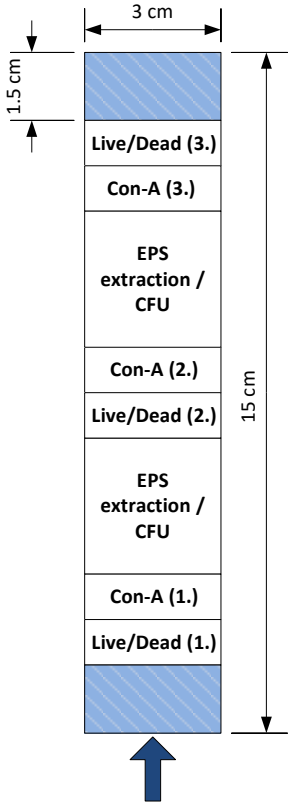

Figure 3.2 Outline of various sections of the fouled membrane used for different membrane autopsies. The arrow indicates the flow direction.

3.2.4.1 Fluorescent staining and CLSM

Segments of membrane were gently washed in 0.85% NaCl solution and stained using SYTO 9 and PI (3 μg ml^{-1} each) or 100 μg ml^{-1} Con-A-FITC (Sigma-Aldrich). The segments were then washed again in NaCl solution to remove excess stain, mounted onto glass slides and viewed using CLSM as detailed above. For each section, z stack (3D) confocal images were obtained from 5 locations covering the membrane surface, and the average biovolume (μm^3) and surface coverage (%) was calculated using IMARIS (Bitplane, version 7.3.1).

3.2.4.2 Viable bacterial counts

Using a cell scraper, the biofilm was removed from each 3 × 3 cm segment of membrane and resuspended in individual tubes containing 3 ml sterile PBS and vortexed for 30 s. For *P. aeruginosa* PAO1, viable heterotrophic counts were determined using a modified Miles and Misra method [146]. In brief, three 10 μl drops of 10^{-1} to 10^{-6} dilutions were pipetted onto nutrient agar. For the mixed RO bacterial community, viable counts were determined by spread plating, in triplicate, 100 μl of 10^{-4}, 10^{-5} and 10^{-6} dilutions on R2A agar (Oxoid). Plates were incubated at room temperature for 24 h before counting. Viable cells were expressed as colony forming units (CFU) cm^{-2} of membrane.

3.2.4.3 EPS extraction and quantification

The remaining bacterial suspension was centrifuged at 18,514 *g* for 10 min and the supernatant was transferred to a clean centrifuge tube for analysis of the soluble EPS fraction. The bound EPS was extracted by adding 2 ml 0.85% NaCl and 12 μl of 37% formaldehyde (Sigma) to the bacterial pellet, the suspension was vortexed and incubated at 4°C for 1 h. After incubation, 2 ml of 1 M NaOH and 0.5 ml MQ water were added, the solution was vortexed and incubated at 4°C for 3.5 h. Subsequently, the bacterial

suspension was centrifuged at 18,514 *g* at 4°C for 20 min, and the supernatant was transferred to a clean centrifuge tube. A blank control consisted solely of the EPS extraction reagents. Using the phenol-H_2SO_4 method[122], the polysaccharide content of the EPS was measured.[147] Briefly, 0.5 ml of 5% phenol (Sigma-Aldrich) and 2.5 ml of concentrated H_2SO_4 (Merck) were added to 1 ml of sample and incubated at room temperature for 10 min. The absorbance of the solution was measured at 492 nm (Shimadzu, model UV1800) and compared against a standard curve generated using glucose (Sigma-Aldrich). The EPS protein content was analysed using the Coomassie (Bradford) Protein Assay kit (Thermo Scientific). A 1 ml volume of the sample was added and mixed with 1 ml of the reagent, incubated at room temperature for 10 min and the absorbance was measured at 595 nm (Shimadzu, model UV1800), as per manufacturer's instructions. Bovine serum albumin (Thermo Scientific) was as a standard for the quantification of proteins.

3.2.4.4 DNA extraction and pyrosequencing

For the RO fouling experiment using the mixed bacterial community, the biofilm was removed from three 3 cm^2 segments of membrane using a cell scraper and used for DNA extraction, so that a detailed comparison of the untreated and PROLI NONOate treated membrane bacterial communities could be made. DNA extraction, pyrosequencing and sequence analysis were then carried out as detailed below.

Pyrosequencing

The DNA samples from both the raw membrane scraping and the R2A culture was sent to Research and Testing Laboratory, Texas, US and sequenced using the "454" pyrosequencing platform, targeting the bacterial community.[148] The selected primers

for the bacterial PCR were Gray519R (5'-GTNTTACNGCGGCKGCTG-3') and Gray28F (5'-GAGTTTGATCNTGGCTCAG-3').[149]

Analysis of sequences

The quality and adaptor trimming of the reads generated from amplicon sequencing was performed using the QIIME (version 1.8.0) package.[150] The trimmed reads were then clustered into representative sequences of operational taxonomic units (OTUs), based on 97% genetic similarity thresholds for species level, with the Uclust algorithm.[151] Chimera screening and depletion was done on the representative sequence using UCHIME.[152] After chimera depletion the sequences were aligned against the Greengenes OTU database [153] using PyNAST.[154] The relative abundance for each OTU identified at the species level was then exported to PRIMER-E (Plymouth Routines in Multivariate Ecological Research) version 629 to calculate the Bray-Curtis distance between each of the samples.

3.3 Results

3.3.1 PROLI NONOate treatment for the prevention of RO membrane biofouling by PAO1

Biofilm formation in the RO module is quite different from the batch systems tested above, where in addition to being a flow through system, the RO module also includes flux, the passage of water through the membrane, which may facilitate transport of bacteria to the surface. Additionally, the cross-flow results in increased aeration, which may result in faster inactivation of NO through binding to oxygen. Therefore, before testing the effect of NO on a mixed species biofilm, the effect of NO on dispersing biofilms of the well characterized bacterium *P. aerugionsa* was first tested. Results from multiple replicate experiments where *P. aeruginosa* was used to foul the membrane in the

absence of PROLI NONOate treatment showed that the TMP rise in both modules was very similar, with only a 0.3% difference in the time required to achieve a maximum TMP increase of 120% (Figure 3.3A). If the experiment was stopped after one module had reached the maximum TMP percentage increase, a maximum TMP percentage difference between the two modules of only 6% was observed. Thus, any difference between module fouling rates observed to be greater than 6% was therefore considered to be significant.

The RO membrane without PROLI NONOate treatment fouled in 140 h, resulting in a TMP increase of 120% (Figure 3.3B). The TMP initially showed a slow increase in TMP, ~20% in the initial 100 h, followed by an abrupt rise in TMP over the next 40 h. Over the same 140 h time period, the TMP of the RO injected with PROLI NONOate every 24 h increased by only 68%, resulting in a 52% difference between the treated and untreated membranes when fouled with *P. aeruginosa*. The biofilm biovolume (total cells) of the treated membrane was 28% less than the untreated membrane (Figure 3.3C). In addition, the viable bacterial count of the treated membrane (3.89×10^6 CFU cm^{-2}) was 18% lower than the untreated membrane (4.72×10^6 CFU cm^{-2}), reflecting the lower bacterial cells numbers present on the membrane. The ratio of dead to live cells was greater in the untreated biofilm (0.34) than in the PROLI NONOate treated biofilm (0.27), revealing that the PROLI NONOate treatment did not have a bacteriocidal effect. Staining with Con-A-FITC revealed that the average polysaccharide biovolume was 20% less for the treated membrane in comparison to the control (Figure 3.3C). This difference was also illustrated by the EPS extraction method, revealing a 52% reduction in polysaccharides associated with the treated membrane. A 25% reduction in protein was also observed for the treated membrane (Figure 3.3C). The treated *P. aeruginosa* biofilm was thinner than the untreated control (24 vs. 32 μm, treated vs. control) and had a lower surface coverage (83% vs. 99%, treated vs. control), with more areas of unfouled membrane (Figure 3.3D).

Collectively, the data clearly show that NO induced dispersal of the *P. aeruginosa* biofilm, resulting in reductions in CFUs, biofilm matrix components and ultimately improving the performance of the RO module. These results demonstrated that NO could potentially be used in the complex RO systems to induce dispersal at concentrations derived from the batch biofilm experiments.

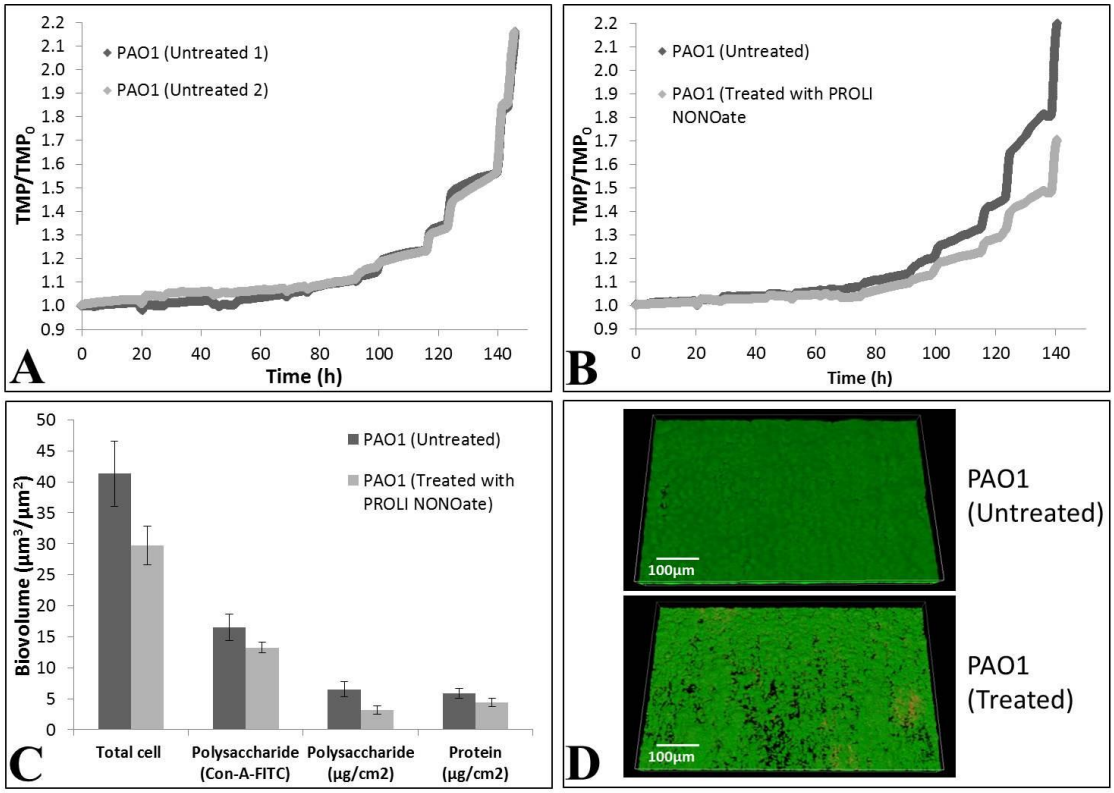

Figure 3.3 A) TMP profiles of the RO system inoculated with *P. aeruginosa*, both cells untreated. B) TMP profiles of the RO system inoculated with PAO1, untreated vs. treated with 8.764 mg l^{-1} PROLI NONOate every 24 h. C) RO membrane autopsy results for untreated vs. treated: biofilm biovolume as determined by staining with SYTO 9 and PI; biofilm biovolume as determined by staining with ConA-FITC; polysaccharide concentration as determined by EPS extraction; protein concentration as determined by EPS extraction. Error bars are +/- one Std. Dev, n = 3. D) *P. aeruginosa* biofilm on untreated vs. treated membranes. Representative confocal images showing biofilm structure via live and dead bacterial cells stained with SYTO 9 and PI. Total magnification ×200. Scale bar = 100 µm.

3.3.2 PROLI NONOate treatment for the prevention of RO membrane biofouling by a mixed RO bacterial community

As described above for PAO1, the natural variability of fouling between the two RO modules was determined in the absence of NO addition. The TMP rise in both modules, when fouled with the R2A cultured mixed RO bacterial community, was similar to that observed for the PAO1, with a 0.4% difference in the time required for a maximum TMP increase of 120%. The TMP profile was similar to that of the *P. aeruginosa*, with a slow initial increase in TMP, ~20% in the initial 92 h, but with a more rapid second stage where the maximum TMP was reached in the next 25 h. If the experiment was stopped after one module had reached the maximum TMP percentage increase, a maximum TMP percentage difference between the two modules was 8%. Any difference between module fouling rates observed to be greater these values was therefore considered to be significant.

The untreated RO membrane fouled in 117 h, resulting in a total TMP increase of 112% (Figure 3.4A). Over the same 117 h time period, the TMP of the PROLI NONOate treated RO module had only increased by 20%, a 92% difference between the NO treated and untreated membranes. The biofilm biovolume (total cells) of the treated membrane was 29% less than the untreated membrane (Figure 3.4B). In addition, the viable bacterial count of the treated (8.85×10^6) membrane was 23% lower than the untreated membrane (1.15×10^7 CFU cm^{-2}), reflecting the lower number of bacterial cells present on the membrane. The ratio of dead to live cells was greater in the untreated biofilm (0.17) than in the PROLI NONOate treated biofilm (0.08), revealing that the PROLI NONOate treatment did not have a bacteriocidal effect. The surface coverage of biofilm (59% in treated vs. 98% in control) and thickness (20 µm vs. 26 µm, treated vs. control) were also significantly lower on the NO treated membrane, with more areas of unfouled membrane

(Figure 3.4C). The EPS extraction method revealed a 48% reduction in polysaccharide and a 66% reduction in protein for the treated membrane biofilm (Figure 3.4B).

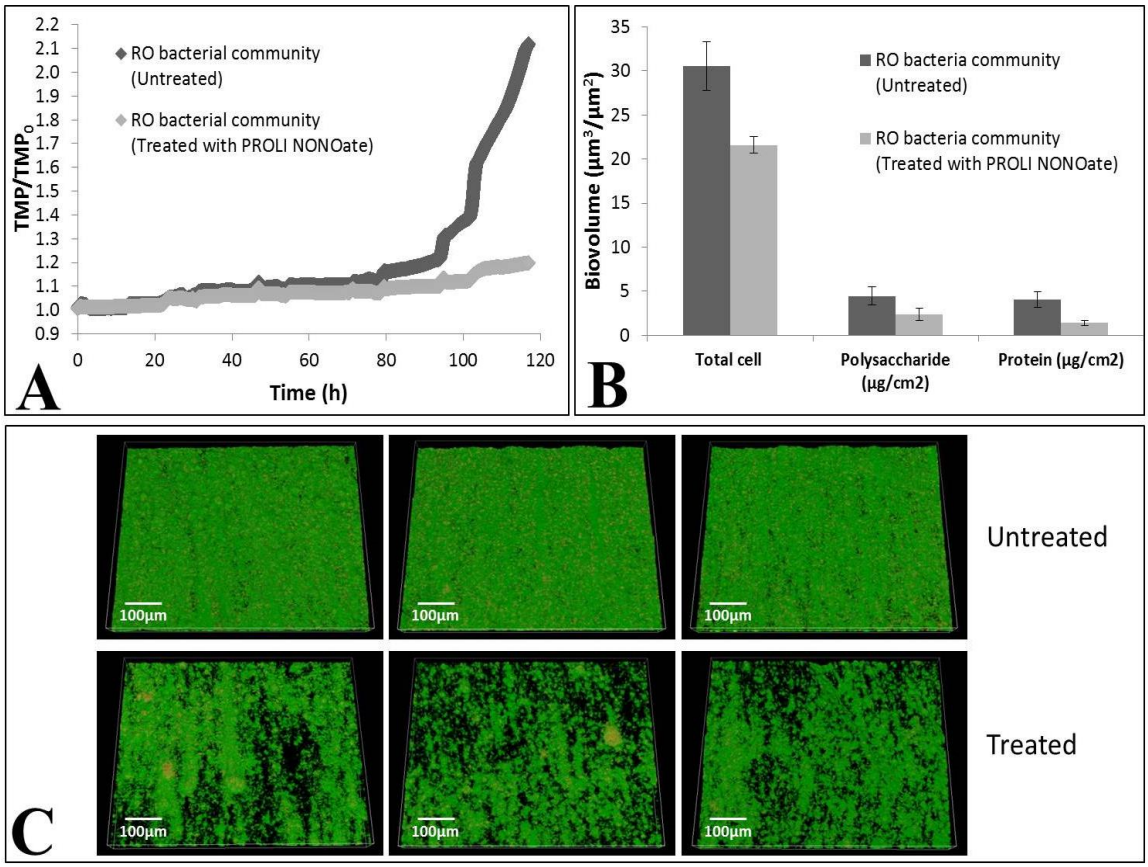

Figure 3.4 A) TMP profiles of the RO system inoculated with the mixed RO bacterial community, untreated vs. treated with 8.764 mg l^{-1} PROLI NONOate every 24 h. TMP values were recorded every 1 min over the experimental period. B) RO membrane autopsy results for untreated vs. treated: biofilm biovolume determined by staining with SYTO 9 and PI; polysaccharide concentration as determined by EPS extraction; protein concentration as determined by EPS extraction. Error bars are +/- one Std. Dev, *n* = 3. C) RO bacterial community biofilm on untreated vs. treated membranes. Representative confocal images showing biofilm structure via live and dead bacterial cells stained with SYTO 9 and PI. Total magnification × 200. Scale bar = 100 µm.

Due to the decreased biofouling rate in the PROLI NONOate treated RO cell, the experiment was repeated. However, rather than ending the experiment when the untreated RO cell had reached the maximum TMP, NO treatment continued in the parallel cell to determine the maximum time that NO treatment could prevent the TMP from reaching its peak pressure. The RO membrane without PROLI NONOate treatment fouled in 115 h, resulting in a total TMP increase of 130% (Figure 3.5). Over the same 115 h time period, the TMP of the RO injected with PROLI NONOate had only increased by 33%, resulting in a difference of 97% between the NO treated and untreated membrane. This is a similar result to the previous experiment, where a 92% reduction in the biofouling rate was observed. However, biofouling could not be prevented indefinitely and the treated RO membrane eventually became fully fouled after 147 h, resulting in a 22% difference in time required to achieve the maximum TMP increase.

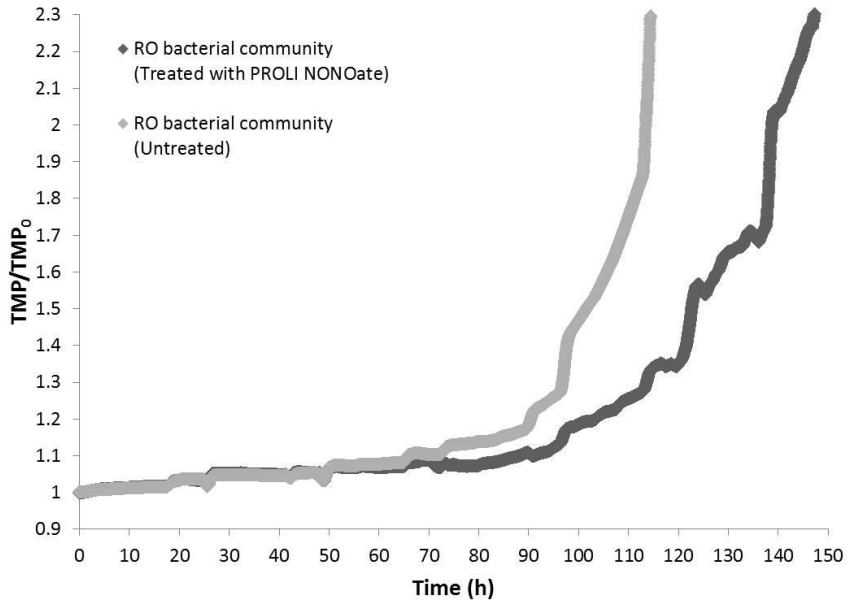

Figure 3.5 TMP profiles of the RO system inoculated with mixed RO bacterial community, untreated vs. treated with 8.764 g l^{-1} PROLI NONOate every 24 h. The RO system was run using feed solution with 31 mg l^{-1} R2A broth and 2 g l^{-1} NaCl, at 30 LMH flux and a CFV of 0.17 m s^{-1}. TMP values were recorded every 1 min over the experimental period.

3.3.3 Industrial RO membrane biofilm community analysis

The raw biofilm scraping taken from an industrial RO membrane from the Kranji NeWater plant, Singapore, was quite diverse, and contained at least 9 bacterial phyla. The scraping samples were represented mainly by the phylum Proteobacteria (91%) followed by Actinobacteria (5.3%) and Bacteroidetes (2.75%) at lower abundances (Figure 3.6).

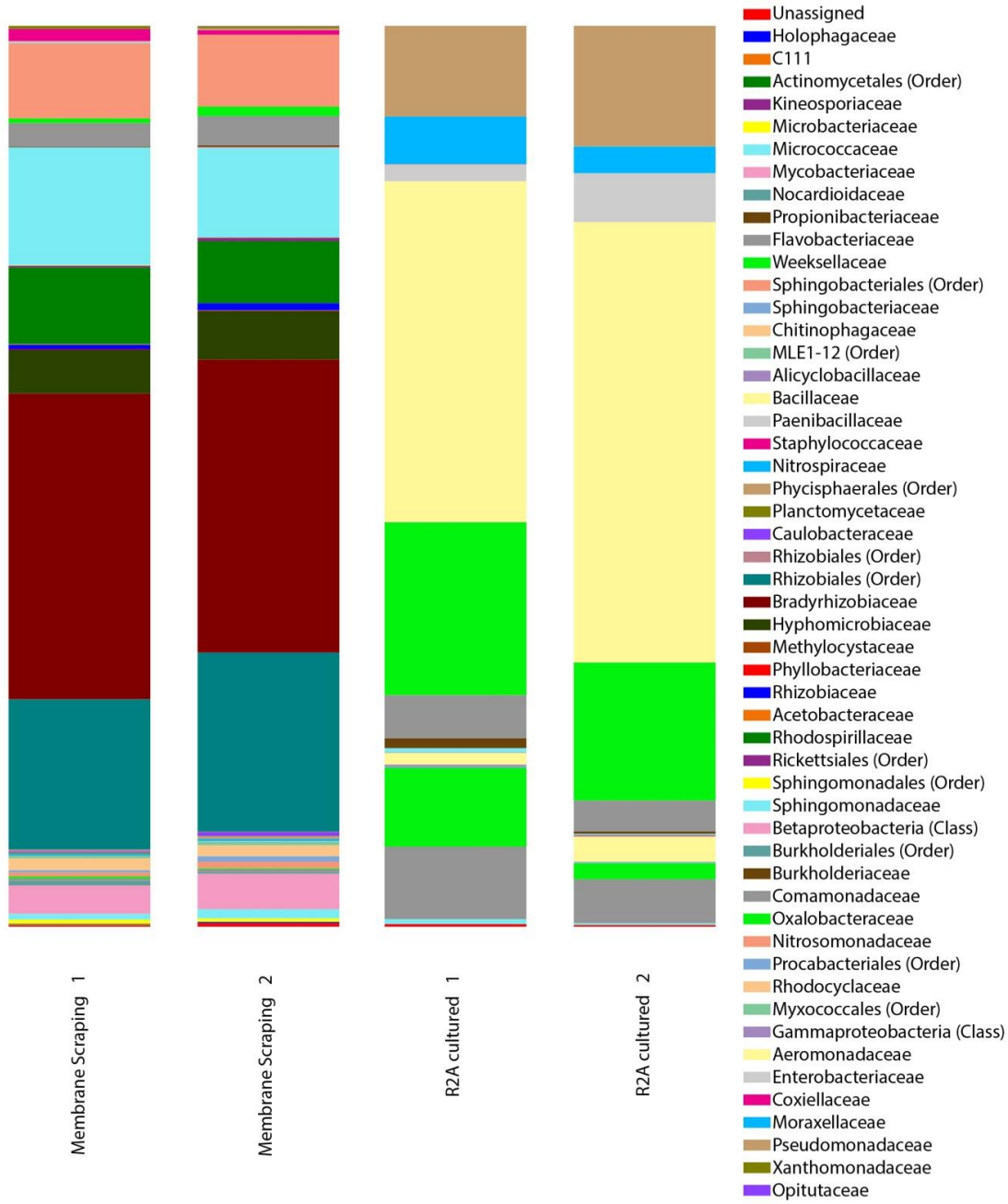

Figure 3.6 Comparison of the relative abundance of the major phylotypes found in the Kranji NEWater membrane biofilm before and after culturing in R2A broth.

The distribution of the Proteobacteria classes revealed that the Alphaproteobacteria class dominated the scraping samples with 77.35% of the Proteobacteria, followed by Betaproteobacteria (12.1%) and Gammaproteobacteria (1.4%). The scraping samples contained at least 53 bacterial families from 29 orders (Figure 3.6). The most abundant families were *Bradyrhizobiaceae* (33% ± 1%), an unknown family of the Order *Rhizobiales* (18% ± 2%), *Sphingomonadaceae* (12% ± 2%), *Nitrosomonadaceae* (8%), *Rhodospirillaceae* (8% ± 1%), *Hyphomicrobiaceae* (5% ± 1%) and *Mycobacteriaceae* (3%). The Bray-Curtis Index at the species level revealed an 87% similarity between duplicate samples. After the raw biofilm scraping was cultured in R2A broth, a shift in dominance was observed. The dominant families after culturing were *Aeromonadaceae* (43% ± 8%), *Oxalobacteraceae* (17% ± 3%), *Pseudomonadaceae* (12% ± 2%) and *Flavobacteriaceae* (6% ± 2%). The communities of the duplicate planktonic samples were very similar, with an 85% similarity at the species level as determined by the Bray-Curtis Index.

3.3.4 Effect of PROLI NONOate on community shift in mixed species RO biofilm

When the bacterial communities of two untreated membrane biofilms from the two biofouling experiments were examined at maximum TMP, the Bray-Curtis Index at the species level revealed a 92% similarity between samples (Figure 3.7), showing good reproducibility of the biofilm community between the parallel cells of the RO system. Despite bacteria of the family *Aeromonadacaceae* being the most abundant in the R2A cultures (Figure 3.6) the dominant bacterial family of the membrane biofilms was *Chitinophagaceae* (23%) (Figure 3.7), suggesting that this organism is a strong biofilm forming organism and thus plays a significant role in the biofouling of RO system membranes. Other dominant bacterial families within the membrane biofilms were

Oxalobacteraceae (23%), *Enterobacteriaceae* (14%), *Comamonadaceae* (13%), *Sphingobacteriaceae* (11%), *Aeromonadaceae* (7%) and *Flavobacteriaceae* (6%) (Figure 3.7). These seven families accounted for 97% of the total biofilm bacteria.

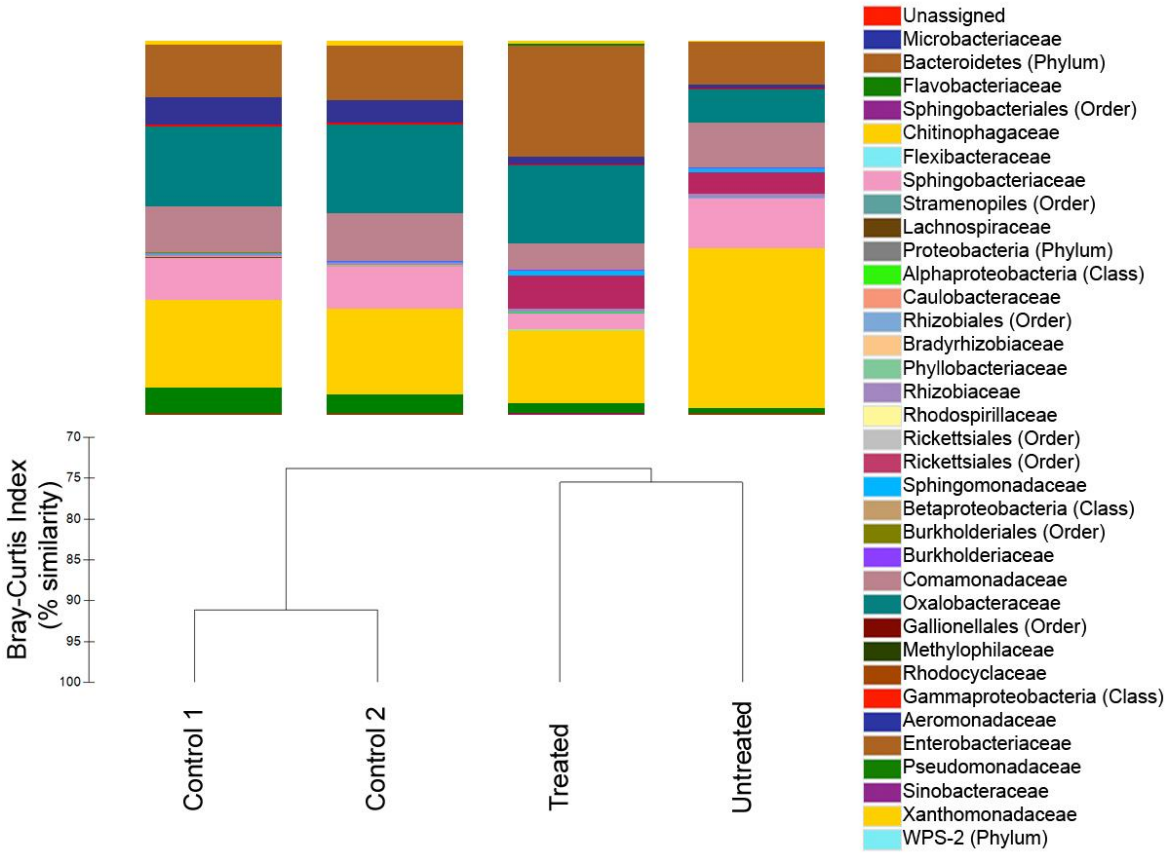

Figure 3.7 Comparison of the relative abundance of the major phylotypes found in the laboratory-scale RO membrane biofilms with and without PROLI NONOate treatment. Similarity of biofilm samples is depicted using a Bray-Curtis Index dendrogram.

The untreated and treated membrane biofilms were examined after 115 and 147 h, respectively, once they had reached maximum TMP. In comparison to the untreated control, dosing with PROLI NONOate led to a decrease in the percentages of *Chitinophagaceae* (decrease from 43% to 20%), *Sphingobacteriaceae* (decrease from 13% to 4%) and *Comamonadaceae* (decrease from 12% to 7%) within the biofilm, but an increase in the percentages of *Oxalobacteraceae* (increase from 9% to 21%), *Enterobacteriaceae* (increase from 11% to 29%), and an unknown Family of the Order

Rickettsiales (increase from 6% to 9%) (Figure 3.7). However, the same six families of bacteria dominated the biofilms of both the treated and untreated membranes. The Bray-Curtis Index at the species level revealed a 76% similarity between samples indicating that the PROLI NONOate treatment did not considerably change the microbial distribution of the membrane biofilm (Figure 3.7). The results from the Bray-Curtis similarity index dendrogram indicated that the variation between the RO runs was higher than the variation between the untreated and PROLI NONOate treated membrane biofilms further suggesting that the NO treatment did not significantly change the biofilm community.

3.4 Discussion

The growing need to improve water production for developed and developing nations has focused attention on membrane based purification methods. However, biofilm formation and biofouling remains a significant issue for the technology and thus there is a real need for novel approaches to control biological fouling. One recent discovery has been that bacteria produce and respond to NO and use this as a natural dispersal signal.[50, 102, 103, 155, 156] Here, the potential of PROLI NONOate to disperse bacteria isolated from fouled industrial RO membranes were investigated, and explored the potential application of PROLI NONOate as an innovative strategy to curb membrane biofouling in a laboratory-scale RO system.

It has been demonstrated that micro-molar concentrations of PROLI NONOate induce biofilm dispersal in a range of bacteria isolated from industrial membrane bioreactor and reverse osmosis (RO) membranes. Interestingly, results showed that different bacteria responded differently to NO exposure, with biofilm dispersal percentages ranging from 10% to 46%. These results correspond with the literature where NO induces biofilm dispersal by stimulating phosphodiesterase activity, which results in the degradation of c-

di-GMP, culminating in changes to gene expression that favour the planktonic mode of growth.[103] While this is the general model for NO induced biofilm dispersal, in some bacteria NO may stimulate biofilm formation [140-142] and it was observed here that NO in fact induced biofilm formation for *Acinetobacter* spp. and *Duganella* spp. The response of these bacterial genera was different to that observed in a former study, when the NO donor compound MAHMA NONOate was employed.[104] This difference is likely a consequence of the growth inhibitory nature of the MAHMA NONOate.[104] Although previous studies have demonstrated that NO exposure does reduce c-di-GMP in P. aeruginosa[103], the biofilm community tested here has a broad range of organisms present and the effect of NO on c-di-GMP levels reduction in mixed communities need to be further investigated in future work as it is still a hypothesis at this stage. In addition, each NO donor compound has a different half-life/release rate of NO, which may have impacted the bacteria differently. Overall, the mixed biofilm effects are similar for both NO donor compounds tested and hence, overall the data say that it is not easy to predict effects on mixed communities, under realistic conditions by using single species.

Previous studies have only investigated NO induced biofilm dispersal of *P. aeruginosa* and other bacterial species in batch experiments.[50, 102, 104, 157, 158] However, in this study, it has been shown that addition of a NO donor compound to a laboratory-scale RO system can significantly reduce the rate of biofouling by both a single species of *P. aeruginosa* and also, more importantly, a mixed bacterial consortium isolated from a fouled industrial RO membrane. In the mixed bacterial community, dosing with PROLI NONOate led to a decrease in the biofilm percentages of *Chitinophagaceae*, *Sphingobacteriaceae* and *Comamonadaceae* but an increase in the percentages of *Oxalobacteraceae*, *Enterobacteriaceae* and an unknown Family of the Order *Rickettsiales*. It therefore also seems apparent in this study that whilst the dispersal of some bacteria is induced during exposure to low levels of NO, biofilm formation may be

encouraged in others. It is important to note that pyrosequencing does not provide an absolute quantification of the number of each organism present, only a relative abundance. Therefore, it is possible that all of these organisms are generally dispersed, but their individual responses differ, as shown in Figure 3.7, resulting in a change in their relative abundances. Despite these different responses, the same six families of bacteria dominated the biofilms of both the treated and untreated RO membranes, with a microbial composition similarity of 76%. Thus, the addition of PROLI NONOate did not significantly change the microbial distribution of the membrane biofilm. In addition, the increase in certain biofilm members did not affect the success of the PROLI NONOate treatment to dramatically reduce the biofouling rate in the RO system. The positive effects of PROLI NONOATE treatment were not only applicable in RO systems. In a biofouling study on membrane bioreactors (MBR), backwashing the membrane module daily with PROLI NONOate reduced fouling resistance by 28.2% over a span of 85 days, reduced EPS production but yet not cause a significant change in the biofilm diversity.[159]

Previous work has shown that whilst the aggregation of bacterial cells on the membrane surface may decrease rejection of salt and permeate flux by a biofilm-enhanced osmotic pressure (BEOP) mechanism, the EPS biofouling layer also negatively affect permeate flux by increasing the hydraulic resistance to permeate flow.[89, 90] A recent study showed that the biofouling rate is dependent on both the quantity of EPS components and the surface coverage of the membrane biofilm, rather than the number of bacterial cells present. A lack of biofilm polysaccharides combined with areas of unfouled membrane dramatically reduced any hydraulic resistance to permeate flow, thus delaying the rate of biofouling.[160] This study showed similar results, where a reduction in EPS constituents (protein and polysaccharide) and a decreased biofilm surface coverage after NO treatment led to significantly lower biofouling rates. A reduction in biofilm cells was also observed

after PROLI NONOate treatment. There is an increasing interest in developing alternative, non-toxic methods to control microbial fouling in membrane based water purification and in particular, there has been a focus on modification of the biofilm development program. For example, Yeon et al. (2009) recently demonstrated that disruption of microbial cell-cell signalling could similarly delay the TMP rise associated with biofouling of a membrane bioreactor.[161] Thus, biologically derived strategies may represent an additional approach for the control of fouling communities.

In addition to testing NO as a novel strategy for biofouling control, this study has contributed to existing knowledge on the structure and diversity of industrial RO membrane biofilm communities. Over the last decade a number of studies have investigated the microbial community composition of RO membrane biofilms.[114, 162-167] The advancement of modern molecular methods, such as pyrosequencing, combined with ever decreasing analysis costs enable current studies to portray a detailed characterisation of sample microbial diversity and abundance. Identifying common bacteria that contribute to the biofouling of industrial RO membranes could enable the development of tailored solutions for its control. The industrial RO membrane biofilm from the Kranji NeWater plant, Singapore, supported a bacterial community dominated by Proteobacteria, with a relatively low abundance of other Phyla. The dominance of Proteobacteria on a fouled industrial RO membrane has been observed in other studies,[114, 162-166, 168] covering RO plants in the Netherlands[114], Australia [166], Israel [165], Italy [167] and Singapore.[162, 164] The dominant Class within this Phylum was observed to be Alphaproteobacteria, also similarly observed in other studies,[114, 162, 164, 166] followed by Betaproteobacteria.[114, 162, 166] Two studies by Bereschenko *et al*. revealed that Betaproteobacteria were dominant over Alphaproteobacteria within immature biofilms, but a reversal of dominance occurred as the biofilm matured.[163, 168] Thus, it is likely that the dominance of

Alphaproteobacteria in the innocula used in this thesis was due to the fact that the membrane had been in use for 5 years before collection of the sample.

A recent study has highlighted the challenges in determining the most problematic and predominant microbial species in a specific water recycling plant because species distribution varies considerably from one plant to another depending on conditions specific to the site such as seasons and feed water quality.[166] However, by comparing the bacterial community data from the raw Kranji NeWater membrane scraping in this study with other published work, some common bacteria can be observed to occur on fouled industrial RO membranes. These include bacteria of the Orders: Sphingomonadales [165, 166], Rhizobiales [164, 165], Pseudomonadales [165], Xanthomonadales [165] and Burkholderiales [163, 165]. Bacteria in the Families: Comamonadaceae [114, 163, 165, 168], Nitrosomonadaceae [166], Flavobacteriaceae [166], Microbacteriaceae [166], Pseudomonadaceae [166], Kineosporiaceae [166] and Planctomycetaceae [114]. Bacteria of the genus: Bacillus [104, 162], Bradyrhizobium [162, 166, 168], Rhizobium [166], Sphingomonas [114, 162-164, 166-168], Sphingopyxis [114, 163, 166, 168], Pseudomonas [104, 114, 163, 166, 168], Mycobacterium [114, 166, 168], Hyphomicrobium [114, 163], Acidovorax [114, 163], Janthinobacterium [114], Microbacterium [114, 162, 164, 168], Geothrix [162], Brevundimonas [167], Novosphingobium [168], Sphingobium [168], Acidovorax [168] and Flavobacterium.[168] These bacteria therefore seem to play a significant role in RO membrane biofouling at a number of RO plants covering five different countries, spanning three continents.

Dilute concentrations of PROLI NONOate have been shown to disperse a wide diversity of single species biofilms formed by isolated bacteria from industrial MBR and RO membranes, as well as isolates combined to generate multi-species biofilms.[104] The

dosing of PROLI NONOate every 24 h to a laboratory-scale RO system reduced the rate of biofouling by 92% for a bacterial community isolated from an industrial RO membrane and cultured on R2A. NO treatment led to a cutback in biofilm constituents (polysaccharides, proteins and total cells) as well as biofilm surface coverage and thickness. The dosing of PROLI NONOate also led to a 22% increase in the time taken for the RO module to reach its maximum TMP. Importantly, pyrosequencing analysis showed that the NO treatment did not considerably change the microbial distribution of the membrane biofilm.

However, it is important to note that microbial community present on seawater RO membranes are likely to differ from that of wastewater RO membranes, which will be more indicative of freshwater communities. Accordingly, the synthetic feed used in this study has a composition that was similar to the waste-water, e.g. salt concentrations that were similar to fresh water and not seawater. Furthermore, microbial communities vary from one wastewater treatment plant to another due to differences in physicochemical conditions and this study may not be representative for all wastewater treatment plants. While the seawater community will clearly be different, the same general principles would apply as it was seen that the community that developed in these experiments was quite consistent, giving confidence about the reproducibility of the results. Nonetheless, the NO treatment will need to be validated against a seawater community that is more reflective of the community found on desalination membranes for a more complete set of data to support the application of NO to desalination systems.

While the data presented in this chapter suggests that NO can, in principle, control the biofouling problem, there is a lot of room for improvement in this approach. Currently, the amount of NO donor compound required, and its current cost, would indicate that this approach is not as cost-effective compared to current industrial practices. However, if the

use of NO is shown to give a substantial benefit in terms of fouling control, then the costs involved in chemical synthesis may decrease substantially due to mass production. Along these lines, further work would need to be undertaken to determine the optimum dosing regimen and concentration. It would also be of value to combine the application of NO with a more traditional cleaning agent, such as NaOH, to determine if there is any synergistic effect, and hence a real cost-benefit, that makes the approach more commercially attractive.

As with any chemical approach, environmental toxicity has to be taken into account when the compound of interest is introduced into the environment. PROLI NONOate decomposes via a first order reaction, releasing NO and the naturally occurring amino acid, L-proline, hence there are likely to be no ecotoxicity issues, but this would none the less need to be monitored for certainty, should this strategy be implemented in industrial scale. Overall, the results presented demonstrate strong evidence for the application of PROLI NONOate for control of RO biofouling in an industrial setting and further work to optimise the amounts and timing of application of NO may improve upon the efficacy observed here.

CHAPTER 4 REVERSE OSMOSIS BIOFOULING MODELLING USING A "CANARY CELL" AND NON-INVASIVE BIOFOULING SENSORS FOR IMPROVED MANAGEMENT AND CONTROL OF RO FOULING

4.1 Introduction

Biofouling represents one of the key challenges to reducing costs associated with reverse osmosis based water purification. This is despite current practices such as cleaning in place (CIP), which only partially or temporarily control fouling and restore membrane performance. Ultimately, membranes eventually become irreversibly fouled and its performance can no longer be restored economically and requires replacement.[31] The failure of current antifouling technologies may thus be a consequence of the implementation of cleaning strategies. Typically, this is based on either a defined interval or when the TMP shows a substantial increase, indicating significant fouling. However, such approaches are not likely to completely solve the fouling problem, where current and new, e.g. NO, antifouling strategies do not prevent biofilm development entirely. Thus, in addition to novel antifouling treatments, the control of fouling should be augmented with improved management tools.

Determination of when fouling may occur is particularly difficult for spiral wound modules (SWM) because fouling occurs primarily on the membrane surface which is wrapped around a central core and contained inside an opaque high pressure vessel which makes direct observation almost impossible. Thus, a detection system involving the use of a side-stream or "canary cell" to accurately replicate biofouling at rates that match those of the SWM could be a suitable alternative to direct monitoring in the SWM. The benefits of such a system is that an accurate determination of biofouling within the SWM can be made by performing membrane autopsy of the canary cell without stopping the operation of the SWM and performing destructive analysis on the SWM. The development of a

predictive canary cell that operates in parallel on site has the potential to improve management strategies around when to implement cleaning processes, e.g. early in the fouling process, to improve overall system performance. This also has the potential to greatly reduce plant shutdown frequencies and hence, increase product water production whilst mitigating costs associated with irreversible fouling.

Previous studies have demonstrated that such an approach that can readily detect colloidal fouling in SWM. For example, colloidal silica was used to foul both a SWM as well as a parallel canary under similar hydrodynamic conditions.[169] The increase in TMP was similar for both modules and autopsies of both the SWM and canary cell flat sheet membrane showed a strong correlation in foulant concentrations on both membranes. Coupled with non-invasive monitoring technique such as ultrasonic time domain reflectometry (UTDR), online in-situ measurement of fouling rates can be determined [170] instead of relying on TMP measurements and membrane autopsy methods. However, such an approach has not been established to detect or predict biofouling. This is partly due to the fact that biofouling is an active process, where bacteria in the feed water attach to the membranes and increase in biomass through cellular replication and biofilm formation. Therefore, an appropriate monitoring system must account for these processes to accurately identify when biofouling occurs.

UTDR was evaluated as a non-optical, non-invasive sensor to monitor biofouling, which was shown to have good sub-micron resolution and the ability to study at least two of the three regions affecting membrane processes; the membrane and the fluid boundary layer that includes the membrane-fluid interface and a cake or fouling layer. By investigating the changes in acoustic signals due to a change in the membrane system interface as biofouling progresses, the thickness of the biofilm layer could be estimated.

Another potential non-invasive biofouling monitoring technique is electrochemical impedance spectroscopy (EIS). Like UTDR, it is a non-optical method and does not suffer from the limitation faced by optical methods, making it feasible to employ as a biofouling monitor. By monitoring the changes in the dielectric properties of the membrane system with time, real time information about biofouling could be gathered.

The work presented here is divided in to 3 parts. The first part demonstrates the feasibility of using such a 'canary' system to model biofouling in SWM, the second and third parts describe the possibility of employing UTDR and EIS respectively to monitor biofouling *in situ*.

4.2 Materials and Methods

4.2.1 Canary cell modeling experimental considerations, equipment and materials

NaCl (Sigma–Aldrich) was used as the background electrolyte solution and Milli-Q water (Millipore) was used as the solvent to prepare NaCl solutions for all tests. The NaCl solutions were filtered (0.2 µm Model 597-4520, Nalgene) before use. An industrial, thin-film composite polyamide membrane spiral wound module (Dow, TW30-2540) with a length of 1 m, outer diameter of 61 mm and a nominal membrane surface area of 2.52 m^2 (0.90 m x 0.70 m x 4) was used in the experiments. The permeate spacer, feed spacers and membranes for the canary cell were obtained from an identical spiral wound module.

The canary cell (Figure 4.1) consisted of a rectangular parallel plate crossflow cell (AR Engineering, custom-made) with a membrane area of 0.0186 m^2 (0.31 m x 0.06 m) and received feed water from the same feed tank as the spiral wound module (SWM) via a side stream from the main pipe leading to the SWM.

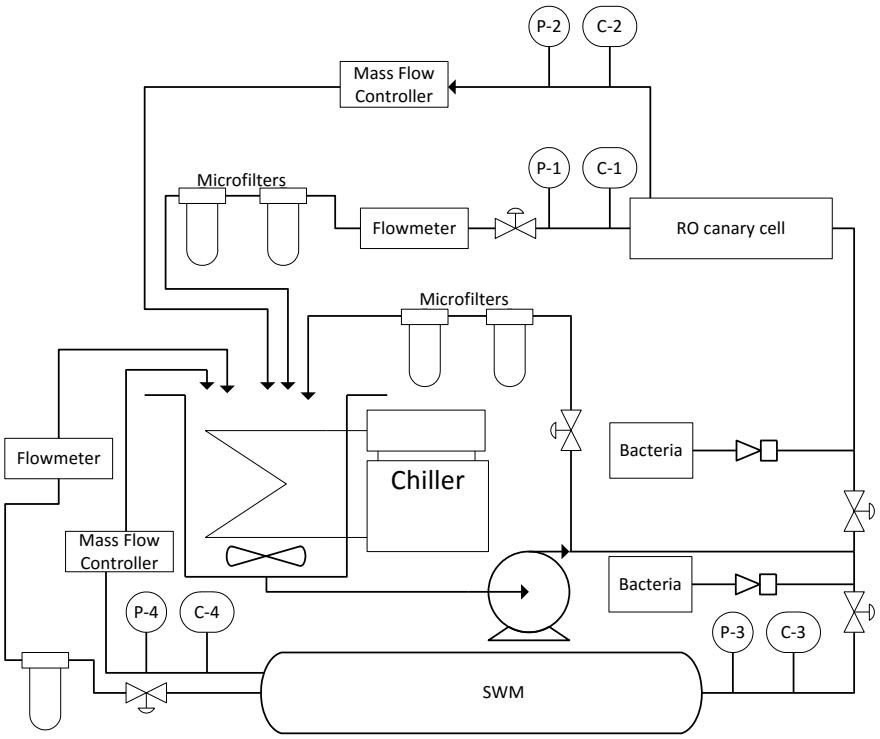

Figure 4.1 Schematic diagram of the crossflow SWM and canary cell RO system used in this study. Feed water was pumped to both the SWM and RO canary cell and both the concentrate and permeate from each flow line were returned to the feed tank to be recycled. P1-P4 represent pressure gauges to measure the pressures at various points in the process in determining TMP. C1-C4 represents conductivity meters to measure the conductivity of the feed and permeate streams at various points. Bacteria were injected into the system right before the SWM and RO canary cell and were filtered off by microfilters before the feed was recycled. Flux and flow rates were controlled by the mass flow controllers and the flow control valves.

A positive displacement pump (HYDRA-CELL, Model D10E) was used to pump water from the 30 l feed tank that was continuously stirred to ensure homogeneity. The temperature of the feed was kept constant at 30˚C (±0.3˚C) using a chiller (Polyscience, Model 9612) controlled by a temperature transmitter (Dwyer, Model 651A-10). The permeate flux for the canary cell and the SWM was controlled by two different mass flow controllers (Brooks Instrument, Model 5882 for the canary cell; Bronkhorst Cori-Tech,

Model M55AAD55OS for the SWM) and the TMP was measured with the use of pressure gauges (Ashcroft, Model 2174). The salinity of the feed and permeate streams for both the canary cell and the SWM were measured using a conductivity meter (Thermo Scientific; Model Alpha Cond 500).

Similar to other biofilms studies [171-173] *Pseudomonas aeruginosa* PA01, one of the best studied biofilm forming organisms, which can also be found in seawater, was used for membrane fouling studies. The bacteria were grown overnight in a 750 ml solution of 5 g l^{-1} Nutrient Broth (NB; Difco) and 2 g l^{-1} NaCl at 30ºC with shaking at 200 rpm. The bacterial cells were subsequently harvested by centrifugation at 18,514 *g* for 10 min. The pellet was washed and resuspended in sterile PBS to an OD_{600} of 0.1. To standardize the bacterial load and to ensure that the bacteria have sufficient nutrients to maintain active growth, the stock bacterial solution was replenished with freshly prepared stock daily.

To ensure that the biofouling rate in the canary cell and the SWM were similar, the rate of nutrients deposited on the membrane with respect to time must be similar and this was achieved by ensuring the Peclet number of the canary cell and the SWM were similar. The Peclet number is defined as the product of the Reynolds number, which describes the hydrodynamics of the fluid and the Schmindt number that describes the diffusive behaviour of the substance contained by the fluid. Theoretically, the Schmindt number is the same for both the canary cell and the SWM since the nutrients and bacteria injected into the system are the same for both. As such, only the Reynolds number needed to be considered here.

The effects of the spacer installed into the SWM and canary cell has to be considered to obtain an accurate Reynolds number since the area taken up by the spacer reduces the effective osmotic area of the membrane. Subsequently, the Reynolds number was calculated for the canary cell and SWM. The method of calculation of Reynolds number

and the effective membrane area after taking into account the effects of spacer is shown below.

The effective crossflow velocity, v, is given by the total flow rate, Q, divided by the effective total cross sectional area [174]

$$v = \frac{Q}{\varepsilon_{sp} h_{sp} w} \quad (4.1)$$

where ε_{sp} is the channel voidage, w is the canary cell channel width and h_{sp} is the height of the spacer used (equal to the feed spacer thickness provided by manufacturer).

Figure 4.2 shows a schematic of the rhomboid type spacers used in the SWM; ε is defined by:

$$\varepsilon = 1 - \frac{\pi d_f^2}{2 l_m h_{sp} \sin\theta} \quad (4.2)$$

where d_f the diameter of spacer filaments, l_m is mesh size, and θ is the angle in Figure 4.2. A digital light microscope (KEYENCE, Model VH-Z100R) was used to measure the dimensions of the spacer used. An average of four measurements was used as the values for l_m and d_f of 2.53 mm and 0.40 mm, respectively. The angle θ of the spacer was 90°.

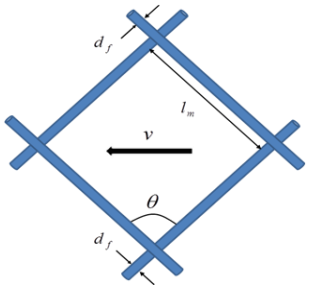

Figure 4.2 Schematic of the rhomboid spacer used, showing the spacer filament diameter d_f, mesh size l_m and angle θ.

The mass balance for the solvent in the canary cell is given by Eq. 4.3:

$$Q_{f,cc} = Q_{0,cc} - J_{cc}L_{cc}w_{cc} \tag{4.3}$$

where $Q_{f,cc}$ and $Q_{0,cc}$ are the amounts of solvent on the feed and outlet side, respectively, of the canary cell, w_{cc} is the width of the canary cell, L_{cc} is the length of the canary cell and J_{cc} is the volumetric permeation flux in the canary cell.

Note that Eq. 4.3 divided by cross-sectional area of the canary cell implies that

$$v_{f,cc} = v_{0,cc} - \frac{J_{cc}L_{cc}}{\varepsilon_{sp}h_{sp}} \tag{4.4}$$

where $v_{f,cc}$ and $v_{0,cc}$ are the effective linear velocities of the liquid on the feed and outlet side, respectively, of the canary cell. Figure 4.3 shows a schematic of the canary cell under constant flux operation.

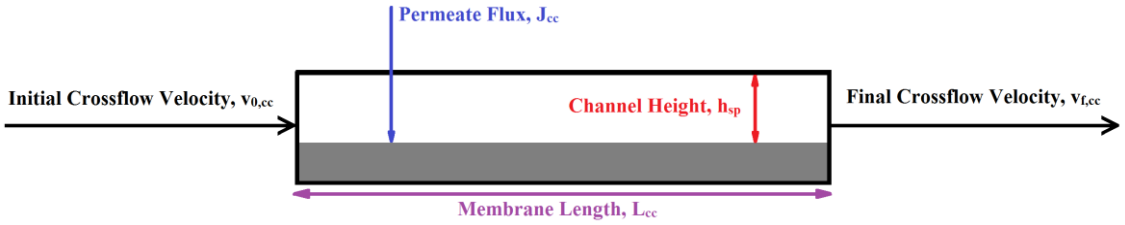

Figure 4.3 Schematic of the canary cell under constant flux operation. As the feed goes into the canary cell with a length of L_{cc} and channel height h_{sp} at an initial crossflow velocity $v_{0,cc}$, some of the water passes through the membrane resulting in permeate flux J_{cc} while the result concentrate exits the canary cell at a final crossflow velocity $v_{f,cc}$.

The mass balance for the solvent in the SWM is given by Eq. 4.5:

$$Q_{f,SWM} = Q_{0,SWM} - 2nJ_{SWM}L_{SWM}w_{SWM} \tag{4.5}$$

Where $Q_{f,SWM}$ and $Q_{0,SWM}$ are the flow rates of the solvent on the feed and outlet side, respectively, of the SWM, w_{SWM} is the width of each membrane leaf in the SWM, L_{SWM} is the length of the SWM, n is the number of membrane leaves in the SWM and J_{SWM} is the volumetric permeation flux in the SWM. Figure 4.4 shows the schematic of the feed channel between two membrane sheets in a spiral wound module under constant flux operation.

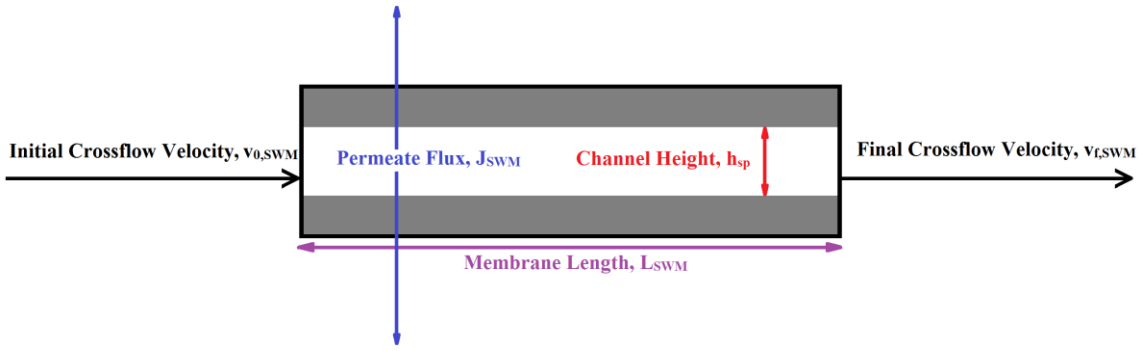

Figure 4.4 Schematic of a channel sandwiched between two membrane sheets in a spiral wound module under constant flux operation. Similar to that of the canary cell, the feed goes into the SWM of length L_{SWM} and channel height h_{sp} at an initial crossflow velocity $v_{0,SWM}$, some of the water passes through the membrane resulting in permeate flux J_{SWM} while the result concentrate exits the SWM at a final crossflow velocity $v_{f,SWM}$.

Note that Eqn. 4.5, divided by cross-sectional area of the SWM, implies that

$$v_{f,SWM} = v_{0,SWM} - \frac{2J_{SWM}L_{SWM}}{\varepsilon_{sp}h_{sp}} \qquad (4.6)$$

Where $v_{f,SWM}$ and $v_{0,SWM}$ are the effective linear velocities of the liquid on the feed and outlet side, respectively, of the SWM.

The Reynolds number is given by Eq. 4.7,

$$\mathrm{Re_i} = \frac{\mathrm{d_h}\rho\left(\mathrm{v_{0,i}}+\mathrm{v_{f,i}}\right)}{2\mu} \tag{4.7}$$

Where the subscript i refers to either the canary cell or spiral wound module and d_h is the hydraulic diameter.

In the presence of the feed channel spacer, the hydraulic diameter is given by

$$d_h = \frac{4\varepsilon_{sp}}{\frac{2}{h_{sp}}+\frac{4(1-\varepsilon_{sp})}{d_f}} \tag{4.8}$$

Substituting Eq. (4.4) into Eq. (4.7) gives the Reynolds number for the canary cell,

$$Re_{cc} = \frac{d_h \rho L_{cc}}{\varepsilon_{sp} h_{sp} \mu}\left(\frac{Q_{0,cc}}{w_{cc}L_{cc}} - \frac{J_{cc}}{2}\right) \tag{4.9}$$

Substituting Eq. (4.6) into Eq. (4.7) gives the Reynolds Number for the SWM,

$$Re_{SWM} = \frac{d_h \rho L_{SWM}}{\varepsilon_{sp} h_{sp} \mu}\left(\frac{Q_{0,SWM}}{n w_{SWM} L_{SWM}} - J_{SWM}\right) \tag{4.10}$$

4.2.2 Canary cell modelling experiment procedures

For all experiments, the membranes in the canary cell were soaked in Milli-Q deionised water for over 12 h. Subsequently, the membranes in the canary cell and the SWM were first compressed at a flux of 50 l m^{-2} h^{-1} (LMH) and a crossflow velocity of 0.1 m s^{-1} overnight with deionised water to achieve a stable flux. The flux then was adjusted to the

desired value and the system was allowed to stabilize before the addition of the filtered salt solution, where 200 g l^{-1} of concentrated NaCl solution and stock Nutrient Broth (NB, difco) solution was added into the feed tank to achieve a final concentration of 2 g l^{-1} of NaCl and 24 mg l^{-1} NB and the system was mixed for 2 h before starting the injection of bacteria via two separate pumps for the canary cell and SWM respectively. At the start of each day, the feed was changed with fresh feed of the same initial composition and 50 cm^3 sample of the feed was removed for total organic carbon analysis to ensure constant nutrients level in the tank after each feed change.

4.2.2.1 Membrane autopsy and biofilm characterization

Nine regions each of approximately 30 cm by 23 cm were obtained by cutting the inner 2 membranes of the SWRO. Then, six 2 x 2 cm^2 samples were cut out from the centre of each region, as illustrated in Figure 4.5.

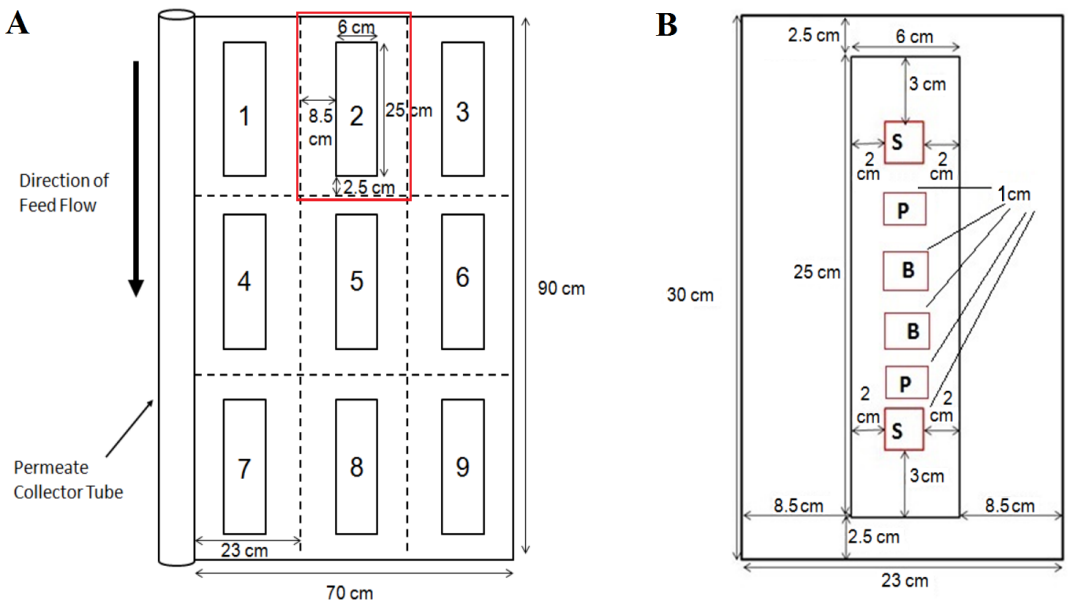

Figure 4.5 (A) The SWM was divided into 9 different regions for spatial analysis. The red box outlines one particular region. (B) A close up view of each region showing six 2 x 2 cm^2 membrane coupons obtained for biofilm analysis (S for polysaccharide analysis, P for protein analysis and B for bacteria cell counts).

The samples were then placed into their corresponding test tubes along with 10 ml of 3.2 g l^{-1} NaOH solution. The 2 x 2 cm^2 samples were analysed for the different foulants according to Figure 4.5B. The tubes were agitated using ultrasonication (Model FB15068, Fisher Scientific) for 1 min to allow the biofilm to detach from the membrane. Each tube was then mixed well with a vortex (Velp Scientifica, Model RX3) for 10 s. Thereafter, 1 ml of solution was withdrawn for CFU counts. Then, the membrane samples were left in the refrigerator at 4˚C for 24 h before being analyzed for EPS and bacterial contents. Similar methods were used for the canary cell.

4.2.2.2 Polysaccharide analysis

Polysaccharides were measured by the colorimetric method [175] where 5 ml of concentrated $H_2SO_4$and 1 ml of 5% wt/vol phenol solution were added to 2 ml of sample solution and left to cool for 10 min so as to dissipate the heat generated by the exothermic reaction upon mixing. Then, 1 ml of each mixture was added into a glass cuvette before being inserted into the UV-VIS spectrophotometer (Shimadzu, Model UV -1800) to obtain the value of absorbance at 490 nm. Using glucose to generate a standard curve, the polysaccharide concentration was determined at an absorbance of 490 nm.

4.2.2.3 Protein analysis

Coomassie (Bradford) Protein Assay Reagent was used to determine the protein concentration, where 1 ml of the assay reagent was mixed with 1 ml of sample solution and was incubated for 10 min. Then, one ml of each mixture was added into a glass cuvette and quantified at 595 nm using a UV-VIS spectrophotometer (Shimadzu, Model UV -1800). Bovine serum albumin (BSA) was used to generate a standard curve for comparison.

4.2.2.4 Bacterial counts

Ten-fold serial dilutions were performed for the bacterial samples using a sterile solution of 2 g l^{-1} of NaCl as the diluent. At each dilution, 100 µl of the solution was transferred to the centre of a sterilized agar plate using a sterile pipette and spread across the plate using a sterile spreader. The sterile agar plates were prepared from a solution containing 8 g l^{-1} of Nutrient Broth (BD Difco) and 14 g l^{-1} of agar (BD, Bacto agar). After spreading the bacteria, the plates where incubated for 1 d at 37˚C and the number of colonies present in each sample were counted.

4.2.3 UTDR biofouling experimental design, equipment and materials

The RO setup used in this chapter was similar to that in section 4.2, with only a few changes. In this study, only the flat sheet canary cell was used, and the UTDR system was fitted to the setup to perform the UTDR measurements, as shown in Figure 4.6.

The ultrasonic transducer (Olympus Model Videoscan, V-109RM), high voltage pulser and receiver (Panametrics 5058PR), and digital oscilloscope (National Instruments, Model PCI-5152) formed the three essential constituents of the UTDR system. An electrical signal was sent from the pulser to excite and create vibrations of piezoelectric crystals in the transducer to generate and receive the ultrasonic waveforms. The digital oscilloscope was used to transform the received ultrasonic waves from the transducer into perceptible waveforms of signal voltages and allowed for the logging of the data for post analysis.

Special considerations were required to successfully adapt the use of UTDR for membrane fouling monitoring. The membrane module surface where the transducer was to be mounted had to be flat and coupled appropriately to allow proper propagation of the acoustic waves through the medium and to avoid unwanted signal attenuation.[107] The

transducers could not be mounted near the extreme ends of the membrane module as the hydrodynamic flow is less stable stable at those positions. To confirm the accuracy of the UTDR measurements, offline CLSM measurements were also performed to complement the UTDR measurements in determining biofilm thickness.

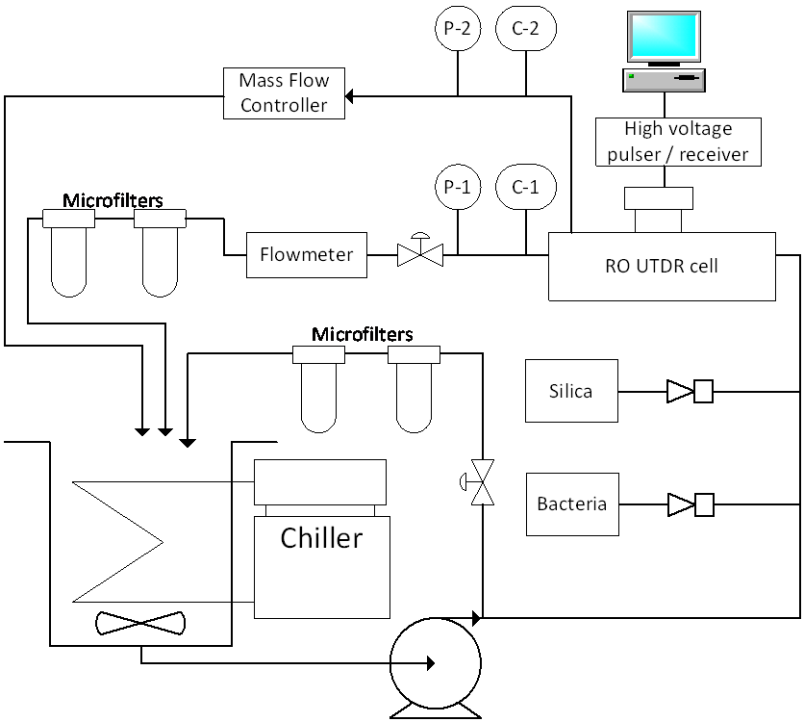

Figure 4.6 Schematic diagram of the RO-UTDR system used in this study. Feed water was pumped to the RO cell and both the concentrate and permeate were returned to the feed tank to be recycled. Both colloidal silica and bacteria were injected into the system right before the RO cell, with the bacteria filtered off by microfilters before the feed was recycled. TMP and salt concentrations were monitored by pressure gauges (P-1 and P-2) and conductivity meters (C-1 and C-2). Flux and flow rates were controlled by the mass flow controllers and the flow control valves. The UTDR system includes a pulser and receiver, an oscilloscope, and a transducer fitted to the RO cell.

4.2.4 RO UTDR biofouling experimental procedure

A series of biofouling experiments ranging from 24 h to 72 h were performed, and for all experiments, the membranes in the canary cell were soaked in Mili-Q water for over 12 h. Subsequently, the membrane in the membrane cell was first compressed at a flux of 50 l m^{-2} h^{-1} (LMH) and a crossflow velocity of 0.1 m s^{-1} overnight with deionised water to achieve a stable flux. The flux then was adjusted to the desired value and the system was allowed to stabilize before the addition of the filtered salt solution, where 200 g l^{-1} of concentrated NaCl solution and stock NB solution was added into the feed tank to achieve a final concentration of 2 g l^{-1} of NaCl and 24 mg l^{-1} NB and the system was mixed for 2 h before starting the injection of bacteria via two separate pumps for the canary cell and SWM respectively. At the start of each day, the feed was changed with fresh feed of the same initial composition and 50 cm^3 sample of the feed was removed for total organic carbon analysis to ensure constant nutrients level in the tank after each feed change.

UTDR analysis was performed every 24 h. To measure the biofilm thickness using UTDR, colloidal silica (0.2 g l^{-1} final concentration) was added into the inlet to increase the biofilm acoustic impedance and was allowed to drain out at the outlet end without returning to the feed tank for 30 min daily. During the 30 min, UTDR measurements were taken and recorded by the oscilloscope. After the 30 min of silica dosing, the system was flushed with synthetic feed solution to remove excess silica before the retentate was returned to the feed tank.

4.2.4.1 Measurement of biofilm thickness using CLSM

At the end of each (24, 48 or 72 h) experiment, the membrane was removed from the module and a section was cut and stained using the LIVE/DEAD BacLight bacterial viability kit (Invitrogen) as per the manufacturer's instructions. The slides were then washed again in 0.85% NaCl to remove excess stain. Live, SYTO-9 stained cells and

dead, propidium iodide (PI) stained cells were visualized by confocal laser scanning microscopy (CLSM) (Nikon eclipse 90i, part of the A1R hybrid confocal spectral imaging system) at a magnification of ×200, with an argon laser (488 nm excitation for SYTO-9) and a diode laser (561 nm excitation for PI). For each section, z stack (3D) confocal images were obtained from 5 locations covering the membrane surface, and the average biovolume (μm^3) and surface coverage (%) was calculated using IMARIS (Bitplane, version 7.3.1).

4.2.5 EIS biofouling experimental design, equipment and materials

The RO-EIS setup is shown in Figure 4.7. The feed water was channeled from a 10 l feed tank using a high-pressure pump (Model F21EASQSFEHQ, Hydra-Cell) to an cross-flow impedance RO module (INPHAZE™). The retentate and permeate were recycled back to the feed tank during the experiment. Temperature of the feed solution was maintained at 24 ± 1^oC with a chiller (PolyScience, Model 9106AA2P). An overhead electric stirrer was used to ensure the homogeneity of the feed solution throughout the experiment. System pressure and flow rates were controlled with the use of back pressure regulators (Swagelok) and flow control valves respectively. Feed and permeate pressures were monitored with pressure gauges (Ashcroft, model302174SD02L600#ZZ). The flow rate of the feed stream were measured by two flow meters (Coleparmer, model PMR1-010640 and model PMR 1-010-210). The salinity of the feed and permeate were monitored using conductivity meters (EUTECH Instruments, model alpha COND500). The permeate flux was controlled by a mass flow controller (Brooks Instrument, model 5882/D1A1/A4B001).

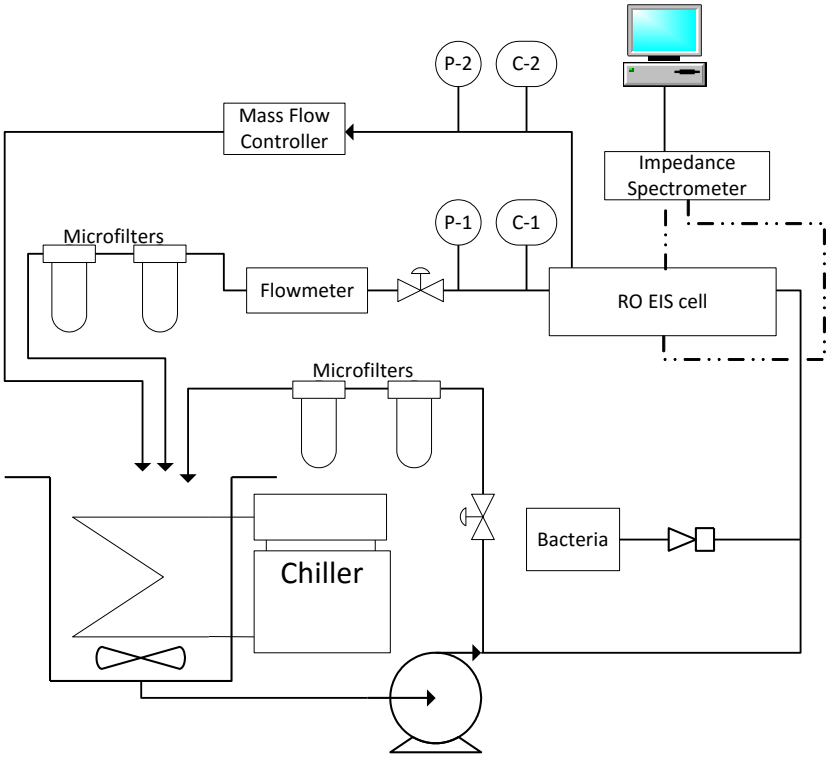

Figure 4.7 Schematic diagram of the RO-EIS setup used in this study. Feed water was pumped to the RO cell and both the concentrate and permeate were returned to the feed tank to be recycled. Bacteria were injected into the system right before the RO cell and filtered off by microfilters before the feed was recycled. TMP and salt concentrations were monitored by pressure gauges (P-1 and P-2) and conductivity meters (C-1 and C-2). Flux and flow rates were controlled by the mass flow controllers and the flow control valves. The RO cell was connected to an impedance spectrometer via specialized electrodes.

4.2.6 EIS experimental procedure

A series of biofouling experiments ranging from 24 h to 120 h were performed, and for all experiments, the membranes were soaked in Mili-Q water for over 12 h. Subsequently, the membrane in the membrane cell was first compressed at a flux of 50 l m^{-2} h^{-1} (LMH) and a crossflow velocity of 0.1 m s^{-1} overnight with deionised water to achieve a stable flux. The flux then was adjusted to the desired value and allowed to stabilize before the

addition the filtered salt solution, where 200 g l^{-1} of concentrated NaCl solution and stock NB solution was added into the feed tank to achieve a final concentration of 2 g l^{-1} of NaCl and 24 mg l^{-1} NB and the system was mixed for 2 h before starting the injection of bacteria via two separate pumps for the canary cell and SWM respectively. At the start of each day, the feed was changed with fresh feed of the same initial composition and 50 cm^3 sample of the feed was removed for total organic carbon analysis to ensure constant nutrients level in the tank after each feed change.

EIS analysis was performed at regular intervals. These measurements, inclusive of the phase difference between the current and voltage, were recorded through a dedicated software (Inphaze™, Sydney). The measured information then yielded the capacitance and conductance of the sample at each of the known frequencies. Each EIS spectrum over the frequencies ranges from 0.1 to 100,000 Hz requires about 30 min of recording time.

4.3 Results

4.3.1 Correlation of TMP and membrane autopsy between the SWM and canary cell

It was observed that under similar hydrodynamic conditions, both the SWM and the canary cell exhibited similar TMP profiles. At 25 LMH there was only a 6.18% and 2.39% difference in TMP between the SWM and canary cell at the end of the biofouling experiment for two replicate runs A and B (Figure 4.8) respectively. The experiments were also conducted at 35 LMH, and both the SWM and the canary cell showed similar TMP profiles as well, with differences of 12.70% and 5.27% in final TMP between the SWM and canary cell for replicated runs C and D respectively. Periodic spikes and fluctuations in TMP occurred at the time of feed change, where the feed was changed in batches, resulting in temporary changes in the temperature of the feed and thus the TMP. In both cases, it was noteworthy that the canary cell showed a slightly higher increase in

TMP than the corresponding SWM. This showed that the canary cell was more sensitive to the onset of biofouling than the SWM, making it a viable early warning monitoring tool.

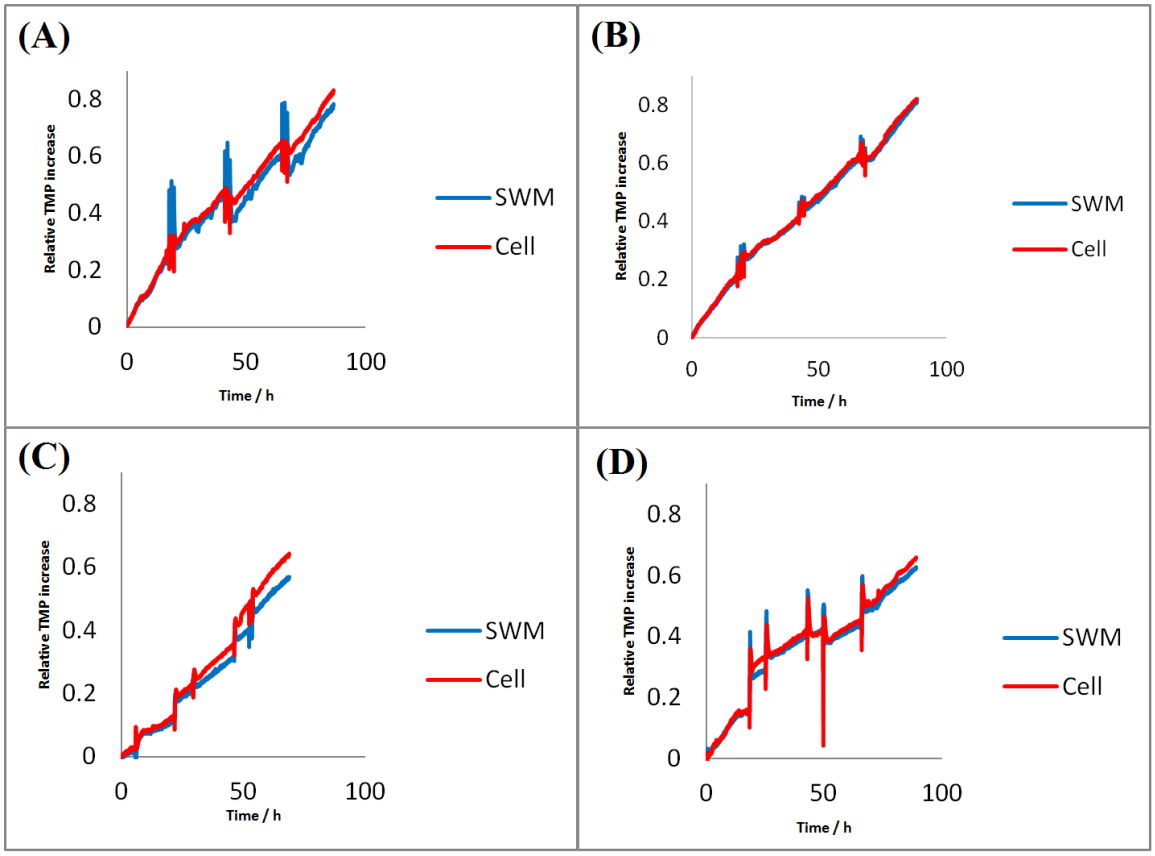

Figure 4.8 TMP profiles of replicate RO biofouling processes with the SWM in parallel with the canary cell operating at a flux of (A and B) 25 LMH and (C and D) 35 LMH.

Figures 4.9, 4.10 and 4.11 represent the respective concentrations of protein, bacteria and polysaccharides isolated from the membranes collected from SWM and the canary cells. It is interesting to note that in general, the concentration of foulants was highest at region 1, which was closest to the inlet, while the concentration at region 9, the farthest away from the inlet, was generally the lowest. This suggests a trend of decreasing foulant concentration as the regions progress horizontally and vertically in distance from the inlet, which was predicted in previous simulation studies.[176] Local flux decreases across the module length from the inlet to the outlet due to the pressure loss along the feed channel.

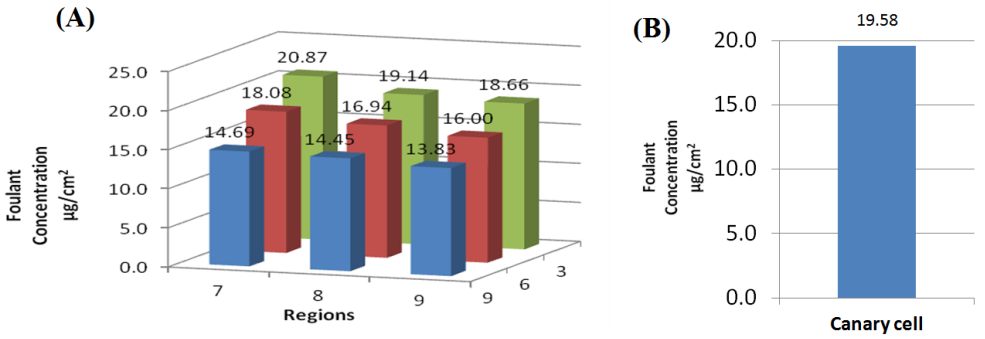

Figure 4.9 Protein concentration distribution across the membrane sections of the SWM (A) and on the canary cell membrane (B).

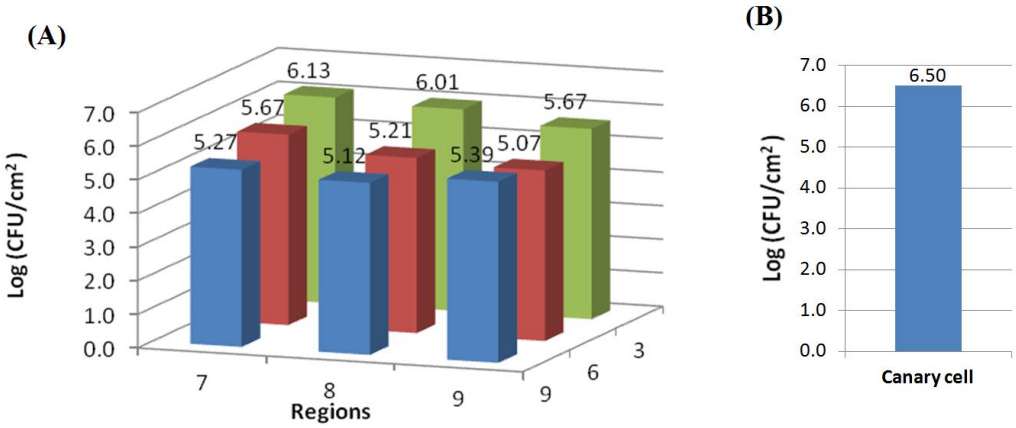

Figure 4.10 Bacteria concentration distribution across the membrane sections of the SWM (A) and on the canary cell membrane (B).

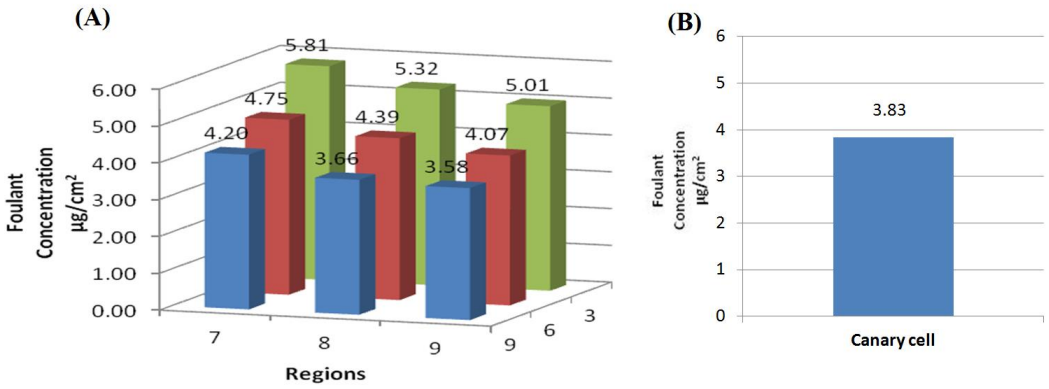

Figure 4.11 Polysaccharide concentration distribution across the membrane sections of the SWM (a) and on the canary cell membrane (b).

The highest flux was achieved at the inlet region closest to the permeate tube and the lowest flux is achieved in the opposite corner near the closed end of the permeate channel due to the pressure loss along the permeate channel.

For the SWM, region 1 had the highest concentration of protein (20.87 µg cm^{-2}), bacteria (1.99 x 10^6 CFU cm^{-2}) and polysaccharide (5.81 µg cm^{-2}) as it was the region nearest to the inlet and permeate tube, where localized flux was the highest. Region 9 had the lowest concentration of protein (13.83 µg cm^{-2}) and polysaccharide (3.58 µg cm^{-2}) as it was the region near the outlet furthest away from the permeate tube. However, region 9 did not have the lowest concentration of bacteria (2.45 x 10^5 CFU cm^{-2}) even though it was the region near the outlet furthest away from the permeate tube. This could be due to slight difference in the time different regions were exposed to the environment during membrane autopsy. The corresponding canary cell did not experience a significant pressure drop across the cell as opposed to that of the SWM due to its relatively smaller area. Hence, the foulant concentration across the membrane was assumed to be uniform and had a difference of 13.4%, 15.1% and 15.5% in protein, bacteria and polysaccharide concentration respectively compared to the SWM average.

4.3.2 UTDR biofouling monitor

Over the course of up to 72 h, the TMP was observed to only increase up to about 5.1% (Figure 5.2). However, UTDR and CLSM analysis revealed that there was a significant amount of biofilm that formed as early as 24 h after the start of the experiment. Within 24 h, biofilm thickness was approximately 9.23 µm (UTDR) and 7.81 µm (CLSM). An additional 48 h only caused the biofilm thickness to increase to 13.07 µm (UTDR) and 10.40 µm (CLSM), or about 33% to 42%.

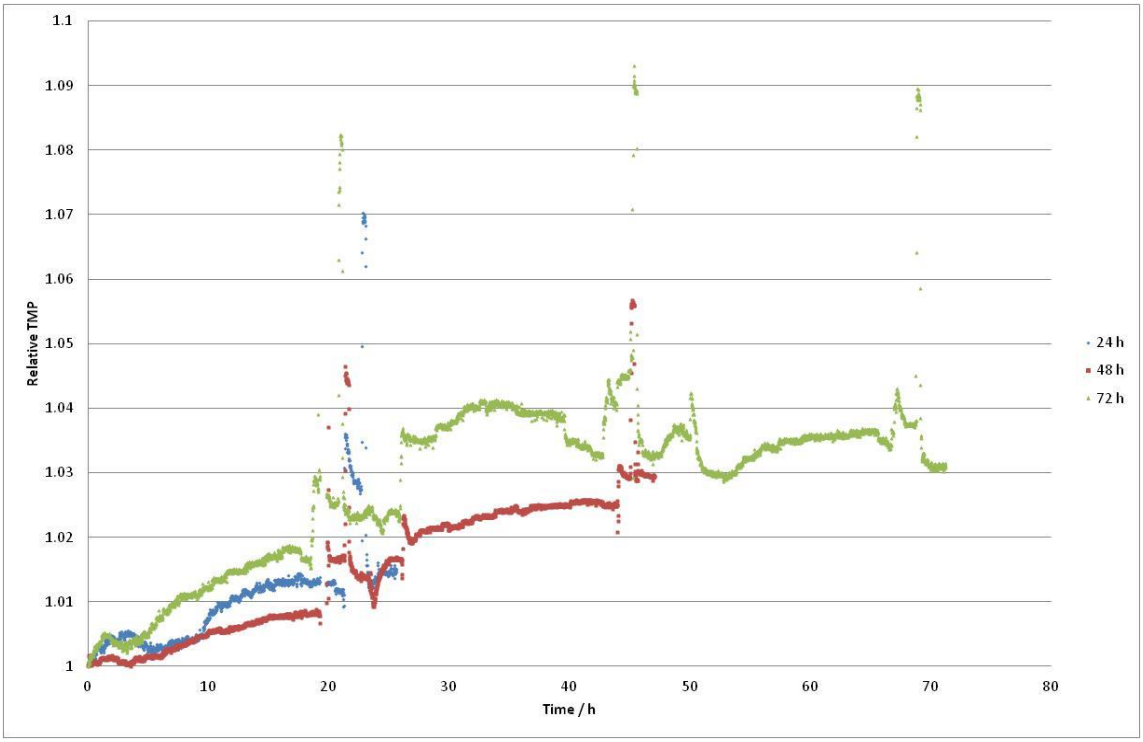

Figure 4.12 TMP profile for 24 h (blue), 48 h (red) and 72 h (green) biofouling experiment running at crossflow conditions at flux of 35 LMH.

Figure 4.13 shows one UTDR signal measured after 24 h, where peaks A and B were identified as the peaks responsible for the membrane/foulant-feed solution interface and the membrane-bottom plate interface respectively, based on calculations using the velocities of sounds in the materials involved, namely Perspex (2800 m s^{-1}), water (1500 m s^{-1}) and polymeric membrane (2000 m s^{-1}).[170] By measuring the difference in peak arrival times as the fouling progresses, the biofilm thickness can be determined.

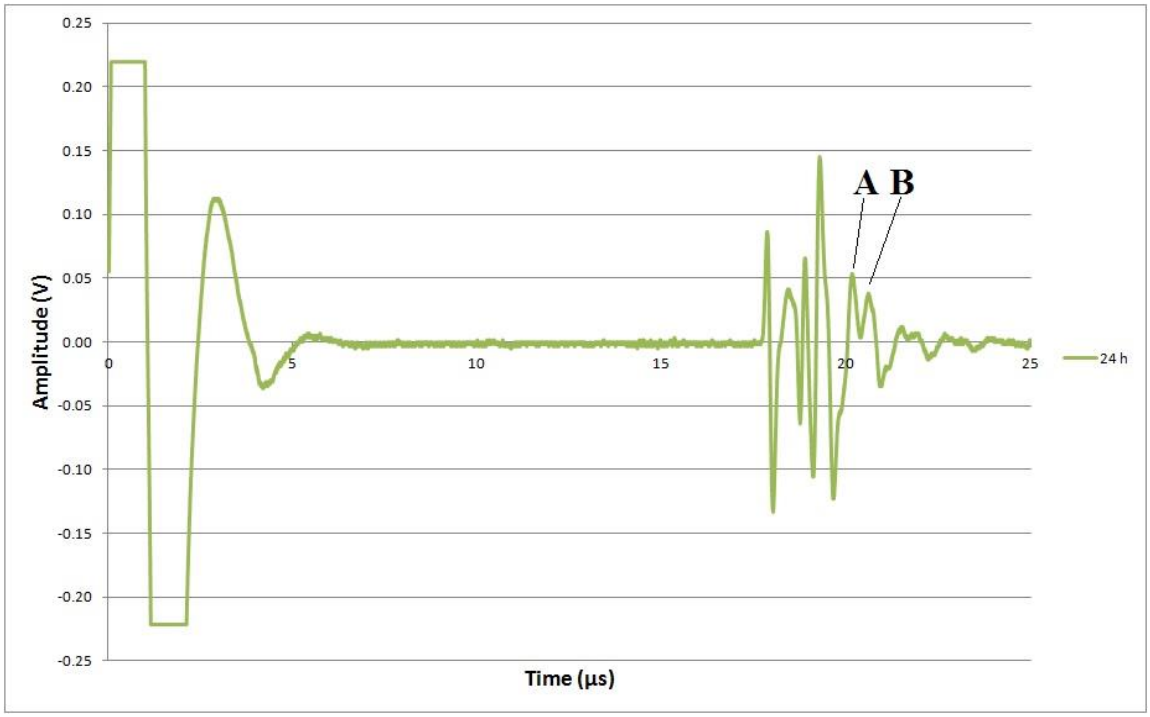

Figure 4.13 UTDR waveform signal after 24 h of biofouling. Peaks A and B were identified as the peaks of interest.

Table 4.1 summarises the biofilm thickness measured by both UTDR and CLSM compared to the actual TMP increase during 24, 48 and 72 h of biofouling. Biofilm thickness determined via UTDR measures are 15.3% to 26% higher than corresponding thickness determined via CLSM analysis.

Table 4.1 Correlation between TMP, UTDR and CLSM analysis.

Biofouling duration (h)	TMP rise	Biofilm thickness (UTDR) / µm	Biofilm thickness (CLSM) / µm	% difference
24	1.9%	9.23	7.81	15.3
48	3.4%	10.76	7.96	26.0
72	5.1%	13.07	10.40	20.4

4.3.3 EIS biofouling monitor

Several EIS spectra were taken over the 5 d duration of the biofouling experiment and a signature Nyquist plot was derived for each spectrum. Figure 4.14 shows the overlay of all the Nyquist plots over the period of the experiment. It can be seen that as fouling progresses, the Nyquist plot shifted towards a lower real impedance (Z_{re}) until a point (at about 1.71 d) before changing directions and shifting towards higher Z_{re}.

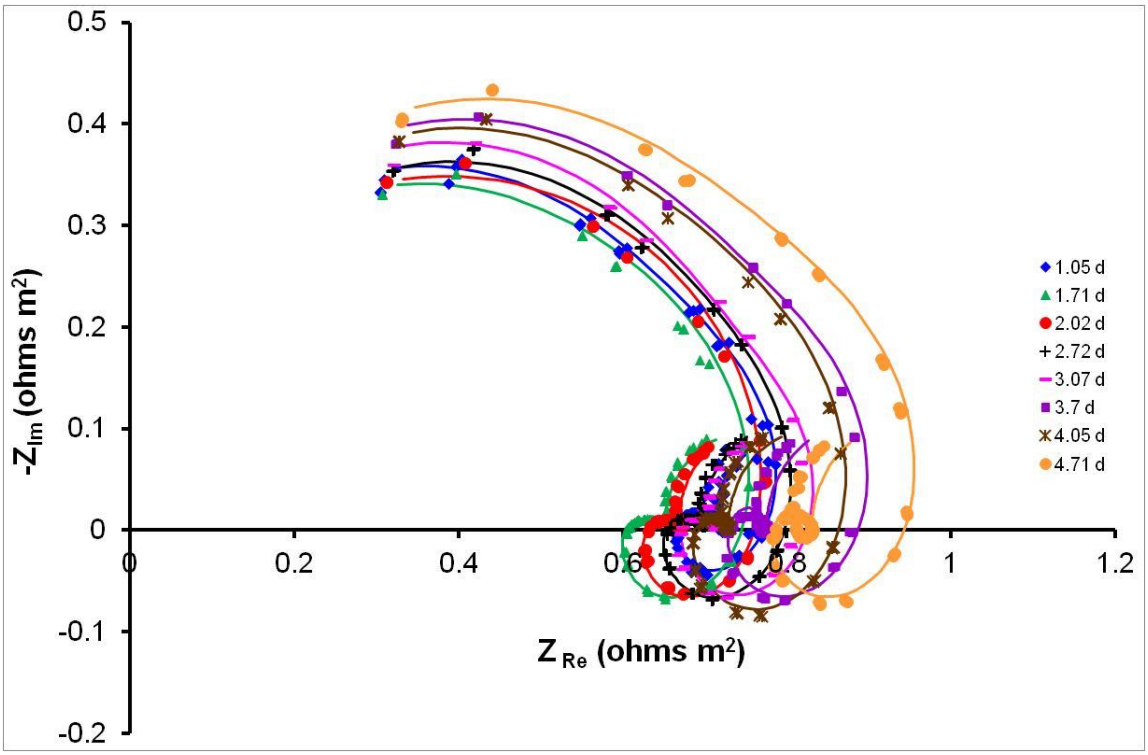

Figure 4.14 Nyquist plot overlay over 5 d biofouling. Each data set corresponds to measurements taken at the same time, and comprises of Z_{Re} and $-Z_{Im}$ measurements over the range of EIS frequencies.

Another way to interpret EIS data is to look at the change in conductance at the diffusion polarization layer (membrane-solution interface) with time, derived from the same Nyquist plots. From Figure 4.15, it can be seen that the conductance increased about 28% at around 1.7 d before decreasing.

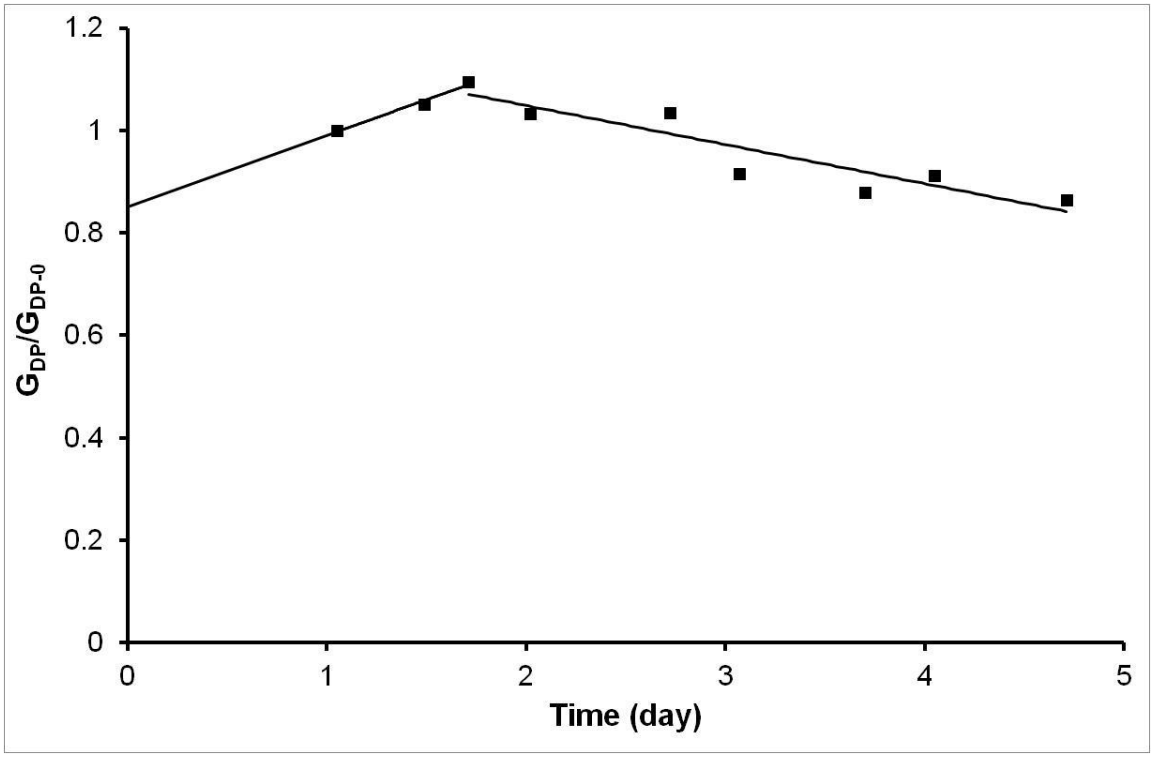

Figure 4.15 Normalised EIS biofouling conductance with time. An increase in y-value indicates an increase in electrical conductance at the membrane boundary or diffusion polarization layer.

4.4 Discussion and conclusions

One of the key aims in biofouling monitoring is to develop a model or a system which can give accurate information regarding the extent of biofouling within a SWM without having to stop the filtration process and perform a membrane autopsy, without just rely on TMP values. A canary cell model was developed to address this problem. The results show that there was a strong correlation between the TMP as well as EPS and bacterial numbers between the canary cell and SWM, thus establishing that not only can the canary cell be used to monitor colloidal fouling, but that it is also suitable as a monitor for biological fouling.

When the biofouling on the SWM was spatially mapped, it was observed that there was a trend of decreasing foulants from the inlet to the outlet and this can be explained through the distribution of foulants along the membrane.[174, 177] As the nutrient concentration decreases from the inlet to the outlet, there is a decrease in the number of bacteria deposited onto the regions with lower nutrient concentration. This may be due to the preferential deposition of bacteria in areas with higher nutrient, due to chemotaxis, as well as the more rapid increase in cell numbers due to utilization of those nutrients and subsequent bacterial growth.[178]

The faster buildup of foulants in the canary cell relative to the average of all regions tested for the SWM can be explained by the nature of biofilm formation. In the early stages of biofilm formation, bacteria adhere to the membrane surface using weak Van Der Waal's forces or hydrophobicity [179] before forming a stronger interaction with the membrane through the secretion of biofilm matrix materials, resulting in irreversible attachment.[180] These forces associated with initial, reversible attachment to the membrane, can be overcome by flowing water with high energy, e.g. elevated cross-flow velocity. Thus, the higher flow rate in the SWM relative to the canary cell may provide this higher dislodging force to reduce or delay the overall initial attachment of bacteria to the membrane surface. The overall effect of this would be a reduced or slowly fouling rate for the SWM compared to the canary cell.

The successful demonstration of the canary cell to simulate biofouling in a SWM strongly supports the implementation of such a system to provide in situ information of biofouling in the SWM, which can be used to manage cleaning regimens to mitigate fouling. This surpasses the current best practice of monitoring changes in the TMP as a proxy for fouling, which is highly limited and can give misleading information. For example, the TMP rise can be due to several factors [181] including foulant and salt accumulation on

the membrane as well as effects of pH [182] and temperature [183] of feed water. The outcome may be more frequent cleaning than necessary or cleaning regimes that are not optimized, which increases operational costs. By reducing over cleaning, there can be substantial financial savings on top of reduced damage to the membrane by chemicals such as chlorine [184] that oxidize the membrane. Moreover, preventing the over usage of biocides and antibiotics on cleaning can reduce severe environmental repercussions of dumping cleaning reagents after cleaning.

In this study, UTDR was established to be a viable technique to monitor biofouling in real time. Traditionally, TMP was used as an indicator to determine the extent of fouling for RO membranes. However, it was observed that while there was only a nominal increase in TMP for up to the first 72 h of biofouling, a substantial amount of biofilm was observed at the membrane surface by both UTDR and CLSM analysis. This showed that TMP is not a good indicator for fouling and that when the TMP rises significantly above critical levels, the amount of biofilm on the membrane surface would have been too thick and dense for it to be removed completely during membrane cleaning.

It was observed that the UTDR measurement always gave a greater value for biofilm thickness as compared to CLSM analysis. This was because UTDR measured peak thickness of the biofilm as compared to the average thickness measured from CLSM analysis. Thus, UTDR may give an overestimate for the detected biofilm thickness, and can serve as a good early warning system. However, both methods do not provide any information regarding other properties of the biofilm, namely the density and porosity of the biofilm, which also contribute to the overall resistance of a fouled membrane.

By measuring the dielectric properties of the membrane cell, EIS was able to provide insights on the type of fouling that is occurring within the membrane system and the rate at which they occur and any changes that develop on the membrane surface. In a previous

study involving organic (bovine serum albumin) fouling, organic fouling resulted in a unidirectional shift towards higher Z_{re}, which is indicative of an overall decrease in conductance.[111] This was proposed to be due to a decrease in the diffusion of NaCl as the organic fouling layer builds up. This was however not the case in biofouling for this study. The initial increase in G_{DP} could be due to the accumulation of bacterial cells at the membrane surface, which increases the overall conductance due to their negatively-charged bacterial cell walls and increasing salt concentration polarization. As EPS is secreted and biofilms start to form, the reverse occurred as the biofilm hindered the salt passage across the membrane, and thus lowering the conductance of the layer. All of these events precede any noticeable increase in TMP and could be identified by EIS almost immediately, suggesting that EIS could potentially be used as an early warning indicator for the onset of biofouling which can enable operators to decide on the best time to apply fouling countermeasures. Further work is in progress to investigate the viability of this technique in monitoring changes in the biofouling layer during traditional cleaning procedures or during application of novel treatment strategies such as NO dozing. Both UTDR and EIS technique can be used in tandem and concurrently to provide complementary information about the biofouling membrane noninvasively, in real time.

To conclude, a method was developed, based on using an in-line flat sheet membrane chamber, dubbed a “Canary Cell” that could be used to monitor membrane fouling as it occurs in a SWM. The results show that both the canary cell and SWM foul at similar rates. The application of such a technology could significantly improve management of desalination processes reliant on SWM as it provides easy access to membrane for comparison. This technology could also be coupled with other in situ biofouling detection techniques such as EIS or UTDR to provide a comprehensive and convenient method of biofouling detection in SWM as well as the efficacy of cleaning regimens. Therefore, this approach can be used to tailor and optimize cleaning strategies for each desalination set-

up and the respective nature of biofouling in order to not only optimize cleaning but also come out with strategies to reduce biofouling.

CHAPTER 5 SUMMARY, CONCLUSIONS AND FUTURE WORK

Since it first emerged in the 1960s, reverse osmosis technology has undergone significant advances and is now one of the most, if not the most, attractive solutions to help meet our global water demands. The cost of water production using membranes has fallen over the past few decades, but is still far from reaching the theoretical thermodynamic limit. Membrane fouling, particularly biofouling, had been the Achilles heel to an otherwise elegant solution to our water needs. Bacteria and other microorganisms settle on membrane surfaces and forms biofilms, resulting in increased transmembrane pressures low water quality. While it is desirable to completely eliminate fouling, this is an unrealistic goal since microorganisms are evolutionarily adapted to biofilm formation and since biofilm formation increases the tolerance of biofilm encased cells to a range of stressors, including biocides.

Thus, it is of utmost importance that we adopt a multi-pronged approach in dealing with biofouling issues in RO. Exopolysaccharides are one of the main components in the biofilm matrix, and thus a greater understanding in its function and purpose is critical in developing strategies to reduce biofilm formation. In single species *P. aeruginosa* PAO1 studies, it was found that the Psl polysaccharide had the greatest impact on RO performance due to its structural properties, resulting in a biofilm that was less permeable to water than a biofilm without Psl. This is supported in another study which showed that Psl promotes highly crosslinked and elastic biofilms.[120] Although Pel appears to have negligible effect on single species biofouling, it was found that Pel promotes the formation of cohesive mixed species biofilms as opposed to Psl, which promotes species segregation in certain biofilms, and these might have a different impact in RO biofouling.[120] The lack of Alg did not significantly impact in biofouling, although an overproduction increased the fouling tendency in single species *P. aeruginosa* biofouling

because of increased biovolume. However, it was found that Alg enhanced the competitive fitness of *P. aeruginosa* in mixed species biofilms.[130] Thus, while Pel and Alg may not be important in fouling by monospecies biofilms of *P. aeruginosa*, it may be very important in mixed species communities, where *P. aeruginosa* facilitates biofilm development in a Pel and or Alg dependent fashion. One approach to deal with fouling issues due to bacterial biofilms is to target these exopolysaccharides. Several polysaccharides isolated from biofilm culture supernatants [185] were found to possess anti-biofilm capabilities. Culture supernatants of *Bacillus licheniformis* SP1 were able to alter biotic surface properties by decreasing cell surface hydrophobicity of *E. coli* and *P. fluorescens* cells.[186] *Lactobacillus acidophilus* A4 polysaccharide was found to down-regulate adhesion factors in *E. coli* O157:H7.[187] PAM galactan polysaccharide from *Kingella kingae* were found to disperse preformed *Staphylococcus epidermidis* biofilms.[188] These and many other anti-biofilm polysaccharides may potentially be used to treat biofouling in RO systems.

There is a need to further study and catalog the effects of other EPS constituents in the formation of mixed species biofilms and how they affect RO membrane performance. For example, it was found that proteins, on top of being an organic foulant [189], were involved in the initial attachment and conditioning of the surface due to hydrophobic interactions between protein non-polar groups and the polymeric membrane [190], which subsequently promotes the adhesion of bacterial cells on this protein layer.[191] Much research has also been done on the fabrication or modification of the membrane surface to achieve the right hydrophobicity to prevent the attachment of organics that form the initial conditioning film, although these efforts have not generally been successful. This is due in part to effects such as concentration polarization driven by flux phenomenon which cannot be eradicated completely. However, such insights can be used in forward osmosis,

where the driving force for water transport is based on osmotic pressure differences instead of hydraulic pressure differences.

Different RO plants around the world experiences biofouling caused by different communities of microorganisms, producing biofilms of varying relative amounts of exopolysaccharides, proteins, DNA, lipids and humic substances due to a fundamental difference in the nature of the feed water.[192] The fouling that these plants experiences are also not limited to biofouling, as other kinds of fouling like inorganic scaling may be of a greater problem due to the nature of the wastewater or seawater that it treats. Therefore it is of importance to isolate communities from different areas and perform geographically-specific research as a strategy developed based on the biofouling community at one site may not work as well on another site.

Just like the constant need for new antibiotics for medical purposes, there is also a constant need to further screen for novel chemical compounds that would ideally prevent or disrupt biofilm formation and are non-toxic. Nitric oxide (NO) is an important biological signal molecule that can induce the dispersal of biofilms. NO has been employed as part of many strategies in the control and regulation of bacterial biofilms. High levels of NO (30 ppm) resulted in biofilm formation in *Nitrosomonas europaea* while low non-toxic levels (<5 ppm) resulted in biofilm dispersal.[140] Low levels of NO also causes *P. aeruginosa* to transition to a planktonic state from the biofilm state, but enhances biofilm formation when NO concentrations increase beyond 25 μM.[50] Here, the effectiveness in using NO in the treatment of RO membrane biofouling, in both single species *P. aeruginosa* and multi-species biofilm was determined (Chapter 3). It was found that the addition of NO donor PROLI NONOate, our compound of interest, was able to reduce the rate of biofouling in both single species *P. aeruginosa* biofilm and mixed

species biofilm isolated from a local wastewater treatment plant. PROLI NONOate also did not significantly alter the community diversity within the mixed species biofilm, which was an important factor as any selection pressure exerted might lead to an emergence of a resistant strain which may give rise to another set of problems (Chapter 3). PROLI NONOate was also shown to have applications in other water purification processes such as membrane bioreactors, where NO addition also resulted in a reduction in biofouling [159], making this compound a viable option in many applications to control biofilms. New solutions for the control of biofouling would have to economically competitive with existing compounds for them to be widely adopted by industry. For example, the cost of chlorine, which is commonly used either for pre-treatment in RO or during backflushing in MBRs, is less than 1 Canadian Dollar per m^3 of treated water in Canada [193]. However, chlorine also has its drawbacks, such as potential damage to membrane integrity as well as the production of chlorine byproducts. Thus, compounds such as the PROLI-NONOate would have to be price competitive or provide a significant improvement in operation, time between cleaning or safety. Alternatively, the NO technology can be used in combination with traditional biocides. For example, it was found that exposure to NO increases the sensitivity of *P. aeruginosa* cells towards tobramycin and hydrogen peroxide, causing a 2 log decline in CFU numbers as opposed to antimicrobial treatments alone.[50] It was also observed that the addition of NO resulted in the reduction of all of the biofilm associated EPS components, consistent with the reduction of biofilm biovolume, but did not appear to selectively affect specific components such as polysaccharides. Therefore, a dual treatment using NO and potential exopolysaccharides-specific agents may further improve anti-biofouling efficiencies, and this is an area worth exploring.

The traditional method of using the rise in TMP to indicate fouling or biofouling is not an ideal approach due to the fact that the SWM is a complex, closed system that does not

allow for dynamic studies (as opposed to endpoint measurements) and that the onset of irreversible biofouling precedes the corresponding increase in TMP. The development of optical monitoring techniques such as Optical Coherence Tomography [194] and the Membrane Fouling Simulator [195] allows for real time biofouling measurement, but requires the use of a specialized cell with a need of a optical window which may pose a problem due to the high pressures generated during a RO process.

The development of a canary cell model was described (Chapter 4) that can simulate real time biofouling rates in an industrial spiral wound module. This represents a novel, additional approach for the detection and monitoring of biofouling, which can be achieved online, in a non-invasive manner that would otherwise be impossible to perform on a spiral wound module. Similarly, ultrasonic time domain reflectometry and electrochemical impedance spectroscopy were investigated for their suitability to provide real-time biofouling information, based on the acoustic and dielectric properties of the biofilm layer. The methods developed here, along with techniques developed in other studies such as feed fouling monitor [196] and NaCl tracer technique [197], are not meant to replace current monitoring techniques employed in industrial treatment plants, but to compliment them in providing more accurate real time information so that plant operators make prompt decisions applying cleaning protocols or membrane replacements to save cost and maximize output. Pilot-scale trials using these technologies are now being carried out in various water treatment plants in Singapore. By combining these methods of detecting and monitoring biofouling with the application of NO-based or other treatment methods, the effects these treatments have on RO performance can be investigated and monitored *in situ*, and optimization of such treatments can be done in real time.

Because biofouling constitutes a significant cost in RO and other water purification operations, it is vital to develop strategies to mitigate and manage fouling. This could be achieved through further studies of the mechanisms controlling biofilm formation, which for example led to the discovery that NO controls dispersal. Alternatively, it may be necessary to continue the development of cheaper, fouling-resistant and longer-lasting membranes to improve operational efficiency. Such strategies must also consider how to manage fouling, since it is unrealistic to expect a solution that will result in no fouling. Thus, monitoring systems that can provide real-time feedback to the operators are an important tool, which can be used to make decisions about when to undertake remedial action such as cleaning. Another interesting application of real time fouling monitors is their ability to provide instantaneous information regarding the efficacy of cleaning protocols. For example, a monitoring system could be used to determine when sufficient NO has been added to reduce the fouling to acceptable levels, thus improving the application of such novel fouling control strategies.

References

[1] P. H. Gleick, *Water in crisis: A guide to the world's fresh water resources*: Oxford University Press, 1993.

[2] R. F. Service, "Desalination freshens up," *Science,* vol. 313, pp. 1088-1090, Aug 25 2006.

[3] WRI. Available: http://www.wri.org/

[4] M. A. Shannon, P. W. Bohn, M. Elimelech, J. G. Georgiadis, B. J. Marinas, and A. M. Mayes, "Science and technology for water purification in the coming decades," *Nature,* vol. 452, pp. 301-310, Mar 20 2008.

[5] C. Fritzmann, J. Lowenberg, T. Wintgens, and T. Melin, "State-of-the-art of reverse osmosis desalination," *Desalination,* vol. 216, pp. 1-76, Oct 5 2007.

[6] M. Busch and W. E. Mickols, "Reducing energy consumption in seawater desalination," *Desalination,* vol. 165, pp. 299-312, Aug 15 2004.

[7] B. J. Feinberg, G. Z. Ramon, and E. M. V. Hoek, "Thermodynamic analysis of osmotic energy recovery at a reverse osmosis desalination plant," *Environmental Science & Technology,* vol. 47, pp. 2982-2989, 2013.

[8] C. Bellona and J. E. Drewes, "The role of membrane surface charge and solute physico-chemical properties in the rejection of organic acids by NF membranes," *Journal of Membrane Science,* vol. 249, pp. 227-234, Mar 1 2005.

[9] J. Radjenovic, M. Petrovic, F. Ventura, and D. Barcelo, "Rejection of pharmaceuticals in nanofiltration and reverse osmosis membrane drinking water treatment," *Water Research,* vol. 42, pp. 3601-3610, Aug 2008.

[10] T. Y. Cath, A. E. Childress, and M. Elimelech, "Forward osmosis: Principles, applications, and recent developments," *Journal of Membrane Science,* vol. 281, pp. 70-87, Sep 15 2006.

[11] Aquatechnology. Available: http://www.aquatechnology.net/reverseosmosistheory.html

[12] winebusiness. Available: http://www.winebusiness.com

[13] M. Mota, J. A. Teixeira, and A. Yelshin, "Influence of cell-shape on the cake resistance in dead-end and cross-flow filtrations," *Separation and Purification Technology*, vol. 27, pp. 137-144, May 1 2002.

[14] S. Loeb, "The Loeb-Sourirajan membrane - how it came about," *Abstracts of Papers of the American Chemical Society*, vol. 180, pp. 1-Cell, 1980.

[15] T. E. Davis, G. W. Skiens, and O. Cotton, "Cellulose triacetate membranes for reverse osmosis," *Abstracts of Papers of the American Chemical Society*, pp. 61-&, 1971.

[16] C. R. Bartels, "A surface science investigation of composite membranes," *Journal of Membrane Science*, vol. 45, pp. 225-245, Aug 1989.

[17] W. J. Lau, A. F. Ismail, N. Misdan, and M. A. Kassim, "A recent progress in thin film composite membrane: A review," *Desalination*, vol. 287, pp. 190-199, Feb 15 2012.

[18] C. Gonzalez-Gago, J. Pisonero, R. Sandin, J. F. Fuertes, A. Sanz-Medel, and N. Bordel, "Analytical potential of rf-PGD-TOFMS for depth profiling of an oxidized thin film composite," *Journal of Analytical Atomic Spectrometry*, 2016.

[19] M. Hill, *standard handbook of environmental engineering*.

[20] B. Penate and L. Garcia-Rodriguez, "Energy optimisation of existing SWRO (seawater reverse osmosis) plants with ERT (energy recovery turbines): Technical and thermoeconomic assessment," *Energy*, vol. 36, pp. 613-626, Jan 2011.

[21] M. Kurihara, N. Kanamaru, N. Harumiya, K. Yoshimura, and S. Hagiwara, "Spiral-wound new thin-film composite membrane for a single-stage seawater desalination by reverse-osmosis," *Desalination*, vol. 32, pp. 13-23, 1980.

[22] S. A. Avlonitis, K. Kouroumbas, and N. Vlachakis, "Energy consumption and membrane replacement cost for seawater RO desalination plants," *Desalination,* vol. 157, pp. 151-158, 2003.

[23] L. F. Song and M. Elimelech, "Theory of concentration polarization in cross-flow filtration," *Journal of the Chemical Society-Faraday Transactions,* vol. 91, pp. 3389-3398, Oct 7 1995.

[24] M. C. Porter, "Concentration polarization with membrane ultrafiltration," *Industrial & Engineering Chemistry Product Research and Development,* vol. 11, pp. 234-&, 1972.

[25] Yale. Available: http://www.yale.edu

[26] A. G. Fane, T. H. Chong, and P. Le-Clech, "Fouling in membrane processes," in *Membrane Operations*, ed: Wiley-VCH Verlag GmbH & Co. KGaA, 2009, pp. 121-138.

[27] H. F. Ridgway, M. G. Rigby, and D. G. Argo, "Bacterial adhesion and fouling of reverse-osmosis membranes," *Journal American Water Works Association,* vol. 77, pp. 97-106, 1985.

[28] H. C. Flemming, "Reverse osmosis membrane biofouling," *Experimental Thermal and Fluid Science,* vol. 14, pp. 382-391, May 1997.

[29] P. Stoodley, K. Sauer, D. G. Davies, and J. W. Costerton, "Biofilms as complex differentiated communities," *Annual Review of Microbiology,* vol. 56, pp. 187-209, 2002.

[30] P. Landini, D. Antoniani, J. G. Burgess, and R. Nijland, "Molecular mechanisms of compounds affecting bacterial biofilm formation and dispersal," *Applied Microbiology and Biotechnology,* vol. 86, pp. 813-823, Apr 2010.

[31] H.-C. Flemming, "Microbial biofouling: unsolved problems, insufficient approaches, and possible solutions," in *Biofilm Highlights*. vol. 5, H.-C.

Flemming, J. Wingender, and U. Szewzyk, Eds., ed: Springer Berlin Heidelberg, 2011, pp. 81-109.

[32] H. C. Flemming and J. Wingender, "The biofilm matrix," *Nature Reviews Microbiology,* vol. 8, pp. 623-633, Sep 2010.

[33] H. C. Flemming, "The perfect slime," *Colloids and Surfaces B-Biointerfaces,* vol. 86, pp. 251-259, Sep 1 2011.

[34] J. S. Baker and L. Y. Dudley, "Biofouling in membrane systems - A review," *Desalination,* vol. 118, pp. 81-89, Sep 20 1998.

[35] K. Poole, "Stress responses as determinants of antimicrobial resistance in Gram-negative bacteria," *Trends in Microbiology,* vol. 20, pp. 227-234, 2012.

[36] F. C. Fang, "Antimicrobial reactive oxygen and nitrogen species: Concepts and controversies," *Nature Reviews Microbiology,* vol. 2, pp. 820-832, 2004.

[37] A. Boehm, S. Steiner, F. Zaehringer, A. Casanova, F. Hamburger, D. Ritz, *et al.*, "Second messenger signalling governs *Escherichia coli* biofilm induction upon ribosomal stress," *Molecular Microbiology,* vol. 72, pp. 1500-1516, 2009.

[38] T. Hindré, H. Brüggemann, C. Buchrieser, Y. Héchard, T. Hindre, H. Bruggemann, *et al.*, "Transcriptional profiling of *Legionella pneumophila* biofilm cells and the influence of iron on biofilm formation," *Microbiology,* vol. 154, pp. 30-41, 2008.

[39] H. Mulcahy, S. Lewenza, and S. Bereswill, "Magnesium limitation Is an environmental trigger of the *Pseudomonas aeruginosa* biofilm lifestyle," *PLOS ONE,* vol. 6, p. e23307, 2011.

[40] J. J. Amarasinghe, F. A. Scannapieco, and E. M. Haase, "Transcriptional and translational analysis of biofilm determinants of *Aggregatibacter actinomycetemcomitans* in response to environmental perturbation," *Infection and Immunity,* vol. 77, pp. 2896-2907, 2009.

[41] P. Dirckx, "Biofilm formation in 3 steps," ed: Center for Biofilm Engineering, 2003.

[42] R. A. Al-Juboori and T. Yusaf, "Biofouling in RO system: Mechanisms, monitoring and controlling," *Desalination,* vol. 302, pp. 1-23, Sep 17 2012.

[43] A. G. Gristina, "Biomaterial-centered infection - microbial adhesion versus tissue integration," *Science,* vol. 237, pp. 1588-1595, Sep 25 1987.

[44] M. Hermansson, "The DLVO theory in microbial adhesion," *Colloids and Surfaces B-Biointerfaces,* vol. 14, pp. 105-119, Aug 15 1999.

[45] H. J. Busscher, W. Norde, P. K. Sharma, and H. C. van der Mei, "Interfacial re-arrangement in initial microbial adhesion to surfaces," *Current Opinion in Colloid & Interface Science,* vol. 15, pp. 510-517, Dec 2010.

[46] J. B. Kaplan, "Biofilm dispersal: mechanisms, clinical implications, and potential therapeutic uses," *Journal of Dental Research,* vol. 89, pp. 205-218, Mar 2010.

[47] K. Sauer, M. C. Cullen, A. H. Rickard, L. A. H. Zeef, D. G. Davies, and P. Gilbert, "Characterization of nutrient-induced dispersion in *Pseudomonas aeruginosa* PAO1 biofilm," *Journal of Bacteriology,* vol. 186, pp. 7312-7326, Nov 2004.

[48] M. Gjermansen, P. Ragas, C. Sternberg, S. Molin, and T. Tolker-Nielsen, "Characterization of starvation-induced dispersion in *Pseudomonas putida* biofilms," *Environmental Microbiology,* vol. 7, pp. 894-906, Jun 2005.

[49] K. M. Thormann, R. M. Saville, S. Shukla, and A. M. Spormann, "Induction of rapid detachment in *Shewanella oneidensis* MR-1 biofilms," *Journal of Bacteriology,* vol. 187, pp. 1014-1021, Feb 2005.

[50] N. Barraud, D. J. Hassett, S. H. Hwang, S. A. Rice, S. Kjelleberg, and J. S. Webb, "Involvement of nitric oxide in biofilm dispersal of *Pseudomonas aeruginosa*," *Journal of Bacteriology,* vol. 188, pp. 7344-7353, Nov 2006.

[51] L. Yang, Y. Hu, Y. Liu, J. Zhang, J. Ulstrup, and S. Molin, "Distinct roles of extracellular polymeric substances in *Pseudomonas aeruginosa* biofilm development," *Environmental Microbiology,* vol. 13, pp. 1705-1717, 2011.

[52] L. Friedman and R. Kolter, "Two genetic loci produce distinct carbohydrate-rich structural components of the *Pseudomonas aeruginosa* biofilm matrix," *Journal of Bacteriology,* vol. 186, pp. 4457-4465, Jul 2004.

[53] C. B. Whitchurch, T. Tolker-Nielsen, P. C. Ragas, and J. S. Mattick, "Extracellular DNA required for bacterial biofilm formation," *Science,* vol. 295, pp. 1487-1487, 2002.

[54] K. Murakami, R. Samudrala, B. R. Borlee, A. D. Goldman, D. J. Wozniak, and M. R. Parsek, "*Pseudomonas aeruginosa* uses a cyclic-di-GMP-regulated adhesin to reinforce the biofilm extracellular matrix," *Molecular microbiology,* vol. 75, pp. 827-842, 2010.

[55] P. S. Stewart, "Mechanisms of antibiotic resistance in bacterial biofilms," *International journal of medical microbiology,* vol. 292, pp. 107-113, 2002.

[56] N. Bagge, O. Ciofu, L. T. Skovgaard, and N. Hoiby, "Rapid development in vitro and in vivo of resistance to ceftazidime in biofilm-growing *Pseudomonas aeruginosa* due to chromosomal AE-lactamaseNote," *APMIS. Acta pathologica, microbiologica et immunologica Scandinavica,* vol. 108, pp. 589-600, 2000.

[57] K. D. Xu, M. J. Franklin, C. H. Park, G. A. McFeters, and P. S. Stewart, "Gene expression and protein levels of the stationary phase sigma factor, RpoS, in continuously-fed *Pseudomonas aeruginosa* biofilms," *FEMS microbiology letters,* vol. 199, pp. 67-71, 2001.

[58] K. Lewis, "Riddle of Biofilm Resistance," *Antimicrobial agents and chemotherapy,* vol. 45, pp. 999-1007, 2001.

[59] M. J. Franklin and D. E. Ohman, "Identification of *algI* and *algJ* in the *Pseudomonas aeruginosa* alginate biosynthetic gene cluster which are required for alginate O acetylation," *Journal of Bacteriology,* vol. 178, pp. 2186-95, 1996.

[60] J. R. Govan and V. Deretic, "Microbial pathogenesis in cystic fibrosis: mucoid *Pseudomonas aeruginosa* and *Burkholderia cepacia*," *Microbiological Reviews,* vol. 60, pp. 539-74, 1996.

[61] M. S. Byrd, I. Sadovskaya, E. Vinogradov, H. Lu, A. B. Sprinkle, S. H. Richardson, *et al.*, "Genetic and biochemical analyses of the *Pseudomonas aeruginosa* Psl exopolysaccharide reveal overlapping roles for polysaccharide synthesis enzymes in Psl and LPS production," *Molecular Microbiology,* vol. 73, pp. 622-638, 2009.

[62] J. Overhage, M. Schemionek, J. S. Webb, and B. H. A. Rehm, "Expression of the psl operon in *Pseudomonas aeruginosa* PAO1 biofilms: *PslA* performs an essential function in biofilm formation," *Applied and Environmental Microbiology,* vol. 71, pp. 4407-4413, August 1, 2005 2005.

[63] L. Ma, K. D. Jackson, R. M. Landry, M. R. Parsek, and D. J. Wozniak, "Analysis of *Pseudomonas aeruginosa* conditional Psl variants reveals roles for the Psl polysaccharide in adhesion and maintaining biofilm structure postattachment," *Journal of Bacteriology,* vol. 188, pp. 8213-8221, December 1, 2006 2006.

[64] M. S. Byrd, B. Pang, M. Mishra, W. E. Swords, and D. J. Wozniak, "The *Pseudomonas aeruginosa* exopolysaccharide Psl facilitates surface adherence and NF-κB activation in A549 cells," *Mbio,* vol. 1, August 31, 2010 2010.

[65] K. D. Jackson, M. Starkey, S. Kremer, M. R. Parsek, and D. J. Wozniak, "Identification of psl, a locus encoding a potential exopolysaccharide that is essential for *Pseudomonas aeruginosa* PAO1 biofilm formation," *Journal of Bacteriology,* vol. 186, pp. 4466-4475, July 15, 2004 2004.

[66] L. Ma, M. Conover, H. Lu, M. R. Parsek, K. Bayles, and D. J. Wozniak, "Assembly and development of the *Pseudomonas aeruginosa* biofilm matrix," *Plos Pathogens,* vol. 5, p. e1000354, 2009.

[67] E. E. Mann and D. J. Wozniak, "*Pseudomonas* biofilm matrix composition and niche biology," *FEMS Microbiol Rev,* vol. 36, pp. 893-916, Jul 2012.

[68] L. Friedman and R. Kolter, "Genes involved in matrix formation in *Pseudomonas aeruginosa* PA14 biofilms," *Molecular Microbiology,* vol. 51, pp. 675-690, 2004.

[69] K. Colvin, V. Gordon, K. Murakami, B. Borlee, D. Wozniak, B. R. Borlee, *et al.*, "The Pel polysaccharide can serve a structural and protective role in the biofilm matrix of *Pseudomonas aeruginosa*," *PLoS Pathogens,* vol. 7, p. e1001264, 2011.

[70] M. B. Miller and B. L. Bassler, "Quorum sensing in bacteria," *Annual Review of Microbiology,* vol. 55, pp. 165-199, 2001.

[71] R. Redfield, "Is quorum sensing a side effect of diffusion sensing?," *Trends in Microbiology,* vol. 10, pp. 365-370, 2002.

[72] B. Hense, C. Kuttler, J. Mueller, M. Rothballer, A. Hartmann, J. Müller, *et al.*, "Does efficiency sensing unify diffusion and quorum sensing?," *Nature Reviews Microbiology,* vol. 5, pp. 230-239, 2007.

[73] M. Harmsen, L. A. Yang, S. J. Pamp, and T. Tolker-Nielsen, "An update on *Pseudomonas aeruginosa* biofilm formation, tolerance, and dispersal," *FEMS Immunology and Medical Microbiology,* vol. 59, pp. 253-268, Aug 2010.

[74] W. C. Fuqua, S. C. Winans, and E. P. Greenberg, "Quorum sensing in bacteria: the LuxR-LuxI family of cell density-responsive transcriptional regulators," *Journal of Bacteriology,* vol. 176, pp. 269-75, 1994.

[75] Z. Li and S. K. Nair, "Quorum sensing: How bacteria can coordinate activity and synchronize their response to external signals?," *Protein Science,* vol. 21, pp. 1403-1417, Oct 2012.

[76] S. Schauder and B. L. Bassler, "The languages of bacteria," *Genes & Development,* vol. 15, pp. 1468-1480, Jun 15 2001.

[77] C. Fuqua, S. Winans, and E. P. Greenberg, "CENSUS AND CONSENSUS IN BACTERIAL ECOSYSTEMS: The LuxR-LuxI Family of Quorum-Sensing Transcriptional Regulators," *Annual Review of Microbiology,* vol. 50, pp. 727-751, 1996.

[78] L. Passador, L. Rust, J. M. Cook, M. J. Gambello, and B. H. Iglewski, "Expression of Pseudomonas aeruginosa virulence genes requires cell-to-cell communication," *Science,* vol. 260, pp. 1127-1130, 1993.

[79] S. B. Vonbodman, S. B. von Bodman, K. Piper, and S. Farrand, "Conjugation factor of Agrobacterium tumefaciens regulates Ti plasmid transfer by autoinduction," *Nature,* vol. 362, pp. 448-450, 1993.

[80] B. Bassler, M. Wright, R. Showalter, and M. Silverman, "Intercellular signalling in Vibrio harveyi: sequence and function of genes regulating expression of luminescence," *Molecular microbiology,* vol. 9, pp. 773-786, 1993.

[81] N. A. Whitehead, A. M. L. Barnard, H. Slater, N. J. L. Simpson, and G. P. C. Salmond, "Quorum-sensing in Gram-negative bacteria," *Fems Microbiology Reviews,* vol. 25, pp. 365-404, 2001.

[82] D. G. Davies, M. R. Parsek, J. P. Pearson, B. H. Iglewski, J. W. Costerton, and E. P. Greenberg, "The involvement of cell-to-cell signals in the development of a bacterial biofilm," *Science,* vol. 280, pp. 295-298, Apr 10 1998.

[83] B. Huber, K. Riedel, M. Hentzer, A. Heydorn, A. Gotschlich, M. Givskov, *et al.*, "The cep quorum-sensing system of *Burkholderia cepacia* H111 controls biofilm formation and swarming motility," *Microbiology,* vol. 147, pp. 2517-28, 2001.

[84] B. Tümmler and C. Kiewitz, "Cystic fibrosis: an inherited susceptibility to bacterial respiratory infections," *Molecular Medicine Today,* vol. 5, pp. 351-358, 1999.

[85] C. Van Delden and B. H. Iglewski, "Cell-to-cell signaling and *Pseudomonas aeruginosa* infections," *Emerging Infectious Diseases,* vol. 4, pp. 551-60, 1998.

[86] K. Riedel, M. Hentzer, O. Geisenberger, B. Huber, A. Steidle, H. Wu, *et al.*, "N-acylhomoserine-lactone-mediated communication between *Pseudomonas aeruginosa* and *Burkholderia cepacia* in mixed biofilms," *Microbiology,* vol. 147, pp. 3249-62, 2001.

[87] S. Periasamy and P. E. Kolenbrander, "*Aggregatibacter actinomycetemcomitans* builds mutualistic biofilm communities with *Fusobacterium nucleatum* and *Veillonella* species in saliva," *Infection and immunity,* vol. 77, pp. 3542-3551, 2009.

[88] D. Kara, S. B. I. Luppens, and J. M. Cate, "Differences between single- and dual-species biofilms of *Streptococcus mutans* and *Veillonella parvula* in growth, acidogenicity and susceptibility to chlorhexidine," *European Journal of Oral Sciences,* vol. 114, pp. 58-63, 2006.

[89] M. Herzberg and M. Elimelech, "Biofouling of reverse osmosis membranes: Role of biofilm-enhanced osmotic pressure," *Journal of Membrane Science,* vol. 295, pp. 11-20, 2007.

[90] M. Herzberg, S. Kang, and M. Elimelech, "Role of extracellular polymeric substances (EPS) in biofouling of reverse osmosis membranes," *Environmental Science & Technology,* vol. 43, pp. 4393-4398, 2009/06/15 2009.

[91] V. Lund and K. Ormerod, "The influence of disinfection processes on biofilm formation in water distribution-systems," *Water Research,* vol. 29, pp. 1013-1021, Apr 1995.

[92] S. Sorlini and C. Collivignarelli, "Trihalomethane formation during chemical oxidation with chlorine, chlorine dioxide and ozone of ten Italian natural waters," *Desalination*, vol. 176, pp. 103-111, Jun 10 2005.

[93] G. D. Kang, C. J. Gao, W. D. Chen, X. M. Jie, Y. M. Cao, and Q. Yuan, "Study on hypochlorite degradation of aromatic polyamide reverse osmosis membrane," *Journal of Membrane Science*, vol. 300, pp. 165-171, Aug 15 2007.

[94] J. C. Perrins, W. J. Cooper, J. H. van Leeuwen, and R. P. Herwig, "Ozonation of seawater from different locations: Formation and decay of total residual oxidant - implications for ballast water treatment," *Marine Pollution Bulletin*, vol. 52, pp. 1023-1033, Sep 2006.

[95] B. S. Oh, H. Y. Jang, Y. J. Jung, and J. W. Kang, "Microfiltration of MS2 bacteriophage: Effect of ozone on membrane fouling," *Journal of Membrane Science*, vol. 306, pp. 244-252, Dec 1 2007.

[96] M. Wietz, L. Høj, and M. R. Hall, "Effects of seawater ozonation on biofilm development in aquaculture tanks," *Systematic and Applied Microbiology*, vol. 32, pp. 266-277, 2009.

[97] K. L. Rakness, R. C. Renner, D. B. Vornehm, J. R. Thaxton, *Ozone: Science and Engineering* vol. 10, 1988.

[98] P. J. L. M. Boner. (1999, Wastewater technology fact sheet ozone disinfection. Available: http://water.epa.gov/scitech/wastetech/upload/2002_06_28_mtb_ozon.pdf

[99] L. Passantino, "Effect of low turbidity and algae on UV disinfection performance," *Journal American Water Works Association*, vol. 96, pp. 128-137, Jun 2004.

[100] M. Manefield, T. B. Rasmussen, M. Henzter, J. B. Andersen, P. Steinberg, S. Kjelleberg, *et al.*, "Halogenated furanones inhibit quorum sensing through accelerated LuxR turnover," *Microbiology,* vol. 148, pp. 1119-1127, Apr 2002.

[101] C. D. Bishop and B. P. Brandhorst, "On nitric oxide signaling, metamorphosis, and the evolution of biphasic life cycles," *Evolution & Development,* vol. 5, pp. 542-550, Sep-Oct 2003.

[102] N. Barraud, M. V. Storey, Z. P. Moore, J. S. Webb, S. A. Rice, and S. Kjelleberg, "Nitric oxide-mediated dispersal in single- and multi-species biofilms of clinically and industrially relevant microorganisms," *Microbial Biotechnology,* vol. 2, pp. 370-378, May 2009.

[103] N. Barraud, D. Schleheck, J. Klebensberger, J. S. Webb, D. J. Hassett, S. A. Rice, *et al.*, "Nitric oxide signaling in *Pseudomonas aeruginosa* biofilms mediates phosphodiesterase activity, decreased cyclic di-GMP levels, and enhanced dispersal," *J Bacteriol,* vol. 191, pp. 7333-42, Dec 2009.

[104] R. J. Barnes, R. R. Bandi, W. S. Wong, N. Barraud, D. McDougald, A. Fane, *et al.*, "Optimal dosing regimen of nitric oxide donor compounds for the reduction of *Pseudomonas aeruginosa* biofilm and isolates from wastewater membranes," *Biofouling,* vol. 29, pp. 203-12, 2013.

[105] W. B. Krantz and A. R. Greenberg, "Membrane characterization by ultrasonic time-domain reflectometry," in *Advanced Membrane Technology and Applications*, ed: John Wiley & Sons, Inc., 2008, pp. 879-897.

[106] H. D. K. Li J.X., Sanderson R.D., "The challenge of detecting the very initial onset of biofouling on membranes by novel ultrasonic wavelet technique," in *The International Congress on Membranes and Membrane Processes (ICOM2005), Seoul, Korea. 2005*.

[107] S. T. V. Sim, S. R. Suwarno, T. H. Chong, W. B. Krantz, and A. G. Fane, "Monitoring membrane biofouling via ultrasonic time-domain reflectometry enhanced by silica dosing," *Journal of Membrane Science,* vol. 428, pp. 24-37, Feb 1 2013.

[108] Q. Wang, M. Grätzel, and J.-E. Moser, "Electrochemical impedance spectroscopic analysis of dye-sensitized solar cells," *The Journal of Physical Chemistry B,* vol. 109, pp. 14945-14953, 2005.

[109] F. Mansfeld, "Use of electrochemical impedance spectroscopy for the study of corrosion protection by polymer-coatings," *Journal of Applied Electrochemistry,* vol. 25, pp. 187-202, 1995.

[110] F. Lisdat and D. Schäfer, "The use of electrochemical impedance spectroscopy for biosensing," *Analytical and Bioanalytical Chemistry,* vol. 391, pp. 1555-1567, 2008.

[111] L. N. Sim, Z. J. Wang, J. Gu, H. G. L. Coster, and A. G. Fane, "Detection of reverse osmosis membrane fouling with silica, bovine serum albumin and their mixture using in-situ electrical impedance spectroscopy," *Journal of Membrane Science,* vol. 443, pp. 45-53, 9/15/ 2013.

[112] H. C. Flemming, "Biofouling in water systems – cases, causes and countermeasures," *Applied Microbiology and Biotechnology,* vol. 59, pp. 629-640, 2002.

[113] Y. Miura, Y. Watanabe, and S. Okabe, "Membrane biofouling in pilot-scale membrane bioreactors (MBRs) treating municipal wastewater: Impact of biofilm formation," *Environmental science & technology,* vol. 41, pp. 632-638, 2007.

[114] L. A. Bereschenko, G. H. J. Heilig, M. M. Nederlof, M. C. M. van Loosdrecht, A. J. M. Stams, and G. J. W. Euverink, "Molecular characterization of the bacterial communities in the different compartments of a full-scale reverse-osmosis water

purification plant," *Applied and environmental microbiology*, vol. 74, pp. 5297-304, Sep 2008.

[115] L. N. Huang, H. De Wever, and L. Diels, "Diverse and distinct bacterial communities induced biofilm fouling in membrane bioreactors operated under different conditions," *Environ Sci Technol*, vol. 42, pp. 8360-6, Nov 15 2008.

[116] A. C. Fonseca, R. S. Summers, A. Greenberg, and M. Hernandez, "Extra-cellular polysaccharides, soluble microbial products, and natural organic matter impact on nanofiltration membranes flux decline," *Environmental Science & Technology*, vol. 41, pp. 2491-2497, 2007.

[117] A. Kim, H. Chen, and R. Yuan, "EPS biofouling in membrane filtration: An analytic modeling study," *Journal of Colloid and Interface Science*, vol. 303, pp. 243-249, 2006.

[118] A. Ghafoor, I. Hay, and B. H. A. Rehm, "Role of Exopolysaccharides in *Pseudomonas aeruginosa* Biofilm Formation and Architecture," *Applied and Environmental Microbiology*, vol. 77, pp. 5238-5246, 2011.

[119] K. Colvin, Y. Irie, C. Tart, R. Urbano, J. Whitney, C. Ryder, *et al.*, "The Pel and Psl polysaccharides provide *Pseudomonas aeruginosa* structural redundancy within the biofilm matrix," *Environmental Microbiology*, vol. 14, pp. 1913-1928, 2012.

[120] S. Chew, B. Kundukad, T. Seviour, J. R. C. van der Maarel, L. Yang, S. C. Chew, *et al.*, "Dynamic remodeling of microbial biofilms by functionally distinct exopolysaccharides," *mBio*, vol. 5, pp. e01536-e01536-14, 2014.

[121] M. J. Franklin, D. E. Nivens, J. T. Weadge, and P. L. Howell, "Biosynthesis of the *Pseudomonas aeruginosa* extracellular polysaccharides, alginate, Pel, and Psl," *Frontiers in Microbiology*, vol. 2, 2011-August-22 2011.

[122] H. R. Daniels L, Phillips JA., "Chemical analysis," *Methods for General and Molecular Bacteriology. Edited by P. Gerhardt, R. G. E. Murray, W. A. Wood and N. R. Krieg. American Society for Microbiology, Washington, D.C.*, pp. 512-554, 1994.

[123] S. R. Suwarno, X. Chen, T. H. Chong, V. L. Puspitasari, D. McDougald, Y. Cohen, *et al.*, "The impact of flux and spacers on biofilm development on reverse osmosis membranes," *Journal of Membrane Science*, vol. 405, pp. 219-232, Jul 1 2012.

[124] X. Chen, S. Suwarno, T. Chong, D. McDougald, S. Kjelleberg, Y. Cohen, *et al.*, "Dynamics of biofilm formation under different nutrient levels and the effect on biofouling of a reverse osmosis membrane system," *Biofouling*, vol. 29, pp. 319-330, 2013.

[125] K. Sombatsompop, C. Visvanathan, and R. Ben Aim, "Evaluation of biofouling phenomenon in suspended and attached growth membrane bioreactor systems," *Desalination*, vol. 201, pp. 138-149, 2006.

[126] H. Y. Dang and C. R. Lovell, "Bacterial primary colonization and early succession on surfaces in marine waters as determined by amplified rRNA gene restriction analysis and sequence analysis of 16S rRNA genes," *Applied and environmental microbiology*, vol. 66, pp. 467-475, 2000.

[127] A. MassolDeya, R. Weller, L. RiosHernandez, A. Massol Deyá, L. Ríos Hernández, J. Z. Zhou, *et al.*, "Succession and convergence of biofilm communities in fixed-film reactors treating aromatic hydrocarbons in groundwater," *Applied and environmental microbiology*, vol. 63, pp. 270-6, 1997.

[128] J. Wimpenny, "Ecological determinants of biofilm formation," *Biofouling*, vol. 10, pp. 43-63, 1996.

[129] T. J. O. Wyckoff, D. Wozniak, M. R. Parsek, M. Starkey, R. Keyser, P. Azadi, *et al.*, "Alginate is not a significant component of the extracellular polysaccharide matrix of PA14 and PAO1 *Pseudomonas aeruginosa* biofilms," *Proceedings of the National Academy of Sciences of the United States of America,* vol. 100, pp. 7907-7912, 2003.

[130] S. Periasamy, H. A. S. Nair, K. W. K. Lee, J. Ong, J. Q. J. Goh, S. Kjelleberg, *et al.*, "*Pseudomonas aeruginosa* PAO1 exopolysaccharides are important for mixed species biofilm community development and stress tolerance," *Frontiers in Microbiology,* vol. 6, 2015-August-20 2015.

[131] B. Borlee, A. Goldman, K. Murakami, R. Samudrala, D. Wozniak, and M. Parsek, "Pseudomonas aeruginosauses a cyclic-di-GMP-regulated adhesin to reinforce the biofilm extracellular matrix," *Molecular microbiology,* vol. 75, pp. 827-842, 2010.

[132] C. Whitchurch, T. Tolker Nielsen, P. Ragas, and J. Mattick, "Extracellular DNA Required for Bacterial Biofilm Formation," *Science,* vol. 295, pp. 1487-1487, 2002.

[133] M. Allesen Holm, K. Barken, L. Yang, M. Klausen, J. Webb, S. Kjelleberg, *et al.*, "A characterization of DNA release in Pseudomonas aeruginosa cultures and biofilms," *Molecular microbiology,* vol. 59, pp. 1114-1128, 2006.

[134] C. Mayer, R. Moritz, C. Kirschner, W. Borchard, R. Maibaum, J. Wingender, *et al.*, "The role of intermolecular interactions: studies on model systems for bacterial biofilms," *International Journal of Biological Macromolecules,* vol. 26, pp. 3-16, 1999.

[135] G. O'Toole, H. B. Kaplan, and R. Kolter, "Biofilm formation as microbial development," *Annual Review of Microbiology,* vol. 54, pp. 49-79, 2000.

[136] Z. Lewandowski, H. M. Lappinscott, J. W. Costerton, D. E. Caldwell, D. R. Korber, and H. M. Lappin Scott, "Microbial biofilms," *Annual Review of Microbiology,* vol. 49, pp. 711-745, 1995.

[137] L. Hall Stoodley, J. W. Costerton, and P. Stoodley, "Bacterial biofilms: from the Natural environment to infectious diseases," *Nature Reviews. Microbiology,* vol. 2, pp. 95-108, 2004.

[138] A. Ramesh, D. J. Lee, M. L. Wang, J. P. Hsu, R. S. Juang, K. J. Hwang, *et al.*, "Biofouling in membrane bioreactor," *Separation Science and Technology,* vol. 41, pp. 1345-1370, 2006.

[139] H. Y. Ng, T. W. Tan, and S. L. Ong, "Membrane fouling of submerged membrane bioreactors: impact of mean cell residence time and the contributing factors," *Environ Sci Technol,* vol. 40, pp. 2706-13, Apr 15 2006.

[140] I. Schmidt, P. J. M. Steenbakkers, H. J. M. op den Camp, K. Schmidt, and M. S. M. Jetten, "Physiologic and proteomic evidence for a role of nitric oxide in biofilm formation by *Nitrosomonas europaea* and other ammonia oxidizers," *Journal of Bacteriology*, vol. 186, pp. 2781-8, May 2004.

[141] A. Arruebarrena Di Palma, C. M. Pereyra, L. Moreno Ramirez, M. L. Xiqui Vazquez, B. E. Baca, M. A. Pereyra, *et al.*, "Denitrification-derived nitric oxide modulates biofilm formation in *Azospirillum brasilense*," *FEMS Microbiology Letters,* vol. 338, pp. 77-85, Jan 2013.

[142] L. Plate and M. A. Marletta, "Nitric oxide modulates bacterial biofilm formation through a multicomponent cyclic-di-GMP signaling network," *Molecular Cell,* vol. 46, pp. 449-60, May 25 2012.

[143] J. Zaitseva, V. Granik, A. Belik, O. Koksharova, and I. Khmel, "Effect of nitrofurans and NO generators on biofilm formation by *Pseudomonas aeruginosa*

PAO1 and *Burkholderia cenocepacia* 370," *Research in microbiology,* vol. 160, pp. 353-357, 2009.

[144] M. L. Falsetta, A. G. McEwan, M. P. Jennings, and M. A. Apicella, "Anaerobic metabolism occurs in the substratum of gonococcal biofilms and may be sustained in part by nitric oxide," *Infect Immun,* vol. 78, pp. 2320-8, May 2010.

[145] D. Ager, S. Evans, H. Li, A. Lilley, and C. J. van der Gast, "Anthropogenic disturbance affects the structure of bacterial communities," *Environmental microbiology,* vol. 12, pp. 670-678, 2010.

[146] A. A. Miles, S. S. Misra, and J. O. Irwin, "The estimation of the bactericidal power of the blood," *J Hyg (Lond),* vol. 38, pp. 732-49, Nov 1938.

[147] B. Kamlage, "Methods for General and Molecular Bacteriology.," *Food / Nahrung,* vol. 40, pp. 103-103, 1996.

[148] S. Handl, S. E. Dowd, J. F. Garcia-Mazcorro, J. M. Steiner, and J. S. Suchodolski, "Massive parallel 16S rRNA gene pyrosequencing reveals highly diverse fecal bacterial and fungal communities in healthy dogs and cats," *FEMS Microbiology Ecology,* vol. 76, pp. 301-10, May 2011.

[149] G. C. Baker, J. J. Smith, and D. A. Cowan, "Review and re-analysis of domain-specific 16S primers," *Journal of Microbiological Methods,* vol. 55, pp. 541-55, Dec 2003.

[150] J. G. Caporaso, J. Kuczynski, J. Stombaugh, K. Bittinger, F. D. Bushman, E. K. Costello, *et al.*, "QIIME allows analysis of high-throughput community sequencing data," *Nature Methods,* vol. 7, pp. 335-6, May 2010.

[151] R. C. Edgar, "Search and clustering orders of magnitude faster than BLAST," *Bioinformatics,* vol. 26, pp. 2460-1, Oct 1 2010.

[152] R. C. Edgar, B. J. Haas, J. C. Clemente, C. Quince, and R. Knight, "UCHIME improves sensitivity and speed of chimera detection," *Bioinformatics*, vol. 27, pp. 2194-200, Aug 15 2011.

[153] *Greengenes OTU database* Available: http://greengenes.secondgenome.com/downloads/database/13_5

[154] J. G. Caporaso, K. Bittinger, F. D. Bushman, T. Z. DeSantis, G. L. Andersen, and R. Knight, "PyNAST: a flexible tool for aligning sequences to a template alignment," *Bioinformatics*, vol. 26, pp. 266-7, Jan 15 2010.

[155] A. B. Roy, O. E. Petrova, and K. Sauer, "The phosphodiesterase DipA (PA5017) is essential for Pseudomonas aeruginosa biofilm dispersion," *J Bacteriol*, vol. 194, pp. 2904-15, Jun 2012.

[156] S. Schlag, C. Nerz, T. A. Birkenstock, F. Altenberend, and F. Gotz, "Inhibition of staphylococcal biofilm formation by nitrite," *J Bacteriol*, vol. 189, pp. 7911-9, Nov 2007.

[157] W. C. Tsai, R. M. Strieter, D. A. Zisman, J. M. Wilkowski, K. A. Bucknell, G. H. Chen, *et al.*, "Nitric oxide is required for effective innate immunity against Klebsiella pneumoniae," *Infection and immunity*, vol. 65, pp. 1870-1875, 1997.

[158] G. Charville, E. Hetrick, C. Geer, and M. Schoenfisch, "Reduced bacterial adhesion to fibrinogen-coated substrates via nitric oxide release," *Biomaterials*, vol. 29, pp. 4039-4044, 2008.

[159] J. Luo, J. Zhang, R. Barnes, X. Tan, D. McDougald, A. Fane, *et al.*, "The application of nitric oxide to control biofouling of membrane bioreactors," *Microbial Biotechnology*, vol. 8, pp. 549-560, 2015.

[160] R. J. Barnes, R. R. Bandi, F. Chua, J. H. Low, T. Aung, N. Barraud, *et al.*, "The roles of *Pseudomonas aeruginosa* extracellular polysaccharides in biofouling of

reverse osmosis membranes and nitric oxide induced dispersal," *Journal of Membrane Science,* 2014.

[161] K. M. Yeon, W. S. Cheong, H. S. Oh, W. N. Lee, B. K. Hwang, C. H. Lee, *et al.*, "Quorum sensing: a new biofouling control paradigm in a membrane bioreactor for advanced wastewater treatment," *Environ Sci Technol,* vol. 43, pp. 380-5, Jan 15 2009.

[162] C. L. Chen, W. T. Liu, M. L. Chong, M. T. Wong, S. L. Ong, H. Seah, *et al.*, "Community structure of microbial biofilms associated with membrane-based water purification processes as revealed using a polyphasic approach," *Applied Microbiology and Biotechnology,* vol. 63, pp. 466-73, Jan 2004.

[163] L. A. Bereschenko, A. J. Stams, G. J. Euverink, and M. C. van Loosdrecht, "Biofilm formation on reverse osmosis membranes is initiated and dominated by *Sphingomonas spp*," *Applied and Environmental Microbiology,* vol. 76, pp. 2623-32, Apr 2010.

[164] C. M. Pang and W. T. Liu, "Community structure analysis of reverse osmosis membrane biofilms and the significance of Rhizobiales bacteria in biofouling," *Environ Sci Technol,* vol. 41, pp. 4728-34, Jul 1 2007.

[165] A. Al Ashhab, M. Herzberg, and O. Gillor, "Biofouling of reverse-osmosis membranes during tertiary wastewater desalination: microbial community composition," *Water Res,* vol. 50, pp. 341-9, Mar 1 2014.

[166] C. Ayache, C. Manes, M. Pidou, J. P. Croue, and W. Gernjak, "Microbial community analysis of fouled reverse osmosis membranes used in water recycling," *Water Res,* vol. 47, pp. 3291-9, Jun 15 2013.

[167] C. Chiellini, R. Iannelli, L. Modeo, V. Bianchi, and G. Petroni, "Biofouling of reverse osmosis membranes used in river water purification for drinking purposes: analysis of microbial populations," *Biofouling,* vol. 28, pp. 969-84, 2012.

[168] L. A. Bereschenko, H. Prummel, G. J. Euverink, A. J. Stams, and M. C. van Loosdrecht, "Effect of conventional chemical treatment on the microbial population in a biofouling layer of reverse osmosis systems," *Water Res,* vol. 45, pp. 405-16, Jan 2011.

[169] S. T. V. Sim, T. H. Chong, W. B. Krantz, and A. G. Fane, "Monitoring of colloidal fouling and its associated metastability using Ultrasonic Time Domain Reflectometry," *Journal of Membrane Science,* vol. 401–402, pp. 241-253, 5/15/ 2012.

[170] S. T. V. Sim, W. B. Krantz, T. H. Chong, and A. G. Fane, "Online monitor for the reverse osmosis spiral wound module — Development of the canary cell," *Desalination,* vol. 368, pp. 48-59, 2015.

[171] J. C. Nickel, I. Ruseska, J. B. Wright, and J. W. Costerton, "Tobramycin resistance of *Pseudomonas aeruginosa* cells growing as a biofilm on urinary catheter material," *Antimicrobial Agents and Chemotherapy,* vol. 27, pp. 619-24, 1985.

[172] G. A. O'Toole and R. Kolter, "Flagellar and twitching motility are necessary for *Pseudomonas aeruginosa* biofilm development," *Molecular Microbiology,* vol. 30, pp. 295-304, 1998.

[173] M. Hentzer, K. Riedel, T. B. Rasmussen, A. Heydorn, J. B. Andersen, M. R. Parsek, *et al.*, "Inhibition of quorum sensing in *Pseudomonas aeruginosa* biofilm bacteria by a halogenated furanone compound," *Microbiology,* vol. 148, pp. 87-102, 2002.

[174] J. Schwinge, P. R. Neal, D. E. Wiley, D. F. Fletcher, and A. G. Fane, "Spiral wound modules and spacers," *Journal of Membrane Science,* vol. 242, pp. 129-153, 2004.

[175] M. DuBois, K. A. Gilles, J. K. Hamilton, P. A. Rebers, and F. Smith, "Colorimetric method for determination of sugars and related substances," *Analytical Chemistry,* vol. 28, pp. 350-356, 1956.

[176] J. Schwinge, P. R. Neal, D. E. Wiley, and A. G. Fane, "Estimation of foulant deposition across the leaf of a spiral-wound module," *Desalination,* vol. 146, pp. 203-208, 2002.

[177] A. Alexiadis, D. E. Wiley, A. Vishnoi, R. H. K. Lee, D. F. Fletcher, and J. Bao, "CFD modelling of reverse osmosis membrane flow and validation with experimental results," *Desalination,* vol. 217, pp. 242-250, 2007.

[178] M. Herzberg and M. Elimelech, "Physiology and genetic traits of reverse osmosis membrane biofilms: a case study with *Pseudomonas aeruginosa*," *The ISME journal,* vol. 2, pp. 180-194, 2008.

[179] C. M. Pang, P. Hong, H. Guo, and W.-T. Liu, "Biofilm formation characteristics of bacterial isolates retrieved from a reverse osmosis membrane," *Environmental Science & Technology,* vol. 39, pp. 7541-7550, 2005.

[180] I. M. Marcus, M. Herzberg, S. L. Walker, and V. Freger, "*Pseudomonas aeruginosa* attachment on QCM-D sensors: The role of cell and surface hydrophobicities," *Langmuir,* vol. 28, pp. 6396-6402, 2012.

[181] C. D. Moody, J. W. Kaakinen, J. C. Lozier, and P. E. Laverty, "Yuma desalting test facility: Foulant component study," *Desalination,* vol. 47, pp. 239-253, 1983.

[182] Y. Kaya, H. Barlas, and S. Arayici, "Nanofiltration of Cleaning-in-Place (CIP) wastewater in a detergent plant: Effects of pH, temperature and transmembrane pressure on flux behavior," *Separation and Purification Technology,* vol. 65, pp. 117-129, 2009.

[183] M. F. A. Goosen, S. S. Sablani, S. S. Al-Maskari, R. H. Al-Belushi, and M. Wilf, "Effect of feed temperature on permeate flux and mass transfer coefficient in

spiral-wound reverse osmosis systems," *Desalination,* vol. 144, pp. 367-372, 2002.

[184] C. Whittaker, H. Ridgway, and B. H. Olson, "Evaluation of cleaning strategies for removal of biofilms from reverse-osmosis membranes," *Applied and Environmental Microbiology,* vol. 48, pp. 395-403, 1984.

[185] O. Rendueles, J. B. Kaplan, and J.-M. Ghigo, "Antibiofilm polysaccharides," *Environmental microbiology,* vol. 15, pp. 334-346, 06/26 2013.

[186] S. M. Abu-Sayem, E. Manzo, L. Ciavatta, A. Tramice, A. Cordone, S. M. Sayem, *et al.*, "Anti-biofilm activity of an exopolysaccharide from a sponge-associated strain of *Bacillus licheniformis*," *Microbial Cell Factories,* vol. 10, p. 74, 2011.

[187] Y. Kim, S. Oh, and S. Kim, "Released exopolysaccharide (r-EPS) produced from probiotic bacteria reduce biofilm formation of enterohemorrhagic *Escherichia coli* O157:H7," *Biochemical and Biophysical Research Communications,* vol. 379, pp. 324-329, 2009.

[188] M. Bendaoud, E. Vinogradov, N. Balashova, D. Kadouri, S. Kachlany, and J. Kaplan, "Broad-spectrum biofilm inhibition by *Kingella kingae* exopolysaccharide," *Journal of bacteriology,* vol. 193, pp. 3879-3886, 2011.

[189] W. Ang and M. Elimelech, "Protein (BSA) fouling of reverse osmosis membranes: Implications for wastewater reclamation," *Journal of membrane science,* vol. 296, pp. 83-92, 2007.

[190] P. Pradanos, A. Hernandez, I. Huisman, P. Prádanos, and A. Hernández, "The effect of protein–protein and protein–membrane interactions on membrane fouling in ultrafiltration," *Journal of membrane science,* vol. 179, pp. 79-90, 2000.

[191] S. Walker, J. Redman, and M. Elimelech, "Role of cell surface lipopolysaccharides in *Escherichia coli* K12 adhesion and transport," *Langmuir,* vol. 20, pp. 7736-7746, 2004.

[192] M. T. Khan, M. Busch, V. G. Molina, A.-H. Emwas, C. Aubry, and J.-P. Croue, "How different is the composition of the fouling layer of wastewater reuse and seawater desalination RO membranes?," *Water Research,* vol. 59, pp. 271-282, 8/1/ 2014.

[193] A. Khaleghi-Moghadam and M. H. I. Dore, "Cost and efficacy of water disinfection practices: Evidence from Canada," *Review of Economic Analysis,* vol. 4, pp. 209-223, 2012.

[194] C. Dreszer, A. D. Wexler, S. Drusová, T. Overdijk, A. Zwijnenburg, H. C. Flemming, *et al.*, "In-situ biofilm characterization in membrane systems using Optical Coherence Tomography: Formation, structure, detachment and impact of flux change," *Water Research,* vol. 67, pp. 243-254, 12/15/ 2014.

[195] J. S. Vrouwenvelder, J. A. M. van Paassen, L. P. Wessels, A. F. van Dam, and S. M. Bakker, "The Membrane Fouling Simulator: A practical tool for fouling prediction and control," *Journal of Membrane Science,* vol. 281, pp. 316-324, 9/15/ 2006.

[196] A. H. Taheri, L. N. Sim, T. H. Chong, W. B. Krantz, and A. G. Fane, "Prediction of reverse osmosis fouling using the feed fouling monitor and salt tracer response technique," *Journal of Membrane Science,* vol. 475, pp. 433-444, 2/1/ 2015.

[197] T. H. Chong, F. S. Wong, and A. G. Fane, "Enhanced concentration polarization by unstirred fouling layers in reverse osmosis: Detection by sodium chloride tracer response technique," *Journal of membrane science,* vol. 287, pp. 198-210, 2007.